CHAPTER 2

4-Acyl Pyrazolones and their Zinc (II) Metal Complexes: Synthesis, Characterization and Structural Features

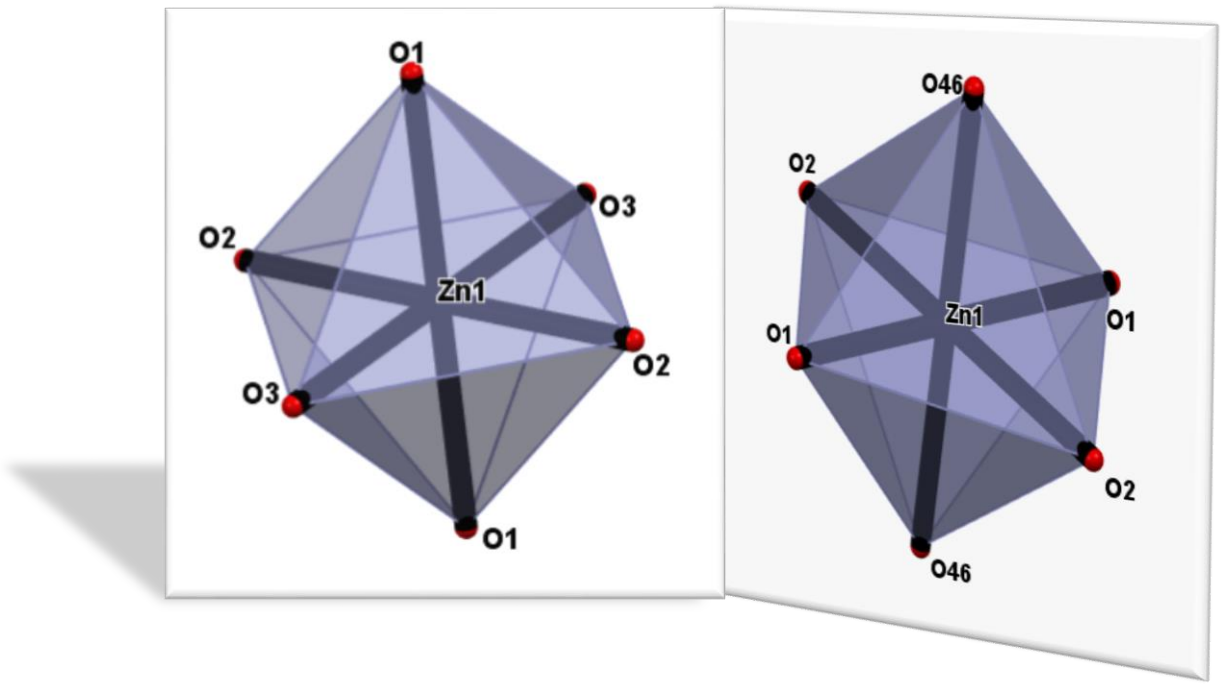

Chapter 2 (Part-a):

Binary Mononuclear Zinc (II) Complexes of 4-acyl Pyrazolones: Synthesis, Characterization and Structural Features.

2.1.1. Introduction

4-Acylpyrazolones history

The reaction between hydrazine or its derivatives and 1, 3 dicarbonyl compound convert into a Pyrazole using an acid catalyst was found by Ludwig Knorr in the last 19th century.[1,2] Knorr has given the synthesis and the correct structure[i] of pyrazolone.[3]

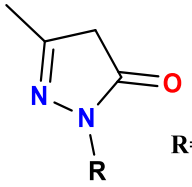

R=-H, substituted aryl group

[I]

Acylpyrazolones having di-ketones are playing a very significant role in coordination chemistry because; it contains a pyrazole fused to a chelating arm. The first synthesis of an acylpyrazolone appeared at the end of the 19th century and in 1959 Jensen has reported an important method of preparation of 1-phenyl-3-methyl-4-acylpyrazol-5-ones.[4,5]

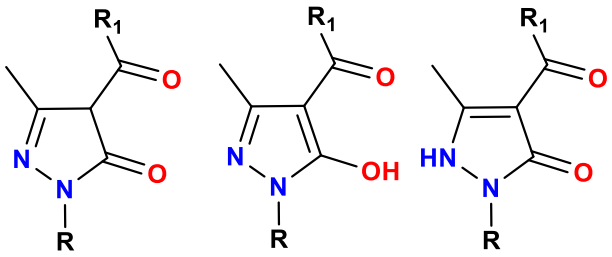

[II] [III] [IV]

From the reported articles and facts it's established that acylpyrazolone exists in different tautomers.[6] The 4-acylpyrazolones having *β*-diketone used as chelating arms with metal in the coordination Chemistry.[7] Pyrazolone based derivatives showing great opportunity due to their wide use in chemical science.[5,8,9] The acyl pyrazolone and its derivatives are highly biological active due to their skeleton. Acylpyrazolones also have been used in general chemistry, biochemistry and medicinal chemistry.[7,10,11] Acylpyrazolone ligands also have been used in complexation with many transition metal.[12–16]

4-Acylpyrazolone in metal complexation

The acylpyrazolones have displayed some interesting coordination modes in the neutral form (II). The enol tautomer can coordinates to the metal in a chelating bidentate O-form (III), as found in the crystal structure of Ba metal complex, where the enolic H is bonded to an external water molecule or also through the ring N atom of the pyrazole (Fig. 2.1.1b), as observed in the crystal structure of Rh metal complex [6,17] The neutral acyl pyrazolone can also coordinate

in O-chelating bidentate keto amino tautomeric form (Fig. 1.1.2), as found in the reported article, and in O-chelating bidentate diketo form (Fig. 1.1.2), as observed in Cr complexes in reported articles.[6,18–21]

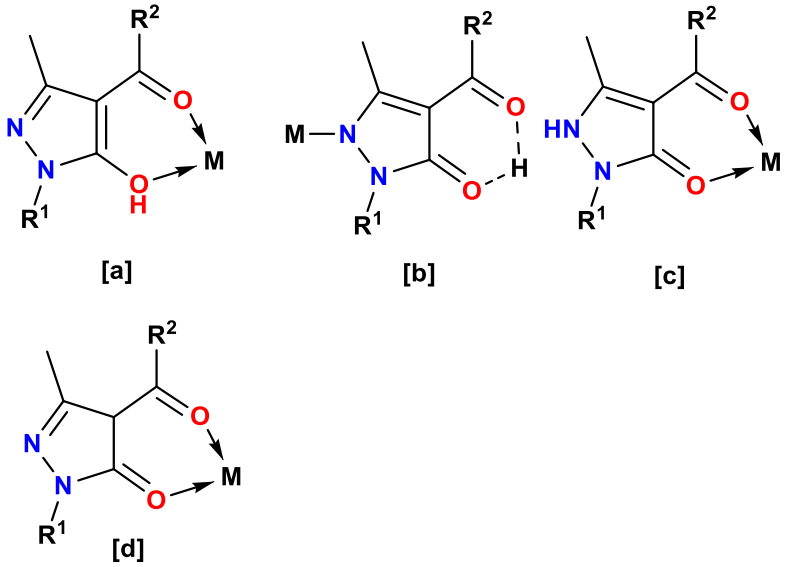

Fig. 2.1.1. Coordination modes of neutral acyl pyrazolones in complexes. Where R^1= Substituted phenyl ring and R^2=Substituted aromatic ring or formyl group or aliphatic chain and M=Metals (Ba, Ca, Sr, Rh).

Acylpyrazolones have involved in H-bonding network with hydrogen atoms of water(Fig. 2.1.1b).[18,22,23] The acylpyrazolonates can also coordinate metals through N2 atom of the pyrazole ring, as observed in silver and lead metal (Fig. 2.1.1).[6,20,21]

Coordination modes of AP presented in the Fig. 2.1.2. Herein, Calcium complexes [Ca(AP-R)$_2$]·xH$_2$O (x = 0, 1/2, 1, 2) (AP=Acylpyrazolone, AP-R=APPh, APMe, APEt, APPr, APBu, APHp) have been synthesised by Ca(OAc)$_2$ and acylpyrazolone in ethanol. In 1995, the first X-ray crystal structures of Ca and Ba acylpyrazolonates have been described.[17,24,25] In [Ca(APPh)$_2$(EtOH)$_2$], the AP-Ph ligands have coordinated in an O2-bidentate fashion, arranged in an *anti*-configuration to each other. The two EtOH molecules have in axial positions (Fig. 2.1.3) involved in an intermolecular extended H-bonding network with N atoms of pyrazole by neighbouring molecular units.[6] In [Ba(APPh)$_2$(APPh)$_2$]·H$_2$O, the Ba atom shows an eight-coordination by two anionic O2- bidentate APPh and two neutral O2-bidentate H-APPh with a water molecule H-bonded to the oxygen atom of a neutral AP-Ph (Fig. 2.1.4).[17,21]

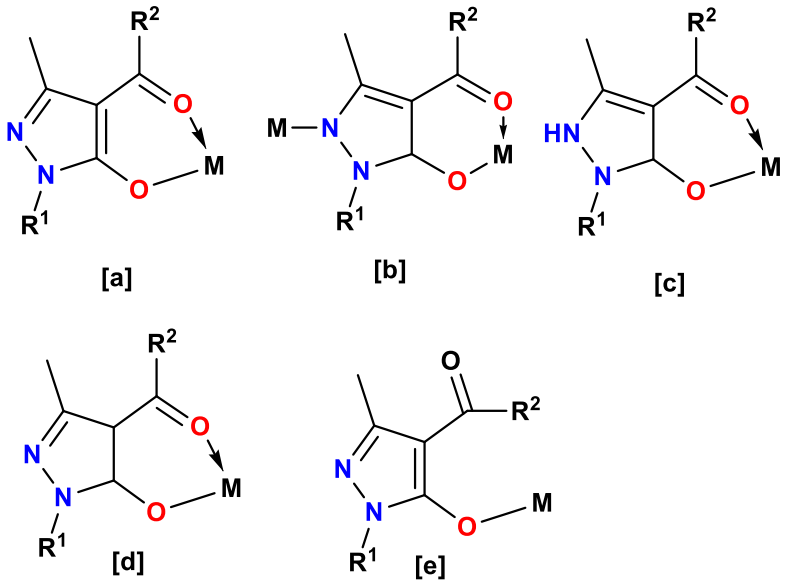

Fig. 2.1.2. Coordination modes of deprotonated anionic acylpyrazolone (AP) with metal in complexation.

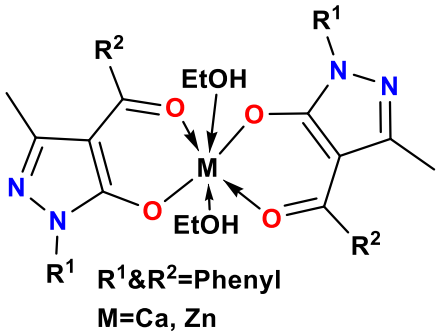

Fig. 2.1.3. Calcium complex $[Ca(AP)_2(EtOH)_2]$ of acylpyrazolone.

The coordination of acylpyrazolone to silver occurs through the O-chelating face and the N of the pyrazole ring in the $[Ag(AP)]_n$ coordination polymers (Fig.2.1.5).[26]

Vanadium complexes $VO(AP)_2(H_2O)$, with hindered substituents in both para- and meta-positions of the phenyl ring of AP ligands, unexpectedly contain the VO(oxo) group located cis to the coordinated water molecule and the AP ligands are in twisted geometry (Fig. 2.1.6), the difference with respect to previous trans geometries being evidently due to the methyl groups in the para position of the phenyl bonded to N1 of pyrazolone.[27,28]

In the complexes $Zn(AP)_2(ROH)_2$(R = Me or Et) the Zn atom is in an inversion center of a distorted octahedral geometry, where the two ethanol molecules are mutually trans (Fig. 2.1.3), while the two bidentate (AP) ligands adopt an anti-configuration.[29] Many of binary zinc

complex of AP, solvent molecules are coordinates opposite site to each other (Fig.2.1.7) and most common geometry distorted octahedral have been obtained.[30–32]

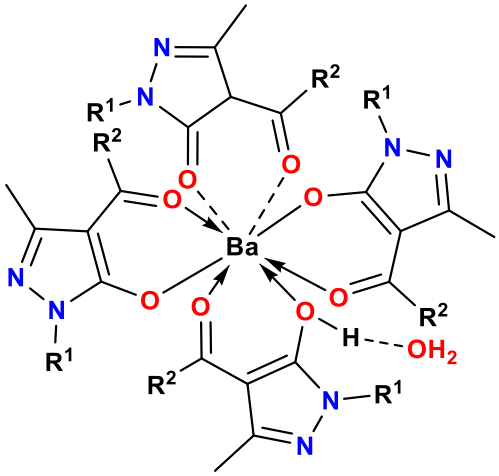

Fig. 2.1.4. Ba complex $[Ba(APPh)_2(APPh)_2]\cdot H_2O$ of acylpyrazolone(AP), where R^1 and R^2 are the phenyl ring in the complex.

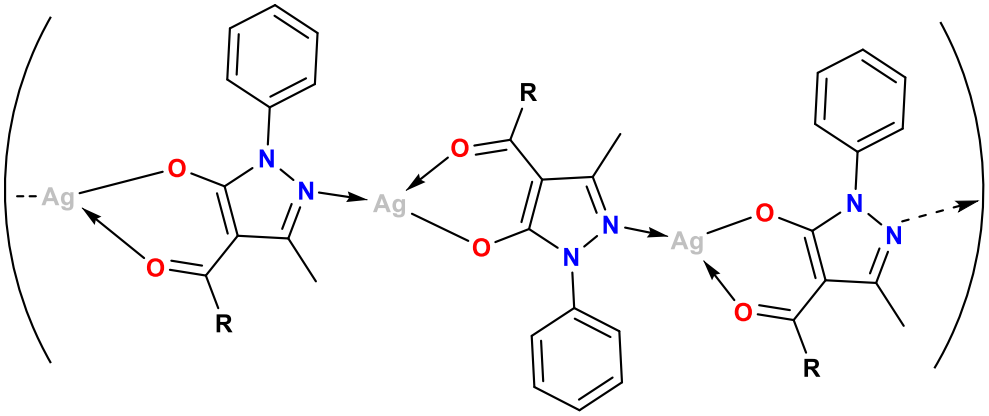

Fig. 2.1.5. Structure of acylpyrazolonates silver complex. Where R= $CF_2CF_2CF_3$/-cyclo-C_6H_{11}/-C(H)=CMe_2.

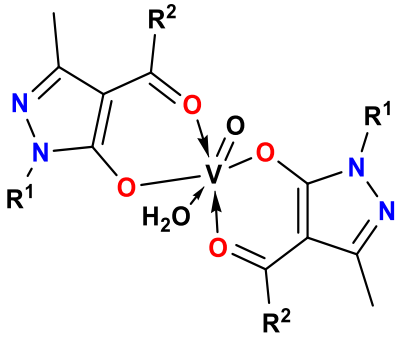

Fig. 2.1.6. Oxo-Vanadium complex. Where R^1 and R^2 are substituted aryl group and an alkyl group.

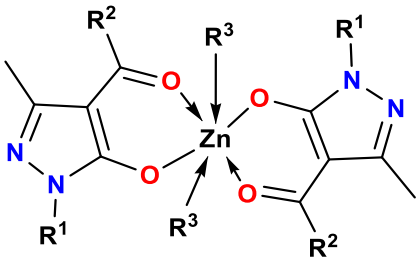

Fig. 2.1.7. Acylpyrazolone based zinc complex. Where R^1 and R^2 are substituted phenyl ring and R^3 are solvents molecules.

Bioactive 4-acylpyrazolone and its complexes

Pyrazolones and their derivatives have been reported for various biologically activities.[6,20,21,26,33] Furthermore, 4-acyl pyrazolones have grabbed more attention of the researcher, as their simple preparation by acylation of substituted pyrazolone and corresponding acid chlorides.[28] Pyrazolones based compounds have much potent of antibacterial activity owing to containing pyrazole and/or pyridazine, chromone, oxazine, furane, and pyrrole rings.[34] H. Luo *et al.* 2016, reported the complexes to have higher cytotoxic activities against HeLa and Eca-109 tumor cells than that of the AP based ligand and cisplatin.[35] I. Shaikh *et. al*. 2019, reported Antimalarial activity of acylpyrazolone and its complexes.[30,36] The catalytic potentials of many metal complexes were investigated. Acylpyrazolone based Ti, Cr, V, Mo, Mn, Cu, Ni, Co and, Zn metal complexes of gives promising catalytic activity.[37]

Zinc in complexation

Zinc as an element, having Atomic Number is 30 and Atomic Mass is 65.39 (30 protons, 30 electrons, 35 neutrons). [38] Zinc Identified as an element in 1746 but known to the Greeks and Romans before 20 BC.[38] In complexes and alloy, zinc has the most common oxidation state is +2. The zinc(II) complexes have composed of two chelating groups of pyrazolone based ligand that adopt an octahedral geometry around the metal ion.[39] Zinc(II) with acyl pyrazolone occupied distorted octahedral geometry in which four sides are occupied by acylpyrazolone moiety and two sides by solvent molecules (Fig.2.1.7).[30,32,36]

Objective and methodology of the present work

Acylpyrazolones are always interested in coordination chemistry in recent years. Zinc(II) complexes of acylpyrazolones and their structural analogues getting attention is continuously progressing after the synthesis of many zinc(II) complex of acylpyrazolone in recent year.[21,28]

In the zinc(II) complexes of acyl pyrazolone, attention was given to the single crystal X-ray analysis of the synthesized complexes, This is might be due to the difficulty in getting good single crystals of d^{10} metal complexes. We were interested in synthesizing the d^{10} complexes of 4-acylpyrazolones and their structural analogues and study their geometry using single crystal X-Ray diffraction technique along with the other spectroscopic and analytical techniques This chapter is dedicated to the synthesis, characterization and crystal study of binary zinc(II) complexes of 4-acyl pyrazolones.

2.1.2. Experimental

2.1.2.1. Materials and method

Solvents used for electrochemical and spectroscopic studies were purified by regular procedures.[40] 1, 4 dioxane, Calcium hydroxide, zinc acetate dihydrate and 2, 2' bi-pyridine were obtained from LOBA Chem. Pvt. Ltd., Mumbai were used as received. Methanol was obtained from Spectrochem. Mumbai, India and methanol was used after distillation. 3-methyl-1-phenyl pyrazolone-5-one, 3-methyl-1(m-chlorophenyl)-pyrazolone-5-one and 3-methyl 1(p-Tolyl) pyrazolone-5-one obtained as gift samples from Shree Sidhdhanath Industries, Sachin.

The synthesized compounds were characterized using different techniques. Infrared spectra (4000-400 cm^{-1}, KBr pellets) of the samples were recorded on a model Bruker alpha FTIR spectrophotometer with 4 scan number. ^{1}H and ^{13}C NMR spectra of the ligands and complexes were recorded with Bruker AV 400 MHz using $CDCl_3$/DMSO-d^6 as a solvent and TMS as an internal reference. The electronic spectra (in DMSO at room temperature) in the range of 200-800 nm were recorded on a model Perkin Elmer Lambda 35 UV-VIS spectrophotometer. Molar conductivity of 1×10^{-3} M solution of the complexes in DMSO was measured at room temperature with a model EQ664A digital direct reading deluxe digital conductivity meter. Zinc content was determined by volumetric analysis after decomposing the complexes with HNO_3.

2.1.2.2. Syntheses of ligands

(i) 4-(4-chlorobenzoyl)-5-methyl-2-phenyl-2,4-dihydro-3H-pyrazol-3-one (L1)

3-methyl-1-phenyl pyrazolone-5-one (0.1 mol, 17.4 g) was dissolved in hot dioxane (80 ml) in a round bottom flask equipped with a mechanical stirrer, separating funnel and reflux

condenser. Calcium hydroxide (0.2 mol, 14.81 g) was added to this solution, followed by 4-chloro benzoyl chloride (0.1 mol, 12.82 mL) added dropwise with precaution, as this stage reaction was exothermic and this whole mass was converted into a thick paste. After the complete addition, the reaction mixture was refluxed for two hours and then it was poured into dilute hydrochloric acid (2 M, 200 ml). The colour crystals (L1) thus obtained were separated by filtration and recrystallized from Rectified spirit. M.P.: 105ºC, Yield: 70.85 %, M.F.: $C_{17}H_{13}ClN_2O_2$ (F.w. 312.75). IR (KBr, cm^{-1}): 1558 (C=N, cyclic), 1589 (C=O, *p*-chloro benzoyl group); 1619(C=O, Pyrazolone ring); ^{1}H NMR ($CDCl_3$, 400MHz): δ *ppm* 2.1 (s) (3H, Pyrazolone C-CH_3), 7.5-7.6 (dd, 4H Ar C-H), 7.4-7.8 (m, 5H Phenyl of pyrazolone); ^{13}C NMR ($CDCl_3$, 100MHz) δ *ppm* 191, 161, 148, 138, 137, 136, 129.3, 129.1, 128.8, 127, 121, 103, 16.[30]

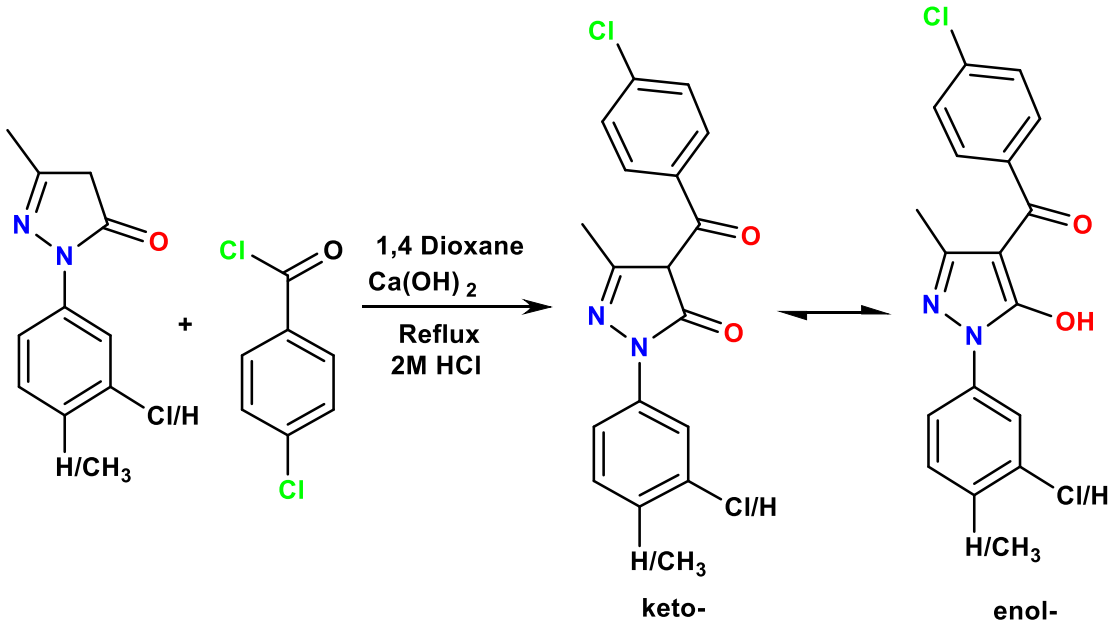

Scheme 2.1.1. Synthesis route of ligands.

(ii) Synthesis of 4-(4-chlorobenzoyl)-2-(3-chlorophenyl)-5-methyl-2,4-dihydro-3H-pyrazol-3-ne (L2).

The synthesized ligand were reported in Shaikh et. al., 2019, [31]. (*See* Scheme 2.1.1) Yield: 72%. M.F.: $C_{17}H_{12}Cl_2N_2O_2$, F.w.: 347.20. M.P.: 105 °C. Λ_m ($S.cm^2.mol^{-1}$): 8.8.FTIR (KBr plates) υ (cm^{-1}): 1625(s) (C=O, amide of pyrazolone), 1590(m) (C=O, 4-chloro benzoyl), 966(s) (N-N of pyrazolone), 1486(m) (aromatic –C-C). ^{1}H NMR ($CDCl_3$) δ ppm: 2.14 (s, 3H,

pyrazolone C–CH_3), 7.28-7.30 (m, 1H, m-chloro ph), 7.39-7.43 (m, 1H, m-chlorophenyl), 7.51-7.63 (m, 4H, *p*-chloro benzoyl), 7.83-7.85 (m, 1H, m-chloro ph), 7.963-7.968 (m, 1H, m-chloro ph). ^{13}C NMR ($CDCl_3$, 100MHz) δ ppm: 16 (-CH_3- pyrazolone), 103, 118, 120, 126, 128, 129, 130, 134, 135, 138, 138, 147 , 162 (C=O, amide of pyrazolone), 190 (C=O, 4-chloro benzoyl).[30]

(iii) Synthesis of 4-(4-chlorobenzoyl)-5-methyl-2-(*p*-tolyl)-2,4-dihydro-3H-pyrazol-3-one (L3)

Synthesized ligand was reported in Shaikh et al., 2019.[30] Yield: 65.5 %, M.F.: $C_{18}H_{15}ClN_2O_2$, (F.w.: 326.78), M.P.: 108ºC, Λ_m ($S.cm^2.mol^{-1}$): 10.1, IR (KBr, cm^{-1}): 1551(C=N, cyclic), 1590 (C=O, 4-chloro benzoyl group) 1625 (m) (C=O, Pyrazolone ring); ^{1}H NMR ($CDCl_3$, 400MHz): *δ ppm* 2.1 (s, 3H, Pyrazolone C-CH_3), 2.38-2.39(m, 1H, -CH-cyclic), 2.4 (s,3H, CH_3-Ar) , 7.28-7.30 (d, 2H, aromatic, *J*=8Hz), 7.50-7.52(m, 2H, aromatic), 7.60-7.62 (d, 2H, *p*-chloro benzoyl-, *J*=8Hz),7.72-7.74 (d, 2H, *p*-chloro benzoyl-, *J*=8Hz); ^{13}CNMR ($CDCl_3$, 100MHz) 16(-CH_3, pyrazolone), 21(-CH_3-tolyl), 30 (CH_3-pyz), 103, 121, 128.7, 129, 130, 131, 135, 136, 138, 147, 160 (C=O, amide of pyrazolone), 191 (C=O, 4-chloro benzoyl).[30] Synthesis of ligands summarized in Scheme **2.1.1**.[30]

2.1.2.3. Synthesis of binary zinc(II) complexes 1-3.

[$Zn(L1)_2(CH_3OH)_2$] (Complex 1)

The complex was synthesized by the following method. The metal salt zinc acetate dihydrate ($Zn(CH_3COO)_2$•$2H_2O$) (0.219 g, 0.001 mol) was dissolved in methanol and the solution was added to a methanolic solution of the ligand (L1) (0.625 g, 0.002 mol). After complete addition, the mixture was refluxed about for 3 hours. The reaction mixture was then filtered and was washed with MeOH and hot water and dried in air. It was recrystallized from $CHCl_3$+MeOH at low temperature. M.P. >200 ºC, Yield 78 %, M.F.: $C_{36}H_{32}Cl_2N_4O_6Zn$ (F.W.: 752.95); IR (KBr, cm^{-1}): 3109 (co-ordinated CH_3-OH), 1613 (C=O, *p*-chloro benzoyl group), 1494 (C=N cyclic), 1457 (C-O, pyrazolone ring), 505 (Zn-O); ^{1}H NMR (DMSO-d6) *δ ppm* 1.6 (s, 3H pyrazolone CH_3-), 7.53-7.42 (dd, 4H, *p*-chloro benzoyl), 7.9-7.1(Ar-H, phenyl of pyrazolone).[30]

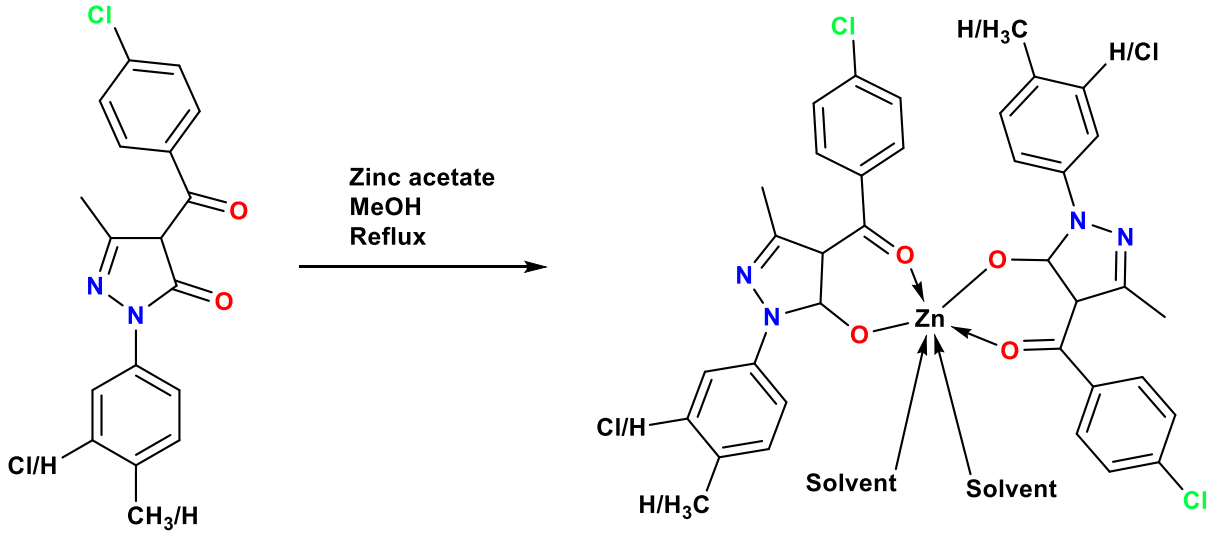

Scheme 2.1.2. Synthesis route of binary zinc (II) complexes **1-3** of 4-acyl pyrazolone. (In the complex **1** coordinated solvent is Methanol, in complex **2** and **3** coordinated solvents are water.)

[Zn(L2)$_2$(H$_2$O)$_2$] (Complex 2)

The complex **2** was synthesised by the previous method which is used for complex **1**. M.P. >200 ºC, Yield 81 %, M.F.: $C_{34}H_{26}Cl_4N_4O_6Zn$ (F.W.: 793.78); IR (KBr, cm^{-1}): 3109 (co-ordinated CH_3-OH), 1612 (C=O *p*-chloro benzoyl group), 1474 (C=N cyclic), 1439 (C-O, pyrazolone ring), 512 (Zn-O); ^{1}H NMR (DMSO-d6) δppm 1.6 (s, 3H pyrazolone CH_3-), 7.42-7.52 (dd, 4H, *p*-chloro benzoyl), 7.1-8.1(Ar-H, phenyl of pyrazolone).[30]

[Zn(L3)$_2$(H$_2$O)$_2$] (Complex 3)

The metal salt zinc acetate ($Zn(CH_3COO)_2$•$2H_2O$) (0.219 g, 0.001 mol) was dissolved in methanol and the solution was added to a cool methanolic solution of the ligand (L3) (0.654 g, 0.002 mol). After complete addition, the mixture was refluxed about for 3 h. The resulting light yellow coloured crystalline compound was collected by filtration. After filtration and the washed product dried in air. Product was recrystallized from DMF at room temperature. M.P.: >200ºC, Yield: 81 %, M.F.: $C_{38}H_{36}Cl_2N_4O_6Zn$ (F. W.: 781.01); IR (KBr, cm-1): 3037 (co-ordinated H_2O), 1598 (C=O *p*-chloro benzoyl group), 1514 (C=N cyclic), 1479 (C-O,

pyrazolone ring), 511 (Zn-O); low solubility in DMSO-d6, ^{1}H NMR (DMSO-d6):δ ppm 1.64 (s,3H, CH_3-pyrazolone), 2.27(s, 3H, CH_3-Ar), 7.5-7.9 (d,4H, *p*-chloro benzoyl), 7.11-7.81(Ar-H, pyrazolone and *p*-chloro benzoyl). Synthesis of complexes **1-3** are summarized in scheme 2.1.2.

2.1.2.4. Single crystal X-ray structure determination

X-ray intensity data of the complexes were collected at room temperature on Bruker CCD area detector diffractometer equipped with graphite mono-chromated MoKα radiation (α = 0.71073 Å). The crystals used for data collection was of suitable dimensions 0.30×0.20×0.20 mm^3 for complex **1-3.** The unit cell parameters were determined by least-squares refinement. Data were corrected for Lorentz, polarization and multi-scan absorption correction. The structures were solved by direct methods using SHELXS97.[41] All non-hydrogen atoms of the molecules were located in the best E-map. Full-matrix least-squares refinement was carried out using SHELXL97[42] ORTEP view diagrams of L2, L3, complex 1 and complex 3 are given in Fig. 2.1.8, 2.1.11, 2.1.14 and 2.1.18, respectively. The geometry of the molecules has been calculated using the software PLATON[43] and PARST[44]. The crystallographic data for the complexes are summarized in Table 2.1.1 and Table 2.1.3. The important bond lengths and bond angles of the complexes are listed in Table 2.1.2, and Table 2.1.4-2.1.7.

2.1.3. Results and Discussion

In this chapter, three zinc complexes have been prepared by following the scheme 2.1.3 described below;

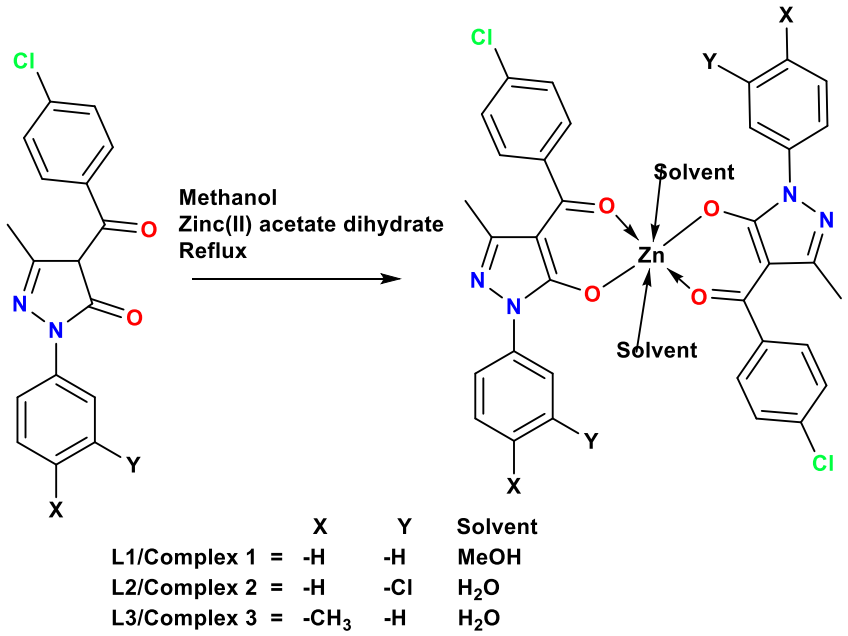

	X	Y	Solvent
L1/Complex 1 =	-H	-H	MeOH
L2/Complex 2 =	-H	-Cl	H_2O
L3/Complex 3 =	$-CH_3$	-H	H_2O

Scheme 2.1.3. Synthesis route of complexes **1-3.**

All these complexes are yellowish solid, stable at room temperature and soluble in DMF and DMSO.

The detailed characterization of these complexes is described in succeeding sections.

2.1.3.1. Crystallographic data of ligands and complexes

(i) Crystal feature of ligand L2.

Ligand **L2** atom numbering scheme presented in Fig. 2.1.8. As shown in the diagram, the C8-O1 (1.243 Å) and C11-O2 bonds (1.222 Å) are near to typical C-O double bonds[45,46] The bond length of C7-C8 is 1.427 Å, near to typical C-C single bonds and the bond length of C8-C9 is 1.390 Å near to C-C double bonds. Furthermore the C7- N1 bond (1.310 Å) is longer than a C-N double bond and since an H atom is attached to N reveals that the ligand is present in the NH amino diketone[45,46]. Selected bond lengths and bond angles for the ligand are given in Table 2.1.2.

Table 2.1.1. Crystal data and structure refinement for **L2** and **L3**.

Code	**L2**	**L3**
Empirical formula	$C_{17}H_{12}Cl_2N_2O_2$	$C_{36}H_{30}Cl_2N_4O_4$
Formula weight	347.20	653.54
Temperature/K	293.0	293
Crystal system	Monoclinic	Triclinic
Space group	$P2_1/c$	P-1
a/Å	15.1886(17)	7.9800(6)
b/Å	9.6726(7)	11.6196(6)
c/Å	11.8403(12)	18.0179(9)
α/°	90	84.835(4)
β/°	112.599(13)	78.544(5)
γ/°	90	72.202(6)
Volume/$Å^3$	1605.9(3)	1558.28(17)
Z	4	2
$\rho_{calc}g/cm^3$	1.4359	1.393
μ/mm^{-1}	0.414	0.256
Crystal size/mm^3	0.3 × 0.2 × 0.2	0.2 × 0.2 × 0.1
Radiation	Mo Kα (λ = 0.71073)	MoKα (λ = 0.71073)
2Θ range for data collection/°	6.88 to 57.74	5.996 to 58.014
Index ranges	$-17 \leq h \leq 20$, $-5 \leq k \leq 13$, $-16 \leq l \leq 8$	$-10 \leq h \leq 10$, $-15 \leq k \leq 15$, $-24 \leq l \leq 24$
Reflections collected	5321	33561
Independent reflections	3299 [R_{int} = *0.0211*, R_{sigma} *=0.0350*]	7546 [R_{int} = *0.0433*, R_{sigma} = *0.0477*]
Data/restraints/parameters	3299/0/209	7546/0/420
Goodness-of-fit on F^2	1.053	1.319
Final R indexes [I>=2σ (I)]	*R_1 = 0.0546, wR_2 = 0.1320*	*R_1 = 0.0729, wR_2 = 0.2059*
Final R indexes [all data]	*R_1 = 0.0880, wR_2 = 0.1481*	*R_1 = 0.1227, wR_2 = 0.2383*
Largest diff. peak/hole / e $Å^{-3}$	0.59/-0.73	1.29/-0.76
CCDC	1985007	1985008

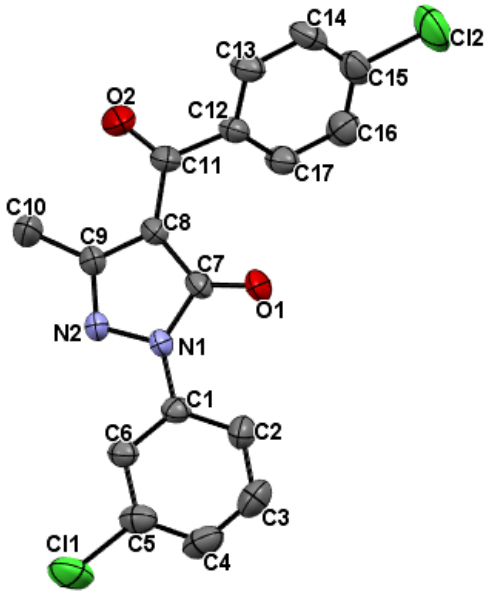

Fig. 2.1.8. ORTEP diagram with ellipsoid 50% probability of ligand L2. H-atoms are omitted for clear structure view.

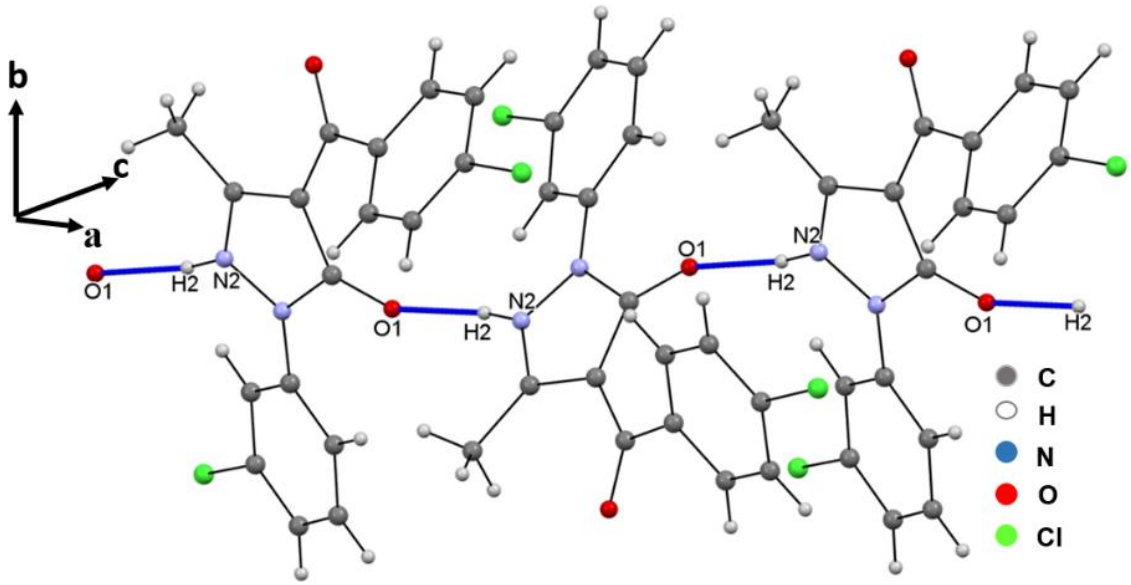

Fig. 2.1.9. Intermolecular H-bond in **L2**. Blueline indicating H-bond between N2-H2…O1.

There is intermolecular hydrogen bonding between the –NH group of one molecule and the carbonyl (C=O) group of the pyrazolone ring of a second molecule of the ligand. The parameters (D-H···A) are as follows: N2-H2 (0.860 Å), H2···O1 (1.790 Å) and N2-O1 (2.631 Å), N2-H2-O1 (165.51^0). The stability of the NH amino diketone form may be due to the

presence of intermolecular hydrogen bonding. Furthermore, in the crystal packing system, molecules arrangement design appear brick wall motif from the 'b' axis (Fig. 2.1.10). O1-C7 (1.243 Å) and O2-C11 (1.222 Å) bond length indicating double bond. C9-N2 (1.314 A) and N2-N1 (1.366 A) both values are very similar to values of a single bond.[47]

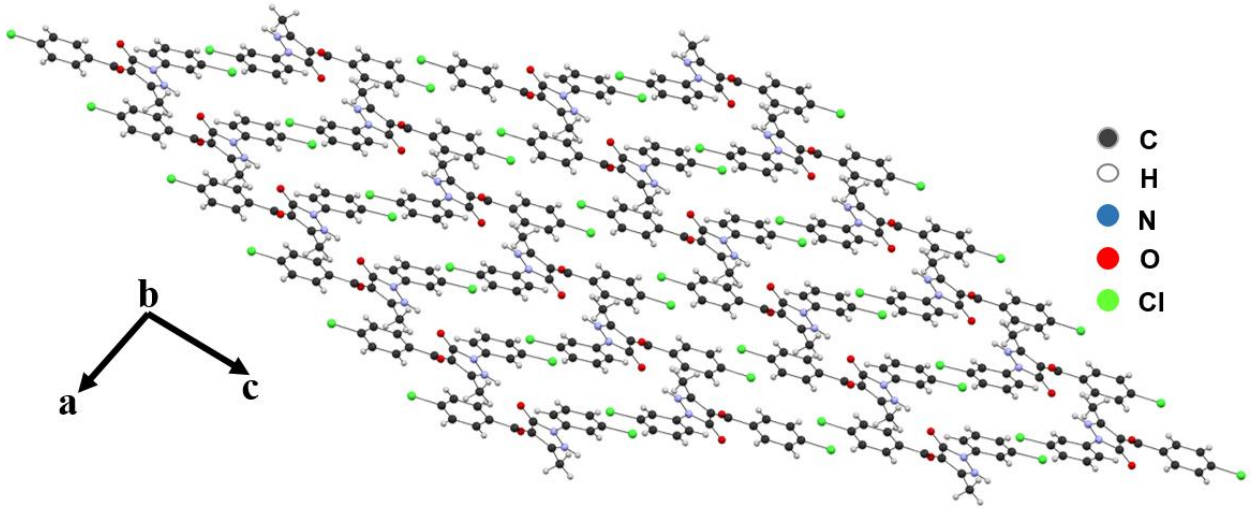

Fig. 2.1.10. Crystal packing system down from the 'b' Axis. Brick wall motif in the crystal packing.

(ii) Crystal features of ligand L3

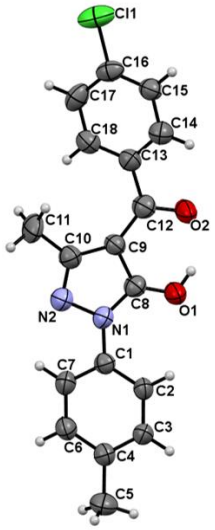

Fig. 2.1.11. ORTEP ellipsoid with 50% probability diagram of L3.

In the ligand L3 crystal data, found two molecules of L3 in the same plane. Selected bond length and bond angles are represented in Table 2.1.3. There is an intramolecular hydrogen bonding between the –OH group of the molecule and the carbonyl (C=O) group of the same ligand. The parameters (D-H··· A) are as follows: O1-H1 (0.820 Å), H1···O2 (1.811 Å) and O1-O2 (2.501 Å), and the angle O1-H1···O2 (140.84^0).

Table 2.1.2. Bond lengths for L2.

Bond length for L2

Atom	Length/Å	Atom	Length/Å
Cl1-C5	1.745(3)	C12-C17	1.379(4)
Cl2-C15	1.743(3)	C12-C13	1.382(4)
C15-C16	1.370(4)	C12-C11	1.495(4)
C15-C14	1.365(5)	O2-C11	1.224(4)
C5-C6	1.377(4)	O1-C7	1.245(3)
C5-C4	1.374(4)	C13-C14	1.394(4)
C9-C10	1.480(4)	C2-C3	1.381(4)
C9-C8	1.396(4)	C8-C11	1.459(4)
C9-N2	1.330(3)	C8-C7	1.436(4)
C6-C1	1.387(4)	C4-C3	1.381(4)
C16-C17	1.386(4)	C7-N1	1.396(3)
C1-C2	1.384(4)	N1-N2	1.384(3)
C1-N1	1.416(3)		

Bond Angles for L2.

Atom	Angle/°	Atom	Angle/°
C16-C15-Cl2	118.6(3)	C12-C13-C14	120.0(3)
C14-C15-Cl2	119.5(3)	C3-C2-C1	119.3(3)
C14-C15-C16	121.9(3)	C9-C8-C11	123.4(3)
C6-C5-Cl1	118.1(2)	C9-C8-C7	106.6(2)
C4-C5-Cl1	119.8(2)	C7-C8-C11	129.8(2)
C4-C5-C6	122.1(3)	C15-C14-C13	119.4(3)
C8-C9-C10	131.2(3)	C5-C4-C3	118.4(3)
N2-C9-C10	119.1(2)	C2-C3-C4	121.1(3)
N2-C9-C8	109.8(2)	O2-C11-C12	118.2(3)
C5-C6-C1	118.6(3)	O2-C11-C8	120.2(3)
C15-C16-C17	118.2(3)	C8-C11-C12	121.5(3)
C6-C1-N1	118.6(2)	O1-C7-C8	132.9(3)
C2-C1-C6	120.5(3)	O1-C7-N1	121.4(3)
C2-C1-N1	120.9(2)	N1-C7-C8	105.7(2)
C17-C12-C13	119.0(3)	C7-N1-C1	130.9(2)
C17-C12-C11	117.7(3)	N2-N1-C1	119.71(19)
C13-C12-C11	123.2(3)	N2-N1-C7	108.7(2)
C12-C17-C16	121.5(3)	C9-N2-N1	109.2(2)

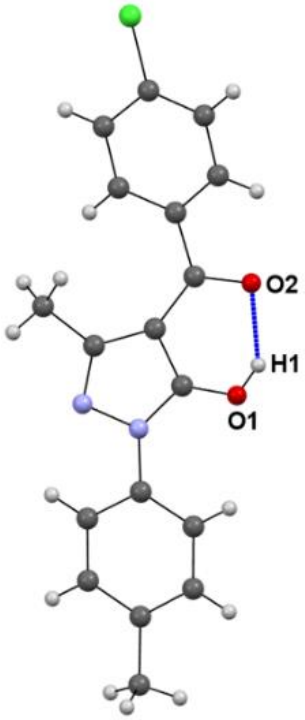

Fig. 2.1.12. Intramolecular H-bond in L3.

Table 2.1.3. Bond Lengths and Angles for L3.

The bond length of L3.

Atom	Length/Å	Atom	Length/Å
C18-C17	1.396(4)	C1-C2	1.374(4)
Cl1-C16	1.713(3)	C1-C7	1.384(4)
C6-C7	1.387(4)	C9-C8	1.437(4)
C15-C14	1.370(4)	C9-C10	1.409(4)
O1-C8	1.267(3)	C9-C12	1.416(4)
O2-C12	1.289(4)	C2-C3	1.387(4)
C13-C14	1.376(4)	C4-C3	1.378(4)
C13-C18	1.382(4)	C4-C6	1.382(4)
C10-C11	1.515(4)	C4-C5	1.505(4)
N2-C10	1.301(4)	C16-C15	1.359(4)
N1-N2	1.415(3)	C16-C17	1.405(5)
N1-C1	1.417(3)	C13-C12	1.489(4)

Bond angles for L3.			
Atom	**Angle/°**	**Atom**	**Angle/°**
N2-N1-C1	119.2(2)	C10-C9-C8	103.6(2)
C8-N1-N2	111.2(2)	C10-C9-C12	140.4(3)
C8-N1-C1	129.5(2)	C12-C9-C8	116.0(3)
C10-N2-N1	105.2(2)	O1-C8-N1	124.4(3)
C15-C16-Cl1	121.3(3)	O1-C8-C9	128.6(3)
C15-C16-C17	120.3(3)	N1-C8-C9	107.1(2)
C17-C16-Cl1	118.4(3)	N2-C10-C9	112.9(3)
C4-C3-C2	121.1(3)	N2-C10-C11	118.2(3)
C14-C13-C12	118.3(3)	C9-C10-C11	128.9(3)
C14-C13-C18	118.5(3)	C4-C6-C7	121.6(3)
C18-C13-C12	123.1(3)	C1-C7-C6	119.0(3)
C2-C1-N1	121.6(3)	C16-C15-C14	120.7(3)
C2-C1-C7	120.2(3)	O2-C12-C9	119.2(3)
C7-C1-N1	118.2(3)	O2-C12-C13	115.7(3)

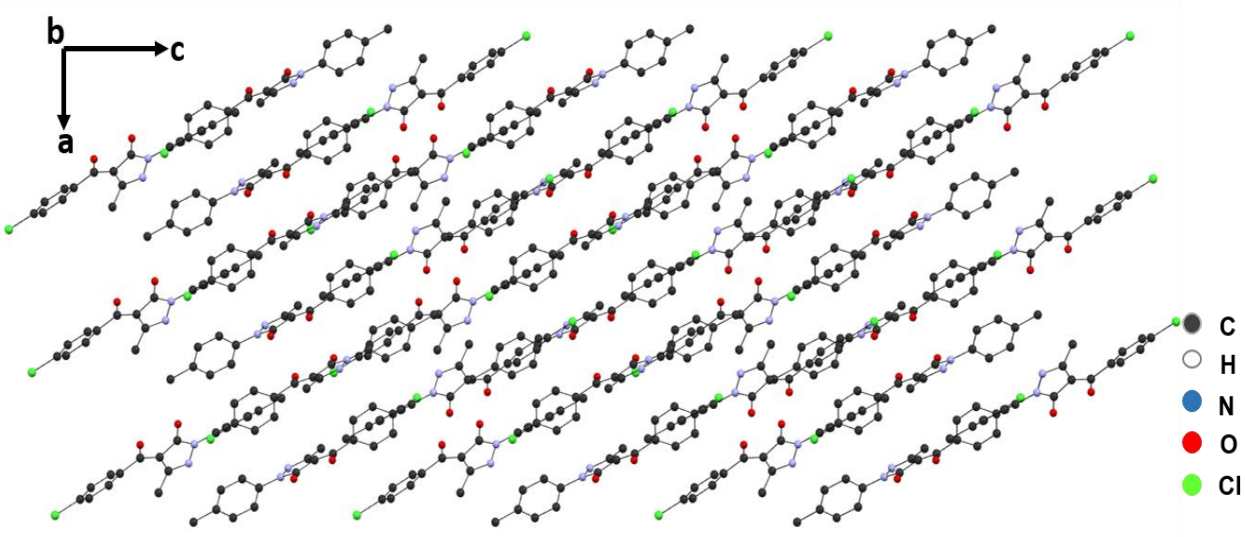

Fig. 2.1.13. Crystal packing down from the 'b' axis. Linear molecules arrangement in the crystal system.

(iii)Crystal features of complex 1 [$Zn(L1)_2(CH_3OH)_2$]

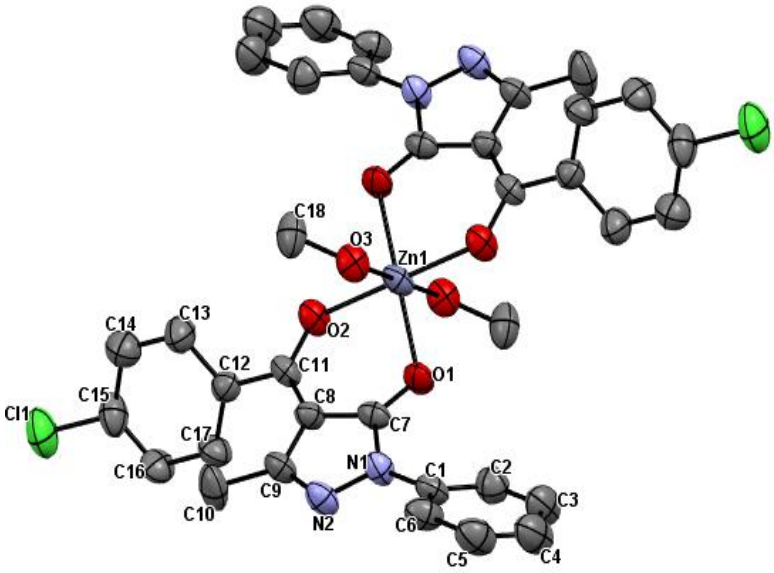

Fig. 2.1.14. ORTEP ellipsoid diagram with 50% probability of complex **1** [$Zn(L1)_2(CH_3OH)_2$]. H-Atoms are omitted for clarity.

The molecular structure and the atom labelling scheme of complex **1** is shown in Fig. 2.1.14. The main bond distances and angles are listed in Table 2.1.5. As shown in Fig. 2.1.14, the Zn(II) is hexa coordinated with four oxygen atoms of two acyl pyrazolone ligands and two oxygen atoms of methanol molecules. Two oxygen donors of both pyrazolone molecules occupy the basal sites of the octahedral structure, whereas the MeOH molecules bind the zinc at the apical site. In this complex, the incorporation of the solvent into the coordination sphere increases the coordination number to six and the geometry around the metal turns into a distorted octahedral. In the complex, the zinc atom occupies a distorted octahedral environment (OH), formed by four oxygen atoms [O(1), O(2), O(1)' and O(2)'] supplied by acyl pyrazolone ligands (Fig. 2.1.15). The fifth and sixth coordination sites are occupied by oxygen atoms of MeOH molecules. The Zn–O distances of the basal plan are Zn(1)- O(1)/O(1)'= 2.089(4) Å and Zn(1)-O(2)/O(2)'= 2.062(4) Å, whereas the axial distance of Zn(1)-O(3)/O(3)' is 2.122(5)Å. The axial metal-oxygen bond distances are longer than basal metal-oxygen bond distances. All atoms of the chelate and pyrazolone rings lie almost in the same plane.[30,32] The Zn(II) atom stays in the centre of the equatorial plane. In the equatorial plane the bond distance between Zn-O(1)/O(1)' and Zn-O2/O(2)' are almost similar. The axial positions are occupied by O(3) and O(3)' of MeOH molecules with the bond length of 2.122 Å.

Table 2.1.4. Crystal data and structure refinement for complex **1** and complex **3**.

Identification code	Complex 1	Complex 3
Empirical formula	$C_{18}H_{16}ClN_2O_3Zn_{0.5}$	$C_{21}H_{21}ClN_3O_3Zn_{0.5}$
Formula weight	376.46	431.54
Temperature/K	293(2)	298
Crystal system	Monoclinic	Triclinic
Space group	$P2_1/c$	P-1
a/Å	11.874(4)	6.9507(6)
b/Å	12.389(3)	10.8579(11)
c/Å	13.239(4)	13.4651(13)
α/°	90	81.567(8)
β/°	115.19(4)	84.854(8)
γ/°	90	89.164(8)
Volume/Å^3	1762.4(10)	1001.17(16)
Z	4	2
ρ_{calc}g/cm^3	1.419	1.432
μ/mm^{-1}	0.899	0.803
F(000)	776.0	448.0
Crystal size/mm^3	0.3× 0.2× 0.2	0.3 × 0.2 × 0.2
Radiation	MoKα (λ = 0.71073)	MoKα (λ = 0.71073)
2Θ range for data collection/°	6.802 to 57.852	6.392 to 58.462
Reflections collected	4467	21607
Independent reflections	3615 [R_{int} = *0.0405*, R_{sigma} = *0.1085*]	4836 *[R_{int} = 0.1736, R_{sigma} = 0.2054]*
Data/restraints/parameters	3615/3/228	4836/0/263
Goodness-of-fit on F^2	1.040	1.026
Final R indexes [I>=2σ (I)]	*R_1 = 0.0865, wR_2 = 0.1995*	*R_1 = 0.0808, wR_2 = 0.1247*
Final R indexes [all data]	*R_1 = 0.1372, wR_2 = 0.2640*	*R_1 = 0.2199, wR_2 = 0.1733*
Largest diff. peak/hole / e Å^{-3}	1.65/-1.28	0.39/-0.45
CCDC	1870326	1870328

The angles O(2)-Zn-O(2)', O(1)-Zn-O(1)' and O(3)-Zn-O(3)' are exactly 180.00°, which shows no deviation from the theoretical value, where angles O(2)-Zn-O(3) and O(2)-Zn-O(3)' are 88.99° and 91.01°, respectively, which reach around to 90°. Therefore, the given coordination geometry around the Zn(II) can be defined as octahedral geometry.[48,49]

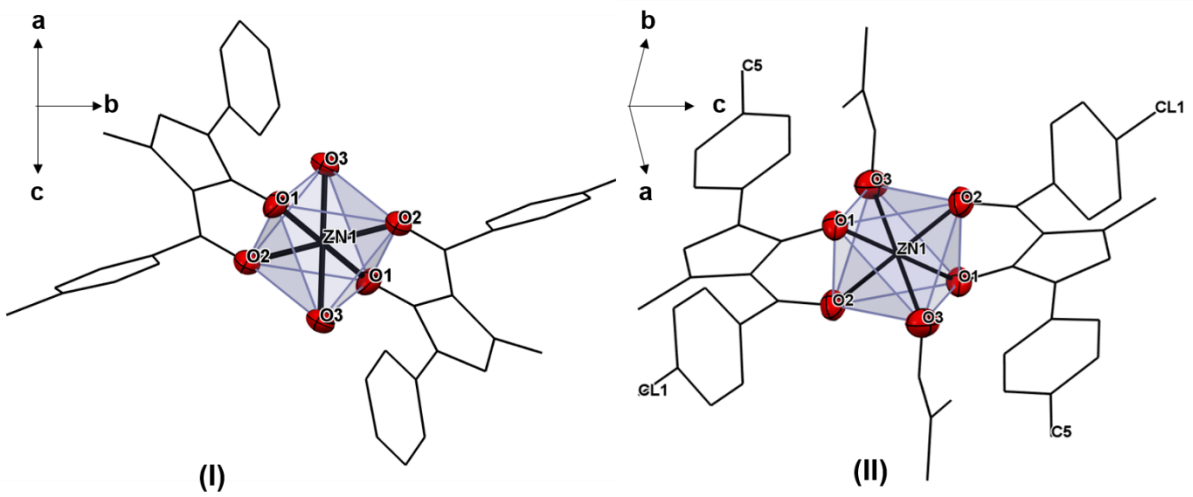

Fig. 2.1.15. The geometry of (I) complex **1** and (II) complex **3** by polyhedral-wireframe style in mercury.

In the crystal structure, the complex molecules are interconnected through intermolecular O3–H3…..N2 hydrogen bonds formed between O3 of the coordinated MeOH molecule and the N2 atom of the pyrazolone ring (Fig. 2.1.16). The packing arrangement of complex **1**, which viewed down the 'a' axis and the 'b' axis, are shown in Fig. 2.1.17.

Table 2.1.5. Bond lengths and angles for complex **1**.

Atom	Length/Å	Atom	Length/Å
Zn1-O1[1]	2.062(4)	C1-C2	1.406(8)
Zn1-O1	2.062(4)	C1-C6	1.381(8)
Zn1-O2	2.089(4)	C8-C7	1.441(8)
Zn1-O2[1]	2.089(4)	C8-C9	1.431(7)
Zn1-O3[1]	2.124(4)	C12-C13	1.390(8)
Zn1-O3	2.124(4)	C12-C17	1.383(8)
Cl1-C15	1.742(7)	C15-C16	1.365(10)
O1-C7	1.256(6)	C15-C14	1.382(10)
O2-C11	1.267(6)	C9-C10	1.503(8)
N1-N2	1.402(6)	C2-C3	1.364(8)
N1-C1	1.402(7)	C6-C5	1.372(9)
N1-C7	1.377(7)	C16-C17	1.403(8)
N2-C9	1.300(7)	C4-C5	1.363(10)

Angles for complex 1			
Atom	**Angle/°**	**Atom**	**Angle/°**
$O1^{1-}$Zn1-O1	180.0	C6-C1-N1	119.6(6)
O1-Zn1-$O2^{1}$	91.45(16)	C6-C1-C2	119.6(6)
$O1^{1-}$Zn1-$O2^{1}$	88.55(16)	C11-C8-C7	122.7(5)
O1-Zn1-O2	88.55(16)	C11-C8-C9	132.3(5)
$O1^{1-}$Zn1-O2	91.45(16)	C9-C8-C7	105.0(5)
O1-Zn1-$O3^{1}$	88.94(16)	O1-C7-N1	124.0(5)
$O1^{1-}$Zn1-$O3^{1}$	91.05(16)	O1-C7-C8	130.8(5)
$O1^{1-}$Zn1-O3	88.95(16)	N1-C7-C8	105.2(5)
O1-Zn1-O3	91.06(16)	C13-C12-C11	120.2(5)
O2-Zn1-$O2^{1}$	180.00(13)	C17-C12-C11	121.5(5)
O2-Zn1-$O3^{1}$	89.24(15)	C17-C12-C13	118.3(6)
O2-Zn1-O3	90.75(15)	C16-C15-Cl1	118.9(6)
$O2^{1-}$Zn1-$O3^{1}$	90.76(15)	C16-C15-C14	121.3(6)
$O2^{1-}$Zn1-O3	89.25(15)	C14-C15-Cl1	119.8(5)
$O3^{1-}$Zn1-O3	180.0	N2-C9-C8	111.6(5)

Symmetry code: ^{1}1-X,-Y,1-Z,

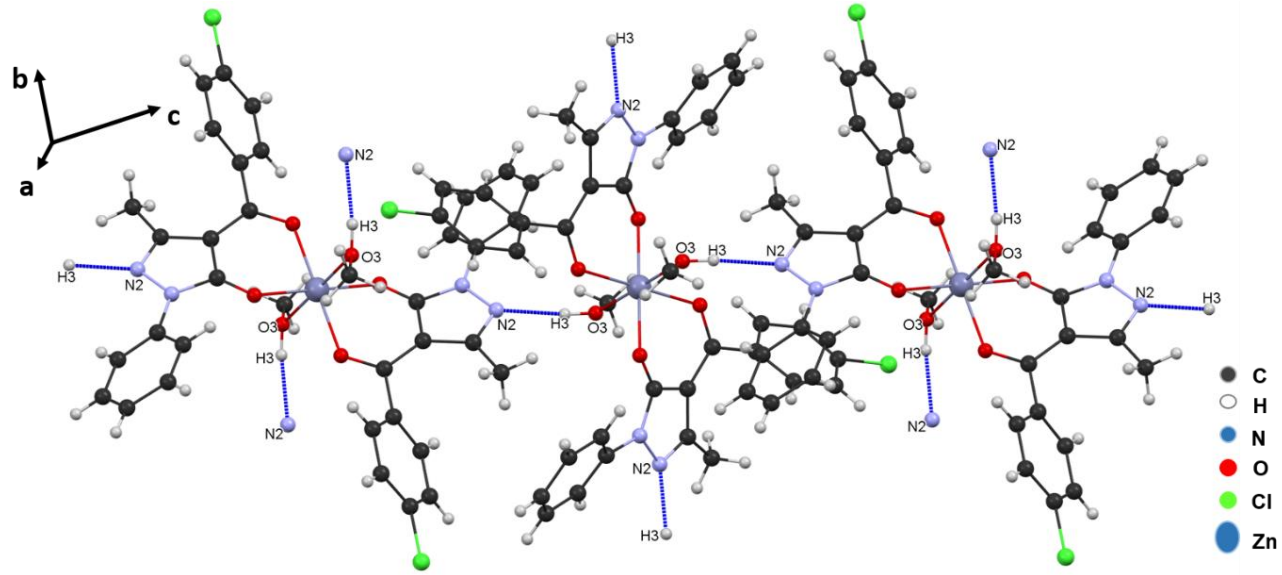

Fig. 2.1.16. Intermolecular H-bond in complex **1.**

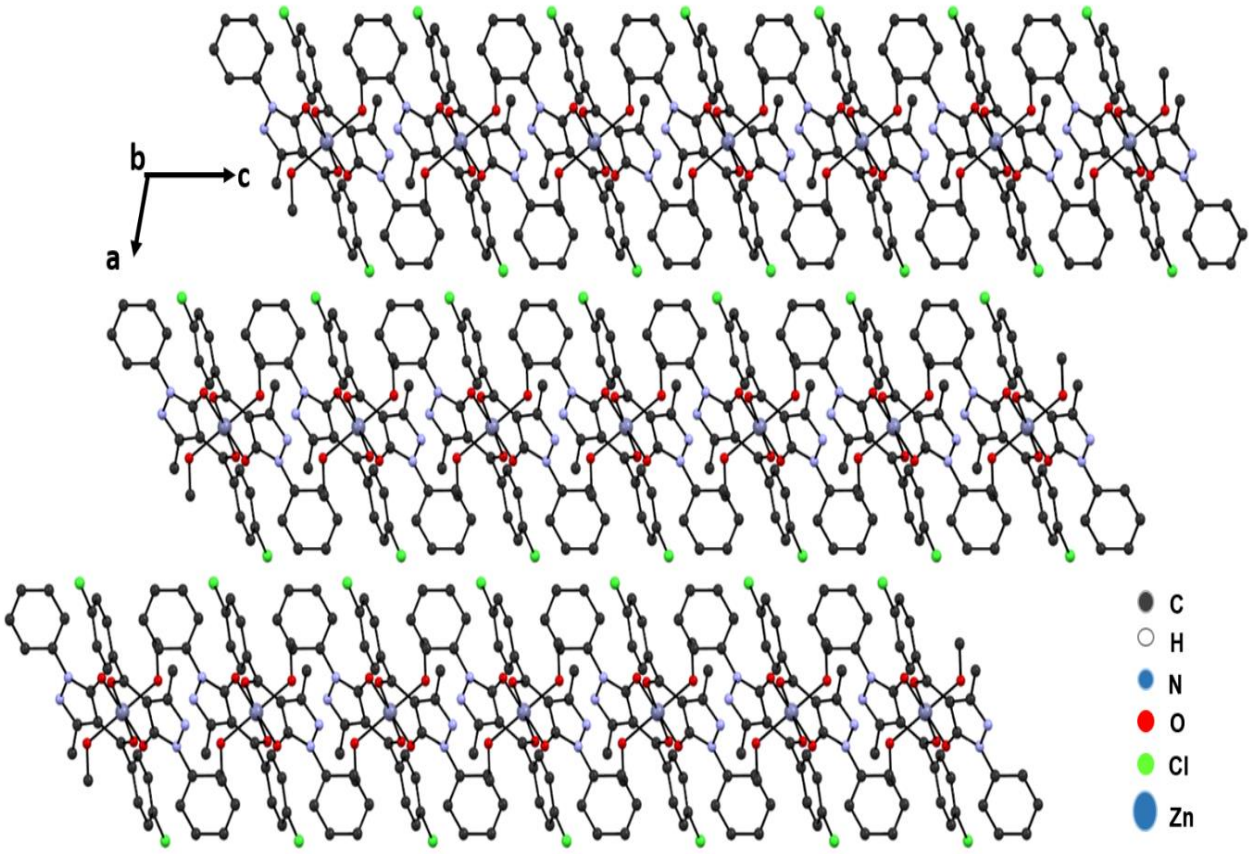

Fig. 2.1.17. Linear layer wise arrangement in complex **1** packing down from the 'b' axis.

Table 2.1.6. Intermolecular O3–H3····N2 hydrogen bonds formed between O3 of the coordinated MeOH molecule and the N2 atom of the pyrazolone ring.

D-H···A	**O3-H3···N2**
D-H	0.890 Å
H…A	2.043 Å
D-A	2.815 Å
∠D-H-A	156.98°
Symmetry code:[1]1-X,-Y,1-Z,	

(ii) Crystal features of Complex 3 [Zn(L3)$_2$(DMF)$_2$]

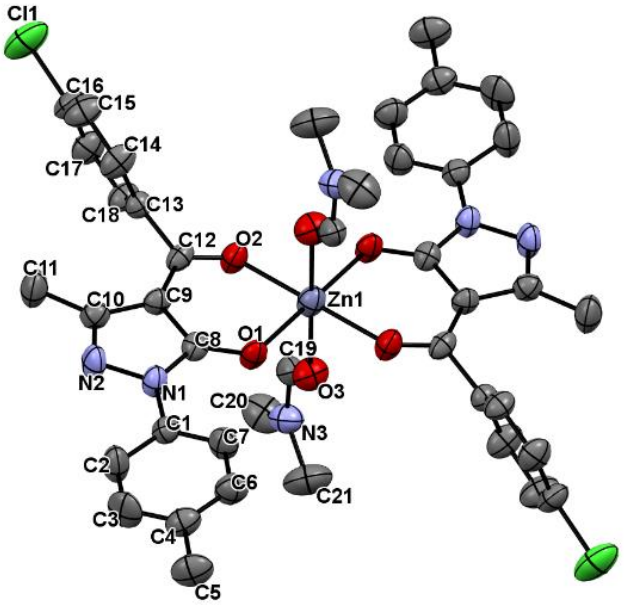

Fig. 2.1.18. ORTEP diagram with ellipsoid 50% probability of complex **3**.

The molecular structure and the atom labelling scheme of complex **3** is shown in Fig. 2.1.19. For crystallization, Complex **3** was dissolved in hot DMF and the filtrate kept for one and a half months for slow evaporation. As the water molecule has weak coordination ability than DMF, coordinated water molecules were replaced by DMF molecules during the crystallization of complex **3**. The main bond distances and angles are listed in Table 2.1.5. As shown in Fig. 2.1.18, the Zn(II) ion is Hexa coordinated by four oxygen atoms of two acyl pyrazolone ligands and two oxygen atoms of DMF molecules. Zn ion is located on a centre of inversion.[30]

The Zn–O distances of the basal plan are Zn(1)- O(1)/O(1)'= 2.092(5) Å and Zn(1)-O(2)/O(2)'= 2.088(05) Å, whereas the axial distance of Zn(1)-O(3) is 2.131(5)Å. Zn(II) situated in the center of the symmetry with no deviation from the equatorial plane. Oxygen atoms [O(1), O(1)', O(2) and O(2)'] of L3 consist of the equatorial plane with the no square plane deviation. Moreover, O(3) and O(3)' are occupied an axial position of octahedral geometry with distance 2.127 Å from the equatorial plane which is similar to bond length of Zn(1)-O(3). Therefore, the octahedral environment, formed by four oxygen atoms supplied by acyl pyrazolones. The fifth and sixth coordination axial sites are occupied by oxygen atoms of the DMF molecules.[30]

The angle O(1)-Zn(1)-O(1)', O(2)-Zn(1)-O(2)' and O(3)-Zn(1)-O(3)' are 180.0(3)º, 180.0(3)º and 180.0(4)º respectively, which are similar to the theoretical value of 180º. All these

observations implied that the geometry around the Zn(II) elongated distorted octahedron.[32,48–50] The crystallographic data of the complex is given in Table 2.1.4.[30]

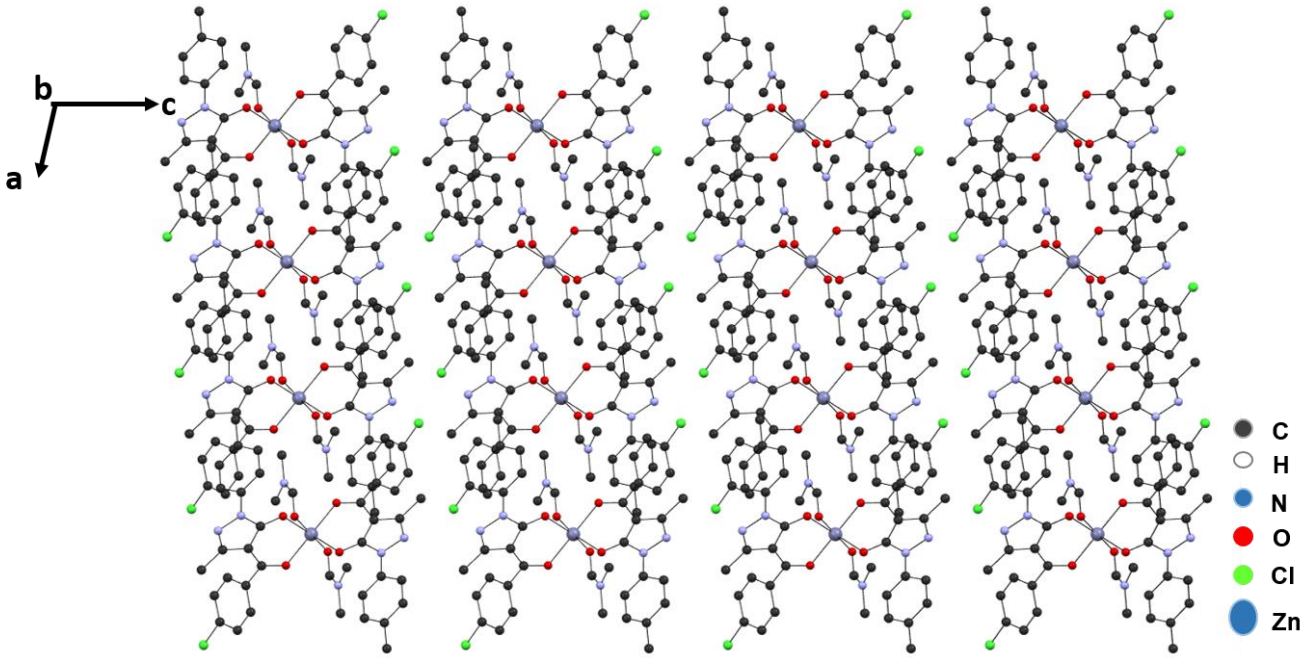

Fig. 2.1.19. Complex **3** crystal packing down from the 'b' axis.

Table 2.1.7. Bond Lengths and Bond Angles for complex **3**.

Bond lengths for complex 3

Atom	Length/Å	Atom	Length/Å
Zn1-O2	2.073(3)	N3-C20	1.450(6)
Zn1-O2^1	2.073(3)	C9-C10	1.424(7)
Zn1-O1^1	2.081(3)	C9-C8	1.422(6)
Zn1-O1	2.081(3)	C10-C11	1.488(6)
Zn1-O3	2.126(4)	C13-C18	1.384(6)
Zn1-O3^1	2.126(4)	C13-C14	1.368(6)
Cl1-C16	1.751(5)	C1-C7	1.354(6)
O2-C12	1.252(6)	C1-C2	1.382(7)
O1-C8	1.262(5)	C6-C7	1.387(6)
O3-C19	1.238(6)	C6-C4	1.347(7)
N2-N1	1.384(5)	C17-C18	1.368(6)
N2-C10	1.296(5)	C17-C16	1.357(7)

Bond Angles for complex 3.			
Atom	Angle/°	Atom	Angle/°
O2-Zn1-O2[1]	180.0	C12-C9-C8	123.9(5)
O2[1-]Zn1-O1	89.78(13)	C8-C9-C10	105.9(4)
O2-Zn1-O1	90.22(13)	N2-C10-C9	110.5(4)
O2[1-]Zn1-O1[1]	90.22(13)	N2-C10-C11	117.5(5)
O2-Zn1-O1[1]	89.78(13)	C9-C10-C11	131.8(5)
O2[1-]Zn1-O3	93.20(14)	C18-C13-C12	120.3(4)
O2-Zn1-O3	86.80(14)	C14-C13-C12	121.3(4)
O2-Zn1-O3[1]	93.20(14)	C14-C13-C18	118.3(4)
O2[1-]Zn1-O3[1]	86.80(14)	O1-C8-N1	123.6(4)
O1[1-]Zn1-O1	180.0	O1-C8-C9	131.3(5)
O1[1-]Zn1-O3[1]	90.68(13)	N1-C8-C9	105.0(4)
O1-Zn1-O3	90.68(13)	C7-C1-N1	123.0(5)
O1-Zn1-O3[1]	89.32(13)	C7-C1-C2	118.6(5)
O1[1-]Zn1-O3	89.32(13)	C2-C1-N1	118.4(5)
O3-Zn1-O3[1]	180.0	C4-C6-C7	121.8(6)
C8-N1-C1	130.7(4)	O3-C19-N3	123.9(5)
O2-C12-C9	124.1(4)	C6-C4-C3	117.6(5)

Symmetry code:[1]-X,1-Y,-Z

2.1.3.2. FTIR spectroscopy

In coordinating chemistry, the IR spectral studies provide valuable information about the coordination sites of the ligand and the compared with that of metal complexes and the peaks which have been changed due to complexation with metal ion is interpreted. A relative study of the IR spectra of ligands and its metal complexes discloses that convinced bands are common and therefore, only important bands, which have been either shifted or newly appeared, are discussed. In the spectra of the free ligands, bands at 1619 cm^{-1} and 1588cm^{-1} are attributed to *ν*(C=O)amide and *ν*(C=O)ketone respectively for L1, and the bands at 1625 cm^{-1} and 1590 cm^{-1} are attributed to *ν*(C=O)amide and *ν*(C=O)ketone respectively for L2 whereas 1625 cm^{-1} and 1590 cm^{-1} is attributed to *ν*(C=O)amide and *ν*(C=O)ketone respectively for L3. In the complexes *ν*(C=O) amide peak disappears and a new peak appears at the range of 1480-1450 cm^{-1} indicating the presence of *ν*(C-O) bond. The *ν*(C=O) ketone changes in the range of 1590-1588 to 1622-1598cm^{-1} in the complexes.[51–53] The IR spectra of the complexes indicate that before binding with a metal ion, the ligand has undergone deprotonation to convert into the

monoanionic form.[47,54–59] FTIR spectra of ligands exhibit the bands within the range 1550–1565cm^{-1} which can be assigned to ν(C=N)(cyclic). In complex **3** it shows the absorption bands within 3000–3150 cm^{-1} which can be assigned to the coordinated water molecules.[30] The complexes show bands around 515-480 cm^{-1} and 425-415 cm^{-1} which are due to the ν(Zn-O) and ν(Zn-N), respectively.[51,60] The IR spectral data are shown in Table 2.1.8. IR spectra of ligands and complexes are presented in Fig. 2.1.20 to Fig.2.1.25.

Table 2.1.8. Important frequencies of FTIR spectral data.

Compound code	Pyrazolone νC=O (cm^{-1})	*p*-chloro Benzoyl νC=O (cm^{-1})	Cyclic νC=N (cm^{-1})	Pyrazolone νC-O (cm^{-1})	νM-O (cm^{-1})
L1	1619	1587	1557	-	-
L2	1625	1590	1516	-	-
L3	1625	1598	1551	-	-
$[Zn(L1)_2(CH_3OH)_2]$ **1**	-	1613	1536	1457	505
$[Zn(L2)_2(H_2O)_2]$ **2**	-	1612	1588	1470	512
$[Zn(L3)_2(H_2O)_2]$ **3**	-	1598	1514	1479	511

FTIR Spectra:

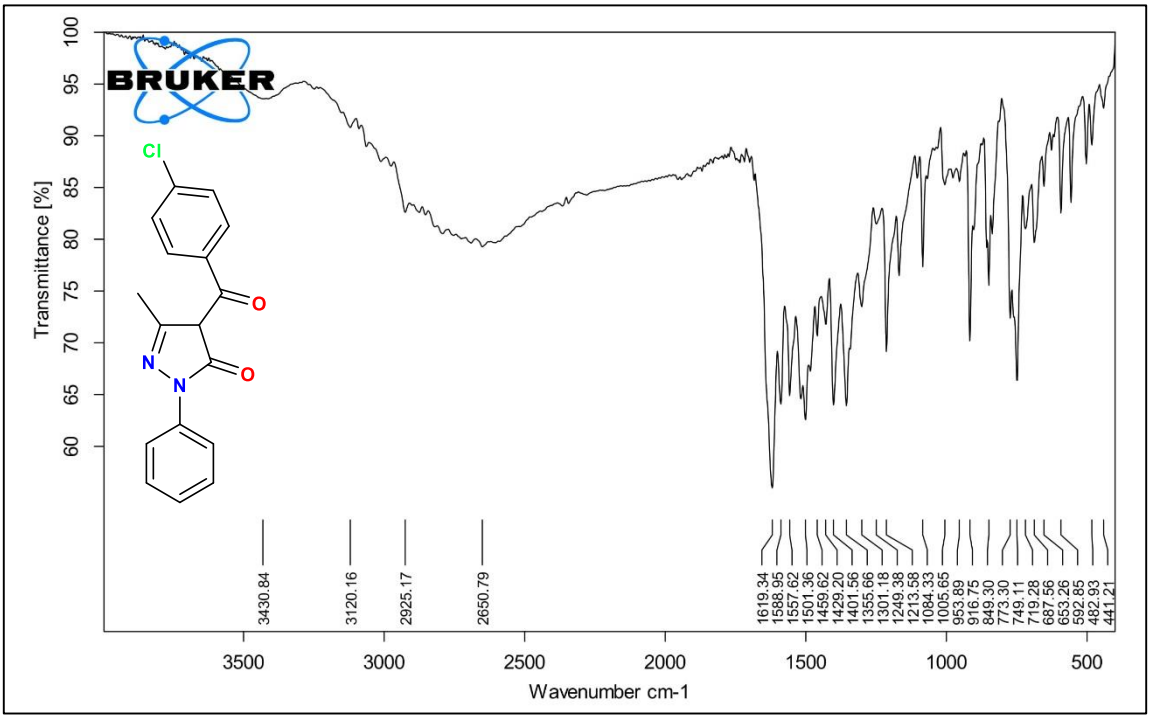

Fig. 2.1.20. FTIR spectrum of ligand L1.

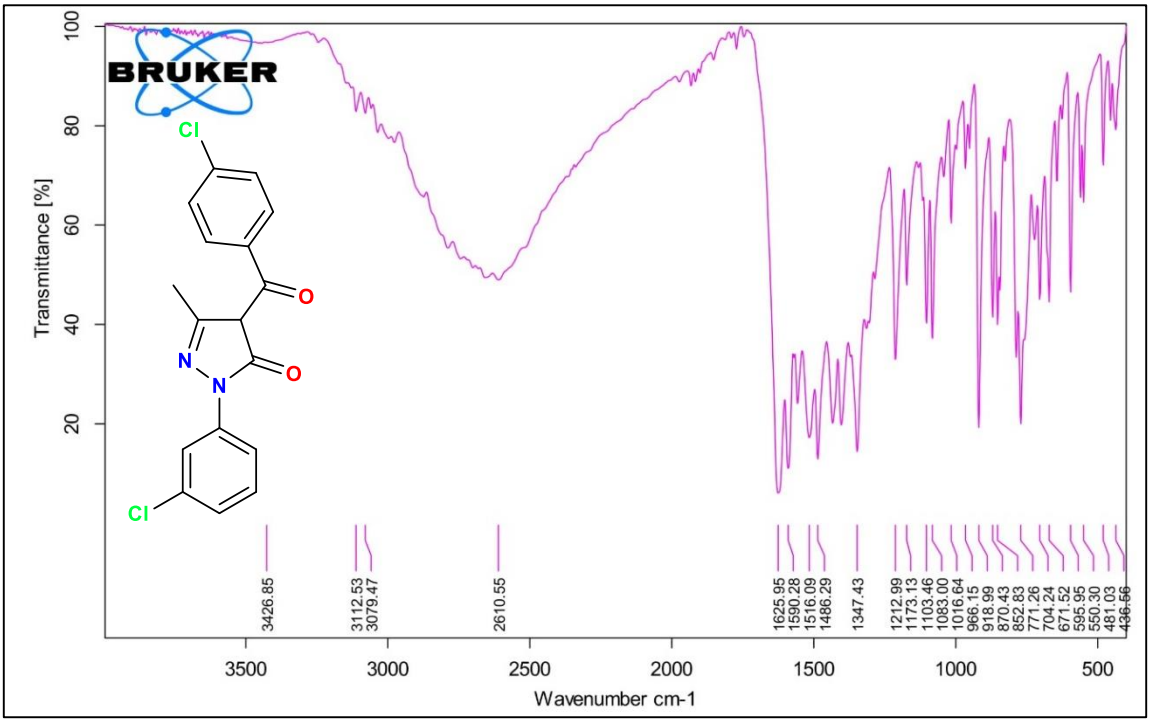

Fig. 2.1.21. FTIR spectrum of ligand L2.

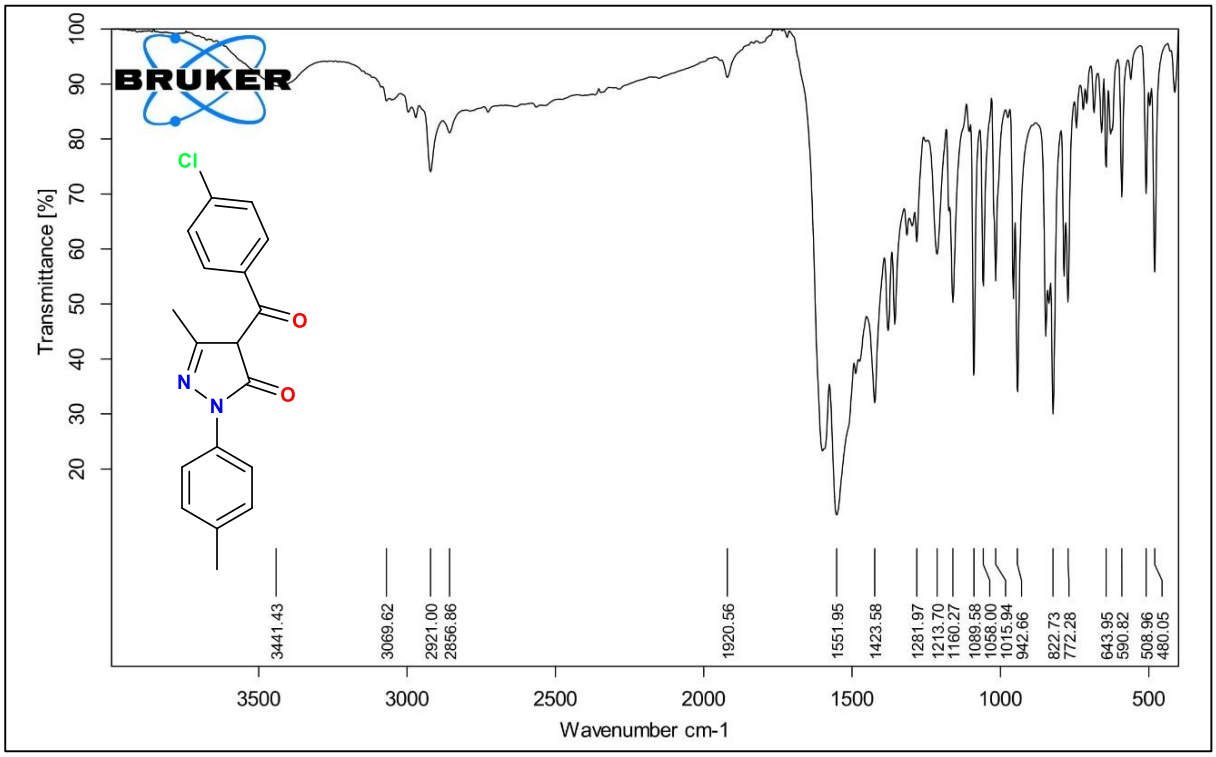

Fig. 2.1.22. FTIR spectrum of ligand L3.

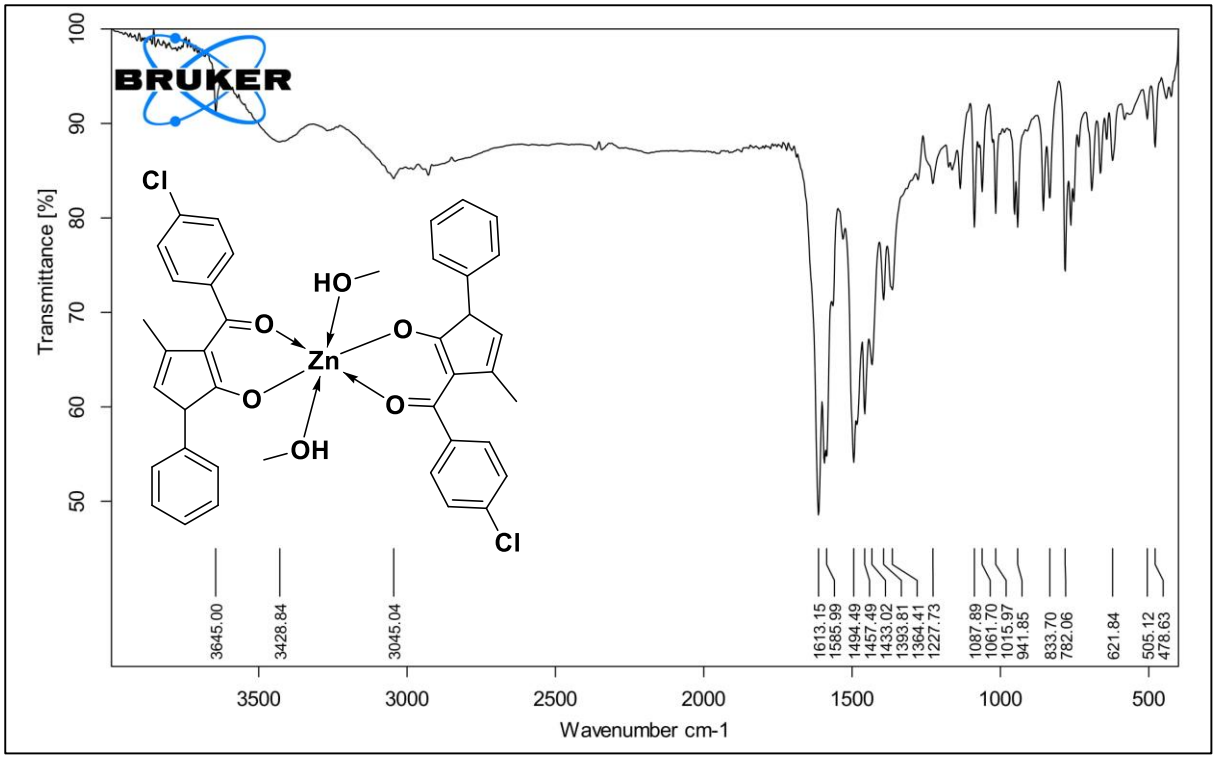

Fig. 2.1.23. FTIR spectrum of complex **1** $[Zn(L1)_2(MeOH)_2]$.

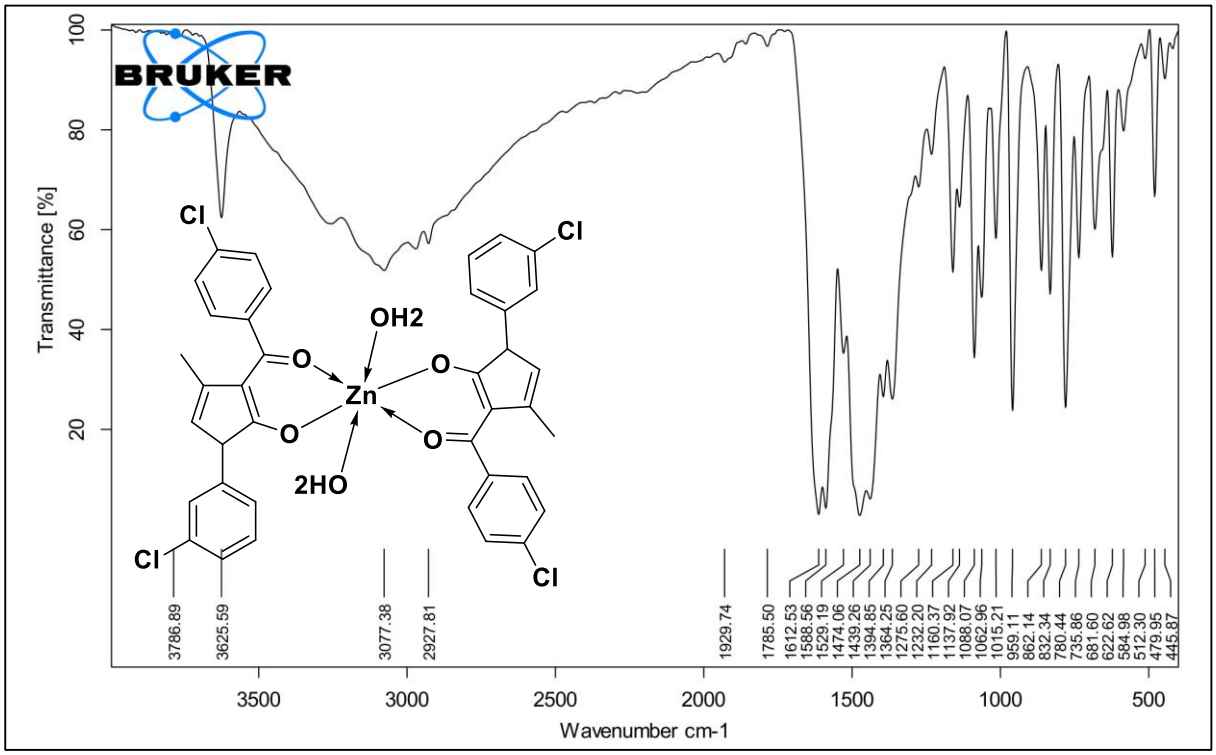

Fig. 2.1.24. FTIR spectrum of complex 2 $[Zn(L2)_2(H_2O)_2]$.

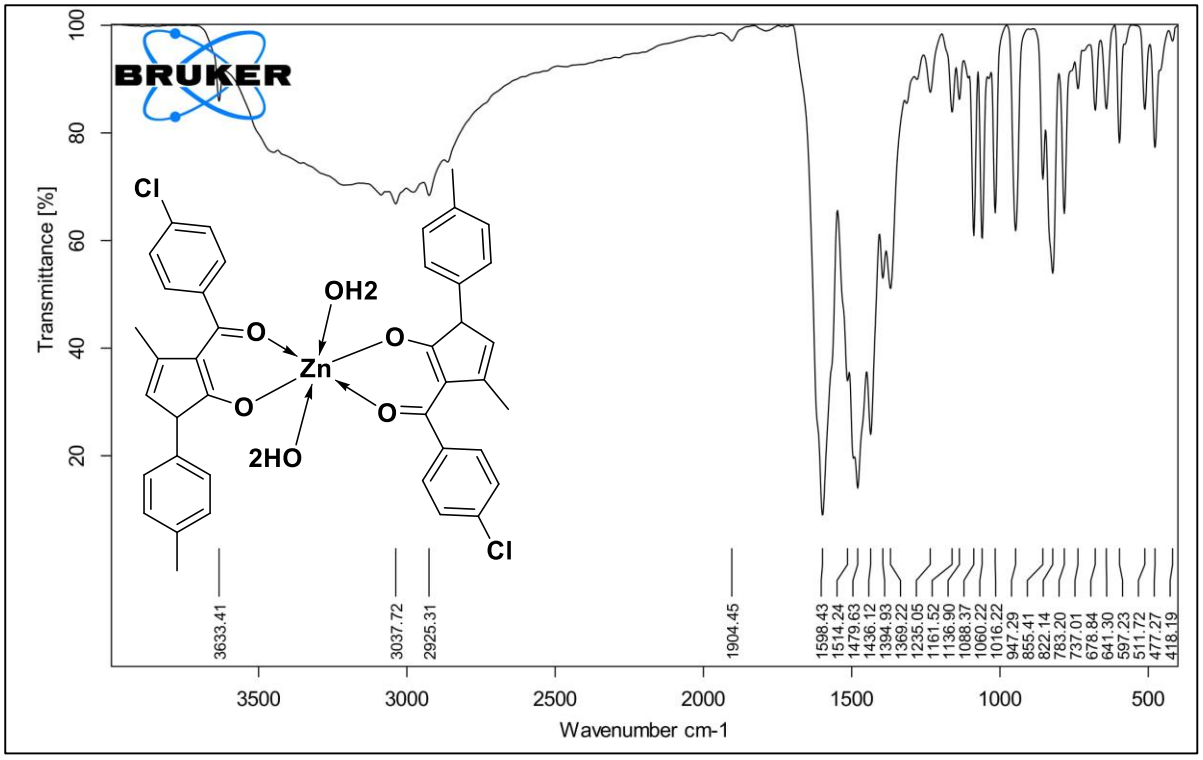

Fig. 2.1.25. FTIR spectrum of complex **3** $[Zn(L3)_2(H_2O)_2]$.

2.1.3.3. NMR spectral studies of ligands (L1, L2 and L3) and complexes 1-3.

The ^1H spectra of ligands L1, L2 and L3 were recorded in $CDCl_3$ at room temperature. The signals due to one methyl group have appeared as singlets at 2.14, 2.13 and 2.12 δ ppm for L1, L2 and L3 respectively. In the aromatic region between 7.25– 7.88 δ ppm, a few doublets and in few cases some overlapping doublets/multiplets are observed due to the aromatic protons. The ^1H NMR spectra of ligands are given in Fig.2.1.26 - 2.1.28. The ^1H NMR spectra of Zn(II) complexes **1-3,** ^1H NMR were recorded in DMSO-d6 at room temperature. ^1H NMR spectra of complexes show signals consistent with the proposed structure.[30] In the ^{13}C NMR spectra of the ligands, the carbon atoms of the methyl groups looked at 15.72, 16.01 and 15.90 δ ppm for L1, L2 and L3 respectively. The Methyl group of Tolyl pyrazolone of L3 appeared at 21.10 δ ppm. The all-carbon atoms of aromatic exhibit signals in the range 120.90–147.70 δ ppm for both ligands. Thirteen signals were observed for ligand L1 indicate the formation of structure. Some of the signals might be overlapped as indicated by the intensity of a few signals. All the carbon signals were found in their expected region.[30] The ^{13}C NMR spectra of ligands and ^1H NMR spectra of complexes are shown in Fig. 2.1.29 - 2.1.34.[30]

^{1}H NMR Spectra of ligands and complexes:

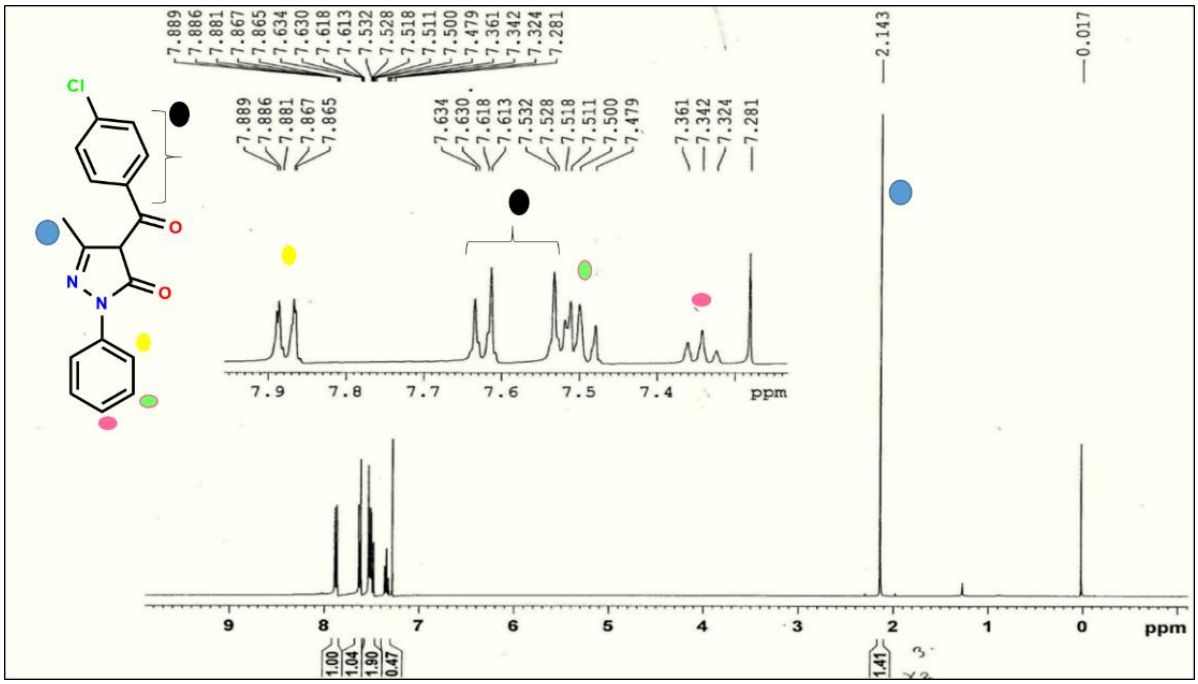

Fig. 2.1.26. ^{1}H NMR spectrum of ligand L1.

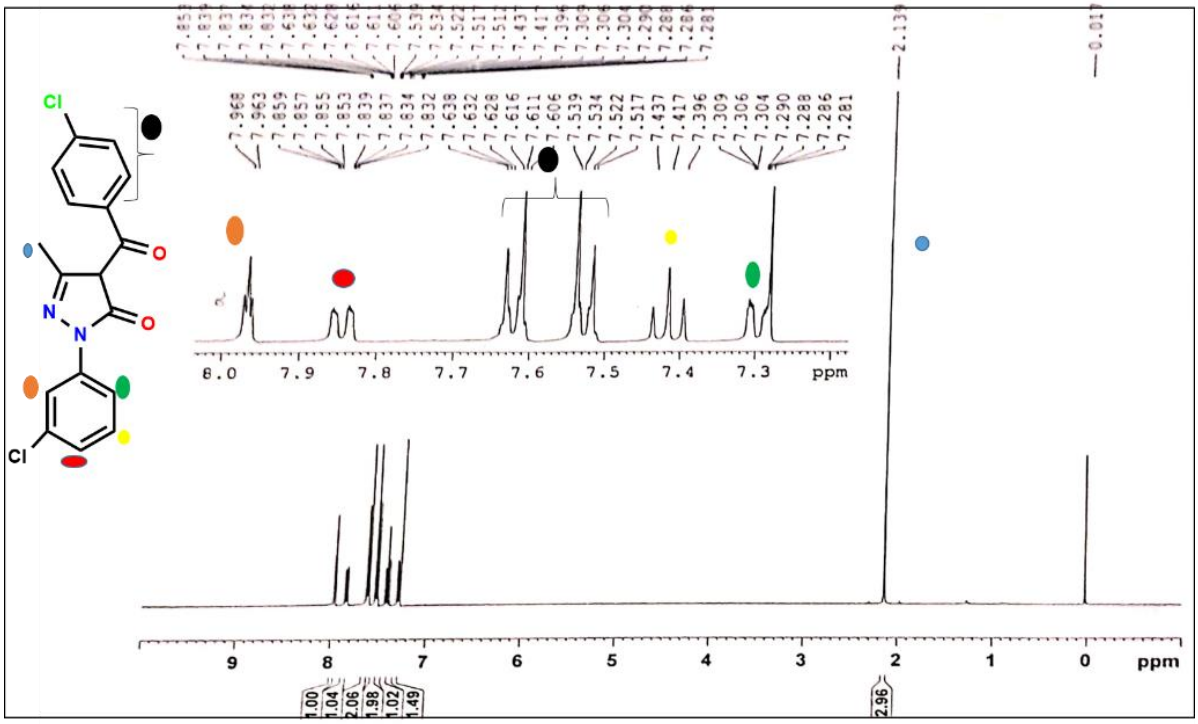

Fig. 2.1.27. ^{1}H NMR spectrum of ligand PCBMPMP.

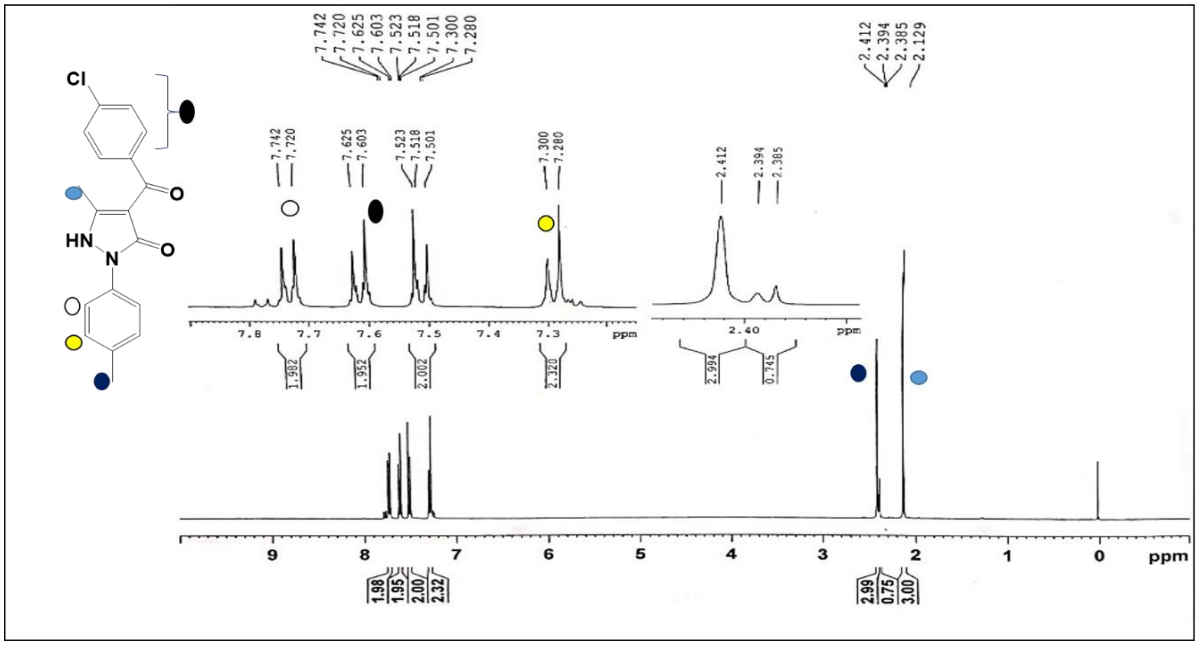

Fig. 2.1.28. ^{1}H NMR spectrum of L3.

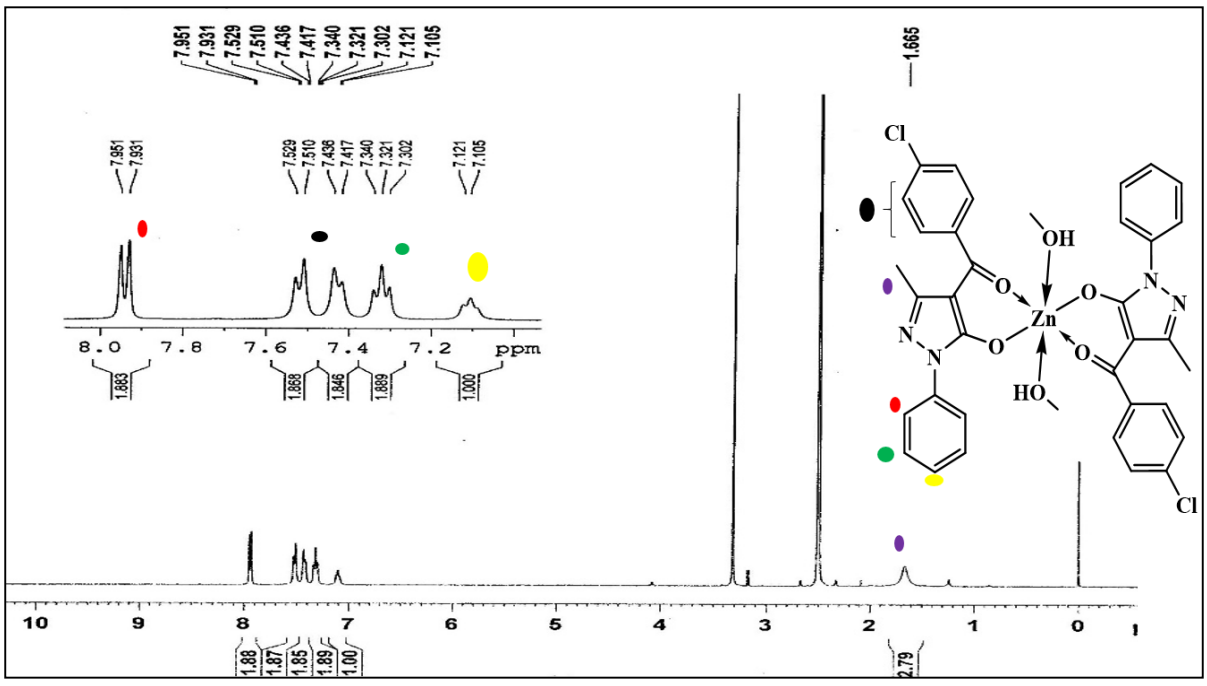

Fig. 2.1.29. ^{1}H NMR spectrum of complex **1** $[Zn(L1)_2(MeOH)_2]$.

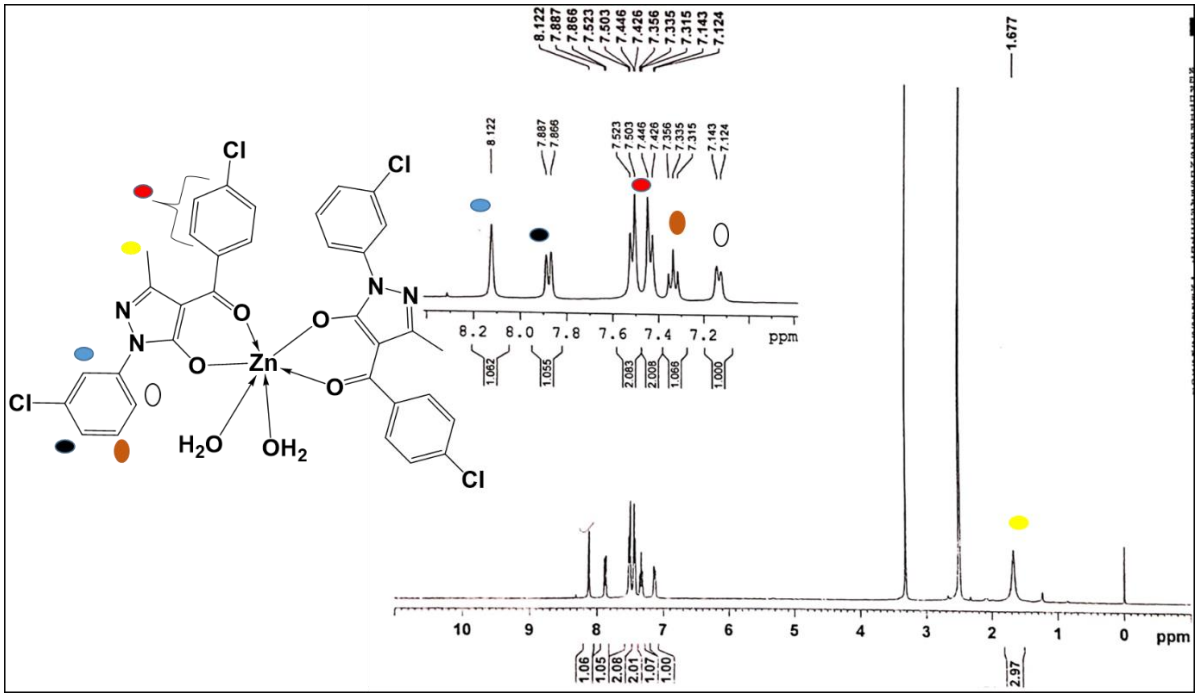

Fig. 2.1.30. ^{1}H NMR spectrum of Complex **2** $[Zn(L2)_2(H_2O)_2]$.

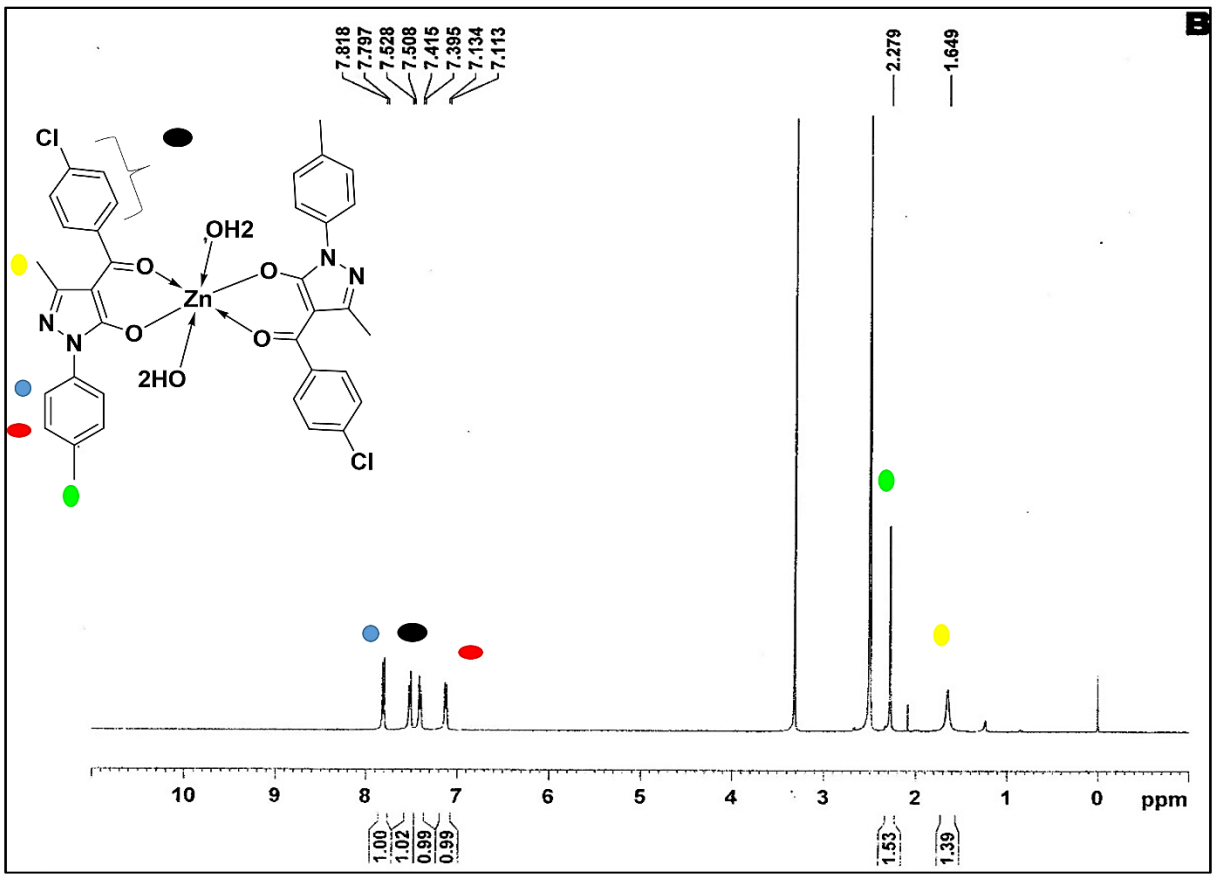

Fig. 2.1.31. ^{1}H NMR spectrum of Complex **3**.

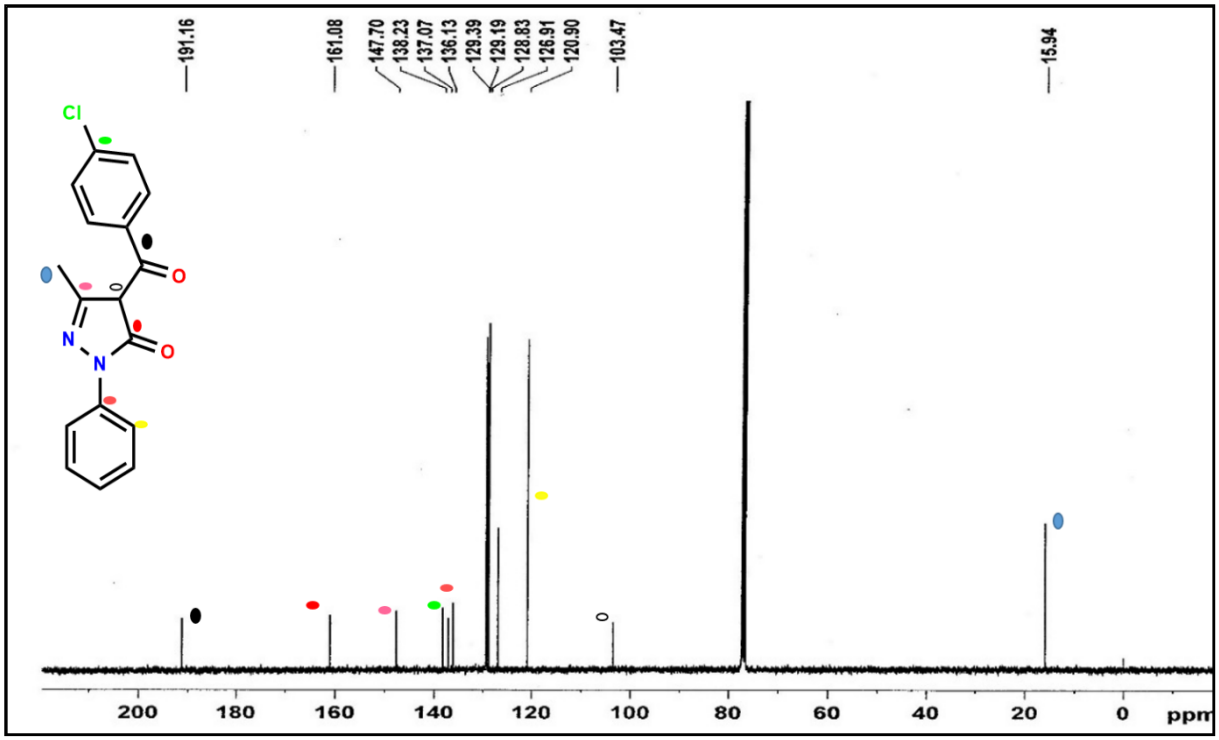

Fig. 2.1.32. ^{13}C NMR spectrum of ligand L1.

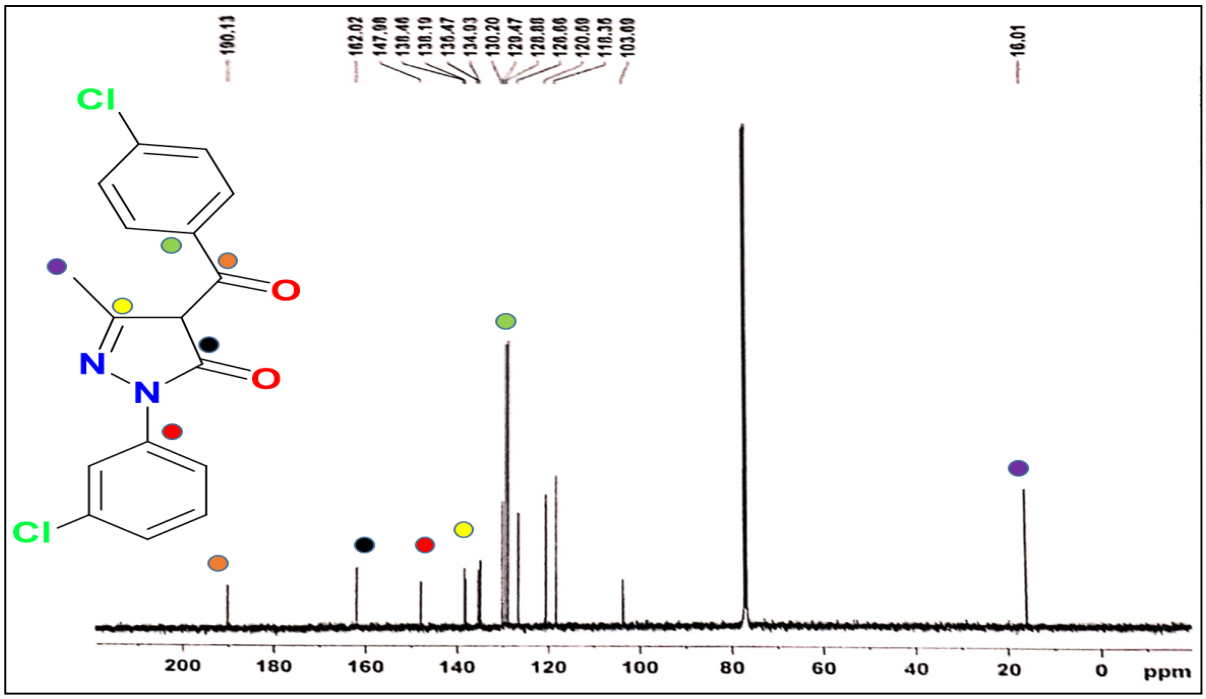

Fig. 2.1.33. ^{13} C NMR spectrum of L2.

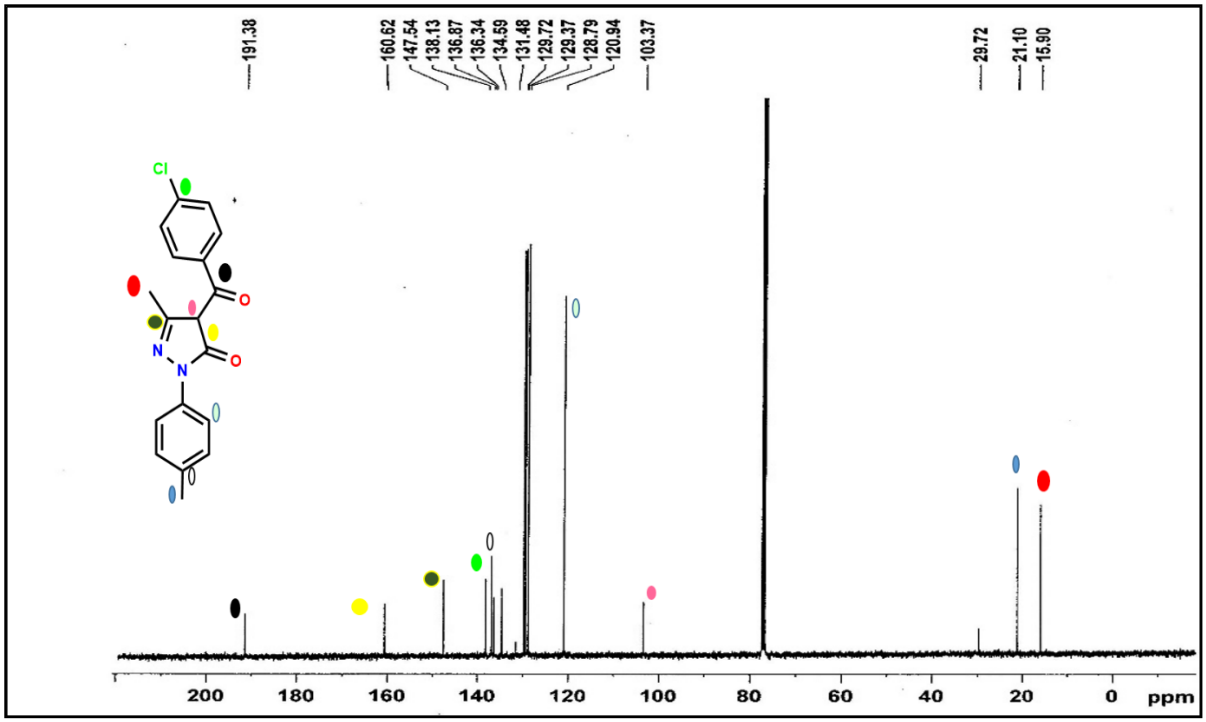

Fig. 2.1.34. ^{13}C NMR spectrum of ligand L3.

2.1.3.4. Thermogravimetric analysis

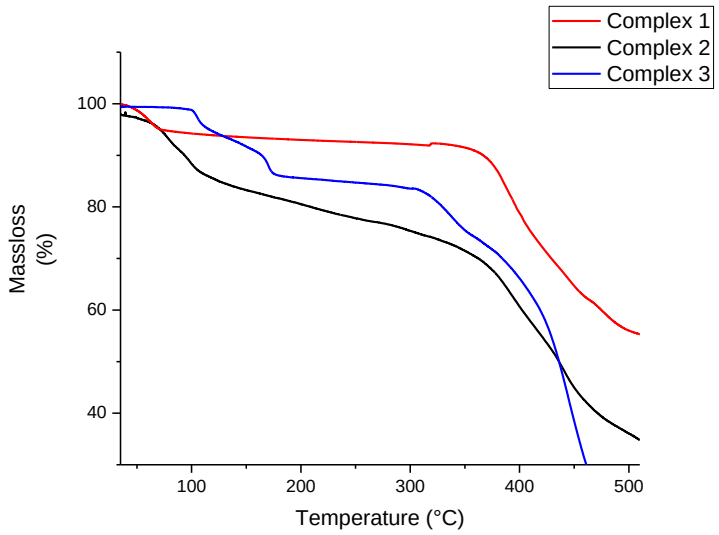

Fig. 2.1.35. TGA graph of **complexes 1-3.**

Binary complexes show the first degradation at up to 100 °C due to the coordinated solvent molecules in the complexes. The second degradation starts after 360 due to pyrolysis of acyl pyrazolone in all complexes (Fig. 2.1.35). Complex **2** and **3** contain water molecule in complex and complex **1** having coordinated MeOH molecule in the complex.[30]

2.1.3.5. Electronic spectral Study

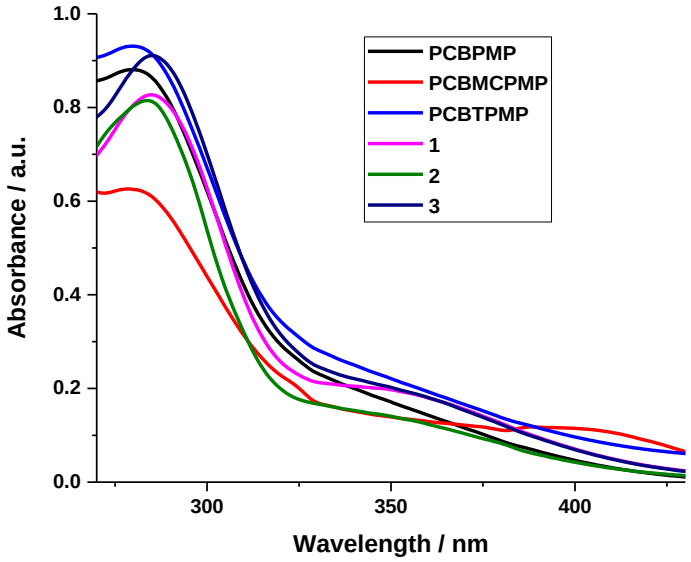

Fig. 2.1.36. Electronic spectra of ligands and complexes.

All complexes were completely soluble in DMSO. In the complexes Uv/Vis spectra, the first intense band is attributed to a ligand-centred (LC) π–π* transition localized on the aromatic rings of the ligand. There is no d-d transition in all complexes due to d^{10} metal. Compounds bearing the coordinated acyl pyrazolone ligands show an intense band at around 275-280 nm, and LMCT band at around 350-360 nm.[30]

2.1.3.6. Molar conductance

The 4- acyl pyrazolones and its complexes having lower molar conductivity and reviled from the reported literature that all complexes are non-electrolyte. The molar conductivity measured for all the three complexes in 10^{-3} M DMSO solution is found to be below 14 ohm^{-1} cm^2 mol^{-1}, so the conductance measurements in DMSO suggest that they are non-electrolytes.[61] The conductivity values are tabulated in Table 2.1.9.[30,61]

Table 2.1.9. Molar conductance of complexes.

Complexes	**Λ_m (ohm^{-1} cm^2mol^{-1})**
1	10.17
2	9.85
3	9.86

Conclusion

The 4-acyl pyrazolone ligands have been prepared by the acylation of pyrazolone derivatives with 4-chloro benzoyl chloride. Ligands have been characterized by **IR, Single crystal X-ray diffraction study, ^{1}H NMR and ^{13}C NMR spectroscopy.** Binary Zn(II) complexes of these ligands have been synthesized and fully **characterized by metal estimation, molar conductance, UV/Vis, FTIR, Thermogravimetric analysis, ^{1}H NMR and single crystal X-ray study**.

References:

1 L. Knorr, *Berichte der Dtsch. Chem. Gesellschaf*, 1883, **16**, 2597–2599.

2 L. Knorr, *Chem. Ber.*, 1884, **17**, 546–552.

3 L. Knorr, *Lieigs Ann. Chem.*, 1887, **238**, 137–219.

4 F. J. PRAKT, *CHEM*, 1897, **55**, 145–171.

5 B. S. Jensen, *Acta Chem. Scand.*, 1959, **13**, 1668–1670.

6 F. Marchetti, C. Pettinari and R. Pettinari, *Coord. Chem. Rev.*, 2005, **249**, 2909.

7 T. Konotsune, K. Kawakubo and T. Yanai, in *Synthesis of Pesticides Chemical Structure and Biological Activity Natural Products with Biological Activity*, Elsevier, 1979, pp. 94–98.

8 M. E. Reichmann, S. A. Rice, C. A. Thomas and P. Doty, *Mol. Weight Size Desoxypentose Nucleic Acid*, 1954, **76**, 3047–3053.

9 J. Singh, *Indian J. Malariol.*, 1956, **10**, 117–129.

10 K. H. Rieckmann, G. H. Campbell, L. J. Sax and J. E. Mrema, *Lancet (London, England)*, 1978, **1**, 22–23.

11 C. Lambros and J. P. Vanderberg, *J. Parasitol.*, 1979, **65**, 418–420.

12 J. S. Valentine, P. A. Doucette and S. Zittin Potter, *Annu. Rev. Biochem.*, 2005, **74**, 563–593.

13 Y. J. Zhong, Y. M. Chen, Y. Q. Sun and G. Y. Yang, *J. Solid State Chem.*, 2005, **178**, 2613.

14 B. Q. Ma, H. L. Sun and S. Gao, *Inorg. Chem.*, 2005, **44**, 837.

15 D. Wang and S. J. Lippard, *Nat. Rev. Drug Discov.*, 2005, **4**, 307–320.

16 Z. Y. Yang, B. D. Wang and Y. H. Li, *J. Organomet. Chem.*, 2006, **691**, 4159–4166.

17 E. Uhlemann, U. Schilde and F. Weller, *Zeitsch. Naturforsch.*, 1995, **B50**, 31–37.

18 F. M. Pettinari, Claudio, Flavio Bonati, Augusto Gingolani, Giancarlo Lobbia, *Gazz. Chim. Ital.*, 1992, **122**, 261–267.

19 R. C. Maurya and D. D. Mishra, *Synth. React. Inorg. Met. Chem.*, 1991, **21**, 845–857.

20 F. Marchetti, C. Pettinari, A. Cingolani, D. Leonesi, A. Drozdov and S. I. Troyanov, *J. Chem. Soc. - Dalt. Trans.*, 1998, **0**, 3325–3333.

21 F. Marchetti, C. Pettinari and R. Pettinari, *Coord. Chem. Rev.*, 2005, **249**, 2909–2945.

22 C. Pettinari, F. Marchetti, A. Gregori, A. Cingolani, J. Tanski, M. Rossi and F. Caruso, *Inorg. Chim. Acta*, 1997, **257**, 37–48.

23 M. F. Mahon, K. C. Molloy, B. A. Omotowa and M. A. Mesubi, *J. Organomet. Chem.*, 1996, **525**, 239–246.

24 X. Y. Chen, S. Z. Zhan and Q. J. Meng, *Transit. Met. Chem.*, 1996, **21**, 345–348.

25 C. Pettinari, F. Marchetti, A. Cingolani, D. Leonesi, G. G. Lobbia and A. Lorenzotti, *J. Organomet. Chem.*, 1993, **454**, 59–66.

26 F. Marchetti, J. Palmucci, C. Pettinari, R. Pettinari, S. Scuri, I. Grappasonni, M. Cocchioni, M. Amati, F. Lelj and A. Crispini, *Inorg. Chem.*, 2016, **55**, 5453–5466.

27 S. Parihar, R. N. Jadeja and V. K. Gupta, *RSC Adv.*, 2014, **4**, 10295–10302.

28 F. Marchetti, R. Pettinari and C. Pettinari, *Coord. Chem. Rev.*, 2015, **303**, 1–31.

29 C. Pettinari, A. Tombesi, F. Marchetti, C. Di Nicola and R. Pettinari, *Aust. J. Chem.*, 2020, **73**, 399–423.

30 I. U. Shaikh, R. K. Patel, V. A. Mevada, V. K. Gupta and R. N. Jadeja, *ChemistrySelect*, 2019, **4**, 8286–8294.

31 I. Shaikh, A. Vohra, R. Devkar and R. Jadeja, *Eur. J. Chem.*, 2019, **10**, 131–138.

32 R. N. Jadeja, M. Chhatrola and V. K. Gupta, *Polyhedron*, 2013, **63**, 117–126.

33 F. Caruso, C. Pettinari, F. Marchetti, M. Rossi, C. Opazo, S. Kumar, S. Balwani and B. Ghosh, *Bioorg. Med. Chem.*, 2009, **17**, 6166–6172.

34 A. Çetin and İ. Bildirici, *J. Saudi Chem. Soc.*, 2018, **22**, 279–296.

35 H. Y. Luo, J. Y. Li, Y. Li, L. Zhang, J. Y. Li, D. Z. Jia and G. C. Xu, *RSC Adv.*, 2016, **6**, 114997–115009.

36 I. Shaikh, R. N. Jadeja and R. Patel, *Polyhedron*, 2020, **183**, 114528.

37 F. Marchetti, C. Pettinari, C. Di Nicola, A. Tombesi and R. Pettinari, *Coord. Chem. Rev.*, 2019, **401**, 213069–213145.

38 Zinc - Element information, properties and uses | Periodic Table, https://www.rsc.org/periodic-table/element/30/zinc, (accessed 16 July 2020).

39 A. Yepremyan, A. Mehmood, S. M. Brewer, M. M. Barnett, B. G. Janesko, G. Akkaraju, E. E. Simanek and K. N. Green, *RSC Adv.*, 2018, **8**, 3024–3035.

40 D. D. P. W. L. F. Armarego, *Purification of Laboratory Chemicals*, Butterworth–Heinemann Publication, 4th edn., 1997.

41 University of Gottingen, *G.M. Sheldrick, SHELXS97 and SHELXL97*, Germany, 1997.

42 C. K. Johnson, *ORTEP II; Report ORNL-5138*, Oak Ridge, TN, 1976.

43 A. L. Spek, *PLATON for Windows*, University of Utrecht, Netherlands, September., 1999.

44 M. Nardelli, *J. Appl. Crystallogr.*, 1995, **28**, 659–665.

45 B. Kumar, K. J. Nakum, R. N. Jadeja, R. Kant and V. K. Gupta, *Acta Crystallogr. Sect. E*, 2015, **71**, 280–281.

46 K. Nakum and R. N. Jadeja, *Zeitschrift für Naturforsch. B*, 2018, **73**, 713–718.

47 K. M. Vyas, R. N. Jadeja, D. Patel, R. V. Devkar and V. K. Gupta, *Polyhedron*, 2014, **80**, 20–33.

48 H. Li, G.-C. Xu, L. Zhang, J.-X. Guo and D.-Z. Jia, *Polyhedron*, 2013, **55**, 209–215.

49 M. H. Sadhu, J. K. Saini, S. S. Ingle and S. B. Kumar, *ChemistrySelect*, 2018, **3**, 6203–6208.

50 R. N. Jadeja, K. M. Vyas, V. K. Gupta, R. G. Joshi and C. Ratna Prabha, *Polyhedron*, 2012, **31**, 767–778.

51 J. Li, L. Zhang, L. Liu, G. F. Liu, D. Z. Jia and G. C. Xu, *Inorg. Chim. Acta*, 2007, **360**, 1995.

52 Z. Wang, H. Zhang, Y. Chen, C. Huang, R. Sun, Y. Cao and X. J. Yua, *J. Solid State Chem.*, 2006, **179**, 1536.

53 X. Hu, L. Zhang, L. Liu, G. Liu, D. Jia and G. Xu, *Inorg. Chim. Acta*, 2006, **359**, 633–641.

54 K. M. Vyas, R. G. Joshi, R. N. Jadeja, R. C and V. K. Gupta, *Spectrochim. Acta. A. Mol. Biomol. Spectrosc.*, 2011, **84**, 256–268.

55 K. M. Vyas, R. N. Jadeja, D. Patel, R. V. Devkar and V. K. Gupta, *Polyhedron*, 2013, **65**, 262–274.

56 J. V.A., K. M. Vyas, J. H. Pandya, V. K. Gupta and R. N. Jadeja, *J. Coord. Chem.*, 2013, **66**, 1094–1106.

57 R. N. Jadeja, K. M. Vyas, K. K. Upadhyay and R. V. Devkar, *RSC Adv.*, 2017, **7**, 17107–17116.

58 R. J. Yadav, K. M. Vyas and R. N. Jadeja, *J. Coord. Chem.*, 2010, **63**, 1820–1831.

59 K. M. Vyas, R. N. Jadeja, V. K. Gupta and K. R. Surati, *J. Mol. Struct.*, 2011, **990**, 110–120.

60 P. U. Maheswari and M. Palaniandavar, *Inorg. Chim. Acta*, 2004, **357**, 901–912.

61 W. J. Geary, *Coord. Chem. Rev.*, 1971, **7**, 81–122.

ChemPubSoc Europe

DOI: 10.1002/slct.201901058

Chemistry SELECT Full Papers

Inorganic Chemistry

Binary and Ternary Zinc(II) Complexes of Acyl Pyrazolones: Synthesis, Spectroscopic Analysis, Crystal Structure and Antimalarial Activity

Irfan U. Shaikh,[a] Rajesh K. Patel,[b] Vishal A. Mevada,[c] Vivek K. Gupta,[d] and Rajendrasinh N. Jadeja*[a]

A new series of Zn^{II} metal complexes of ligands 4-(4-chlorobenzoyl)-5-methyl-2-phenyl-2,4-dihydro-3H-pyrazol-3-one (PCBPMP) and 4-(4-chlorobenzoyl)-5-methyl-2-(p-tolyl)-2,4-dihydro-3H-pyrazol-3-one (PCBTPMP) were prepared and characterized. The nature of bonding and the stereochemistry of the complexes were deduced from ^{1}H and ^{13}C Nuclear Magnetic Resonance (NMR), Fourier-transform infrared spectroscopy (FTIR), thermogravimetric analysis (TGA), Molar conductivity measurements and Single-crystal X-ray diffraction. The analyses indicated that complexes 1, 2 and 3 are mononuclear and exhibited octahedral geometry around Zn^{II}. The potential *in silico* and *in vitro* antimalarial activity inhibits *Plasmodium falciparum* and the same was exhibited by Ligands and Zinc complexes. This would be the first report of the antimalarial activity of Zinc complexes of acyl pyrazolones ligand.

1. Introduction

Acyl pyrazolones are widely used in coordination chemistry due to the nature of the bidentate ligand.[1–5] A wide range of applications has been studied in the field of biological activity of metal complexes of acyl pyrazolone.[4–10] The d^{10} metal complexes of the acyl pyrazolones and their structural analogues showed decent fluorescence properties, antimicrobial and antitumor activity.[3,11–14] In addition to this, docking of all tautomers of this group of ligand on ICAM-1 protein has been performed and suggested that keto-enol tautomerism of acyl pyrazolone has been favoured to act in a biological environment.[1]

Malaria is one of the most dangerous diseases to need serious attention in the present situation.[15] In 2017, an estimated 219 million cases of malaria have been reported worldwide (95% confidence interval [CI]: 203–262 million), as compared to 239 million cases in 2010 (95% CI: 219–285 million) and 217 million cases in 2016 (95% CI: 200–259 million).[16]Heterocydic compounds which contain more than one nitrogen atoms are key structures in a large variety of biochemical processes.[17–19] Thus pyrazolone ligands may be a good candidate to explore as an anti-malarial drug. Metal-based derivatives are still relatively unexplored in anti-malarial drug development. Zinc shows a very important part of the living body.[20,21] A recent report, in which the 7-chloro-4-(1,4,7,10-tetraaza-cyclododec-1-yl)-quinoline-Zn^{II} complex is found to demonstrate a high anti-malarial activity, has motivated us to pursue the present investigation.[22] From literature reports, it is found that this is the first report on the *in vitro* antimalarial activity on Zn^{II} complexes of acyl pyrazolone ligand.

2. Results and discussion

2.1. Crystal structure description of the complexes 1-3

2.1.1. Complex 1

The molecular structure and the atom labelling scheme of complex1 is shown in Figure 1. The main bond distances and angles are listed in Table S2 (Supporting information). As shown in Figure 1, the Zn^{II} ion is hexacoordinated with four oxygen atoms of two acyl pyrazolone ligands and two oxygen atoms of methanol molecules. Two oxygen donors of both pyrazolone molecules occupy the basal sites of the octahedral structure, whereas the MeOH molecules bind the zinc at the apical site. In this complex, the incorporation of the solvent into the coordination sphere increases the coordination number to six and the geometry around the metal turns into a distorted octahedral. In the complex, the zinc atom occupies a distorted octahedral environment (OH), formed by four oxygen atoms [O(1), O(2), O(1)' and O(2)'] supplied by acyl pyrazolone ligands (Symmetry code: (i) 12-X,-Y,2-Z). The fifth and sixth coordination sites are occupied by oxygen atoms of MeOH molecules. The Zn–O distances of the basal plan are Zn(1)- O

[a] *I. U. Shaikh, Dr. R. N. Jadeja*
Department of Chemistry, Faculty of Science, The M.S. University of Baroda, Vadodara 390 002, India
E-mail: rjadeja-chem@msubaroda.ac.in
[b] *Prof. R. K. Patel*
Department of Bioscience, Veer Narmad South Gujarat University, Surat-395007, India
[c] *Dr. V. A. Mevada*
Super Computing Facility, Veer Narmad South Gujarat University, Surat-395007, India
[d] *Prof. V. K. Gupta*
Post-Graduate Department of Physics & Electronics, University of Jammu, Jammu Tawi 180 006, India

Supporting Information for this article is available on the WWW under https://doi.org/10.1002/slct.201901058

Chapter 2(b)

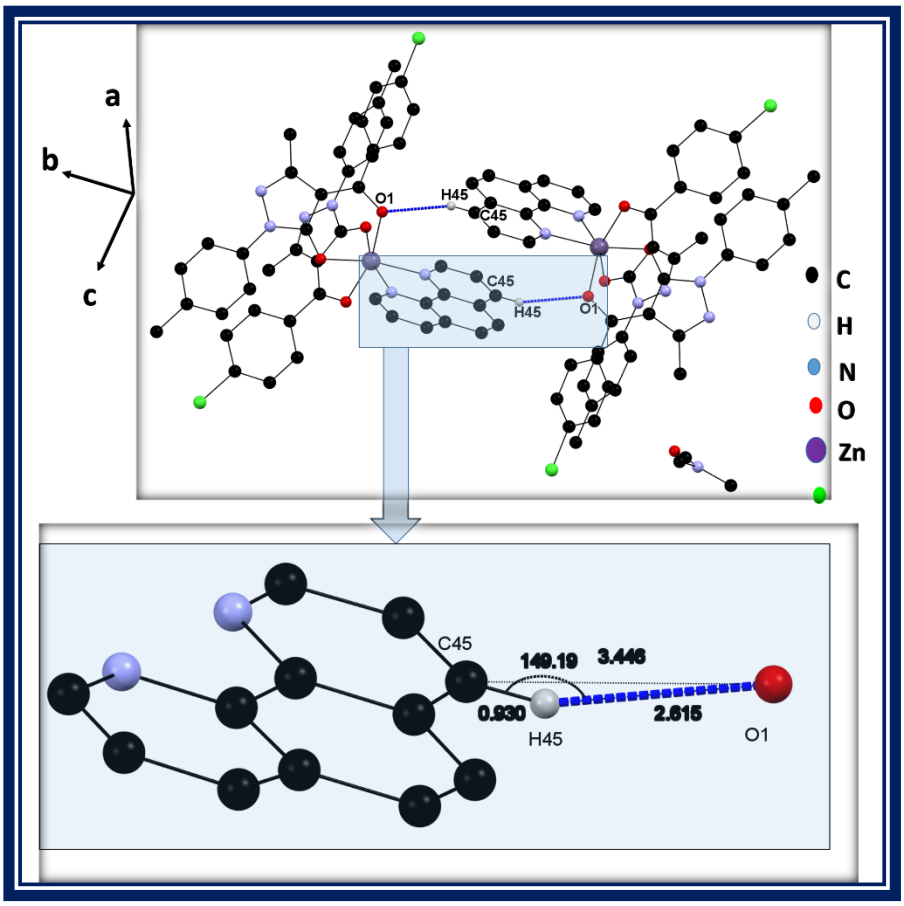

Chapter 2 (Part-b):

Ternary Mixed Ligand Zinc (II) Complexes of 4-Acyl Pyrazolone with 2,2'-Bipyridine and 1,10-Phenanthroline: Synthesis, Characterization and Structural Features

2.2.1. Introduction

4-Acyl pyrazolones are good chelating agent due to having *β*-diketone in the structure moiety. The presence of the pyrazole, stabilized the metal derivative by creating an extensive conjugate system when the double nitrogen containing heterocyclic ring is directly bonded to an aromatic substituent.[1] Mixed ligand Cu(II) complexes of AP and bpy possess slightly distorted square-pyramidal structures (Fig. 2.2.1). Complex [Cu(NCS)(AP)(bpy)] had five-coordinate Cu(II) with two oxygens of bidentate acyl pyrazolones and two nitrogen of 2,2′-bipyridine . Two oxygens from acyl pyrazolone and two nitrogens from 2,2′-bipyridine compose equatorial planes where thiocyanate group attached on an axial plane.[2]

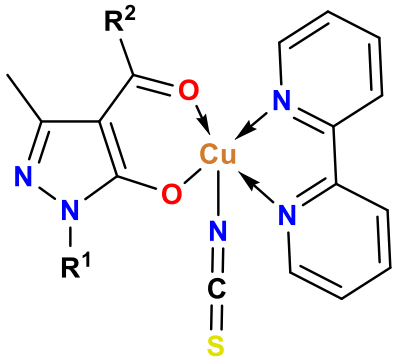

Fig. 2.2.1. Cu(II) complex [Cu(NCS)(AP)(bpy)] has a square-pyramidal environment around Cu(II) ion in the structure configuration, where **R**^{1}= Phenyl ring and **R**^{2}=Methyl.

The Ca(II) complex which general formula is [Ca(AP)$_2$(phen)]. This Ca(II) complex was synthesized by the reaction between the already prepared [Ca(AP)$_2$(H$_2$O)$_2$] and 1,10-phenanthroline (Fig. 2.2.2). In the geometry, two N atoms of phen and two O-atoms of AP have occupied the basal site of the octahedral. Other two O-atoms of AP have settled at axial sites of the geometry.[3]

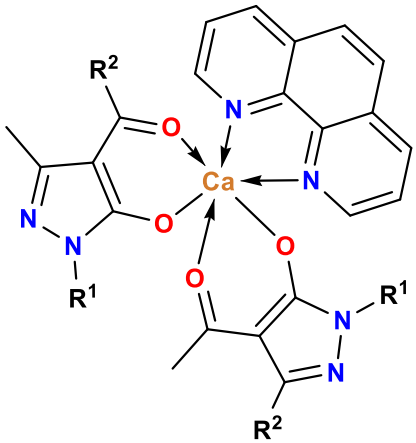

Fig. 2.2.2. Six coordinated Ca(II) complex [Ca(AP)$_2$(phen)].Where **R**^{1}=Phenyl and **R**^{2}=Methyl.

Mixed ligand vanadium complex of AP and bpy (Fig. 2.2.3), in this VO(IV) complex cationic charge has neutralized by chlorate ion (ClO_4^-). In the complex, the basal plan has established by two nitrogen atoms of 2,2′-bipyridine and two oxygen atoms of acyl pyrazolone. The VO (oxo) group has located cis to the coordinated water molecule. The geometry around the vanadium ion has found distorted octahedral (Fig.2.2.3).[4]

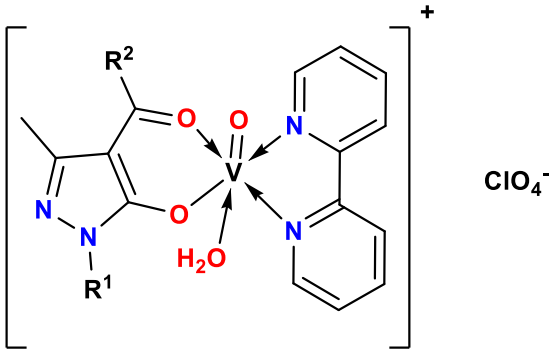

Fig. 2.2.3. A mixed ligand Oxo vanadium cationic complex $[VO(AP)(bpy)(H_2O)]ClO_4$. $\mathbf{R^1}$=phenyl group and $\mathbf{R^2}$= methyl.

Mixed ligand complexes of acyl pyrazolones in biological activity

Mixed ligand complexes of acyl pyrazolones with the secondary ligands have been found very effective in biological activities. 4-Acyl pyrazolone and its mixed ligand Cu complexes have interacted with calf thymus DNA occur through intercalation. They also interacted with bovine serum albumin and are cytotoxic against human lung cancer cell line (A549) and noncancerous rat cardio myoblasts (H9C2) cell lines.[2] A mixed ligand vanadyl cationic complex $[VO(AP)(bpy)(H_2O)]ClO_4$ (Fig. 2.2.3) displayed antibacterial activity against S. aureus, E. coli, and P. aeruginosa.[4]

Mixed ligands zinc(II) complexes, $[Zn(AP^{1/2})_2(L)]$ (**1-6**) (*see* Fig. 2.2.4){AP^1= 3-methyl-1-phenyl-4-stearoyl-5-pyrazolone, AP^2 = 3-methyl-1-phenyl-4-cyclohexylcarbonyl-5-pyrazolone, L = bipy, tmeda or en} were synthesized and the cytotoxicity of the complexes $[Zn(AP^2)_2(bipy)]$ and $[Zn(AP^2)_2(en)]$ has been evaluated in vitro against MCF-7 human breast cancer cell line in a biohybrid membrane system. Results revealed that zinc complexes possess antiproliferative activity inducing apoptosis by activation of caspase-3 and p-JNK.[5] Mixed ligand zinc(II) complex which general formula is $[Zn(PMPAC)_2(phen)]$ (PMPAC = 4-acyl-3-methyl-1-phenyl pyrazolone-5-one) was synthesized by our group. Binding of zinc(II) complex $[Zn(PMPAC)_2(phen)]$ with calf thymus DNA (CT-DNA) was studied by spectroscopic methods and viscosity measurements. Experimental results suggest that the zinc complex has

the ability to form adducts with DNA and to distort the double helix by changing the base stacking (*see* Fig. 2.2.5).[6]

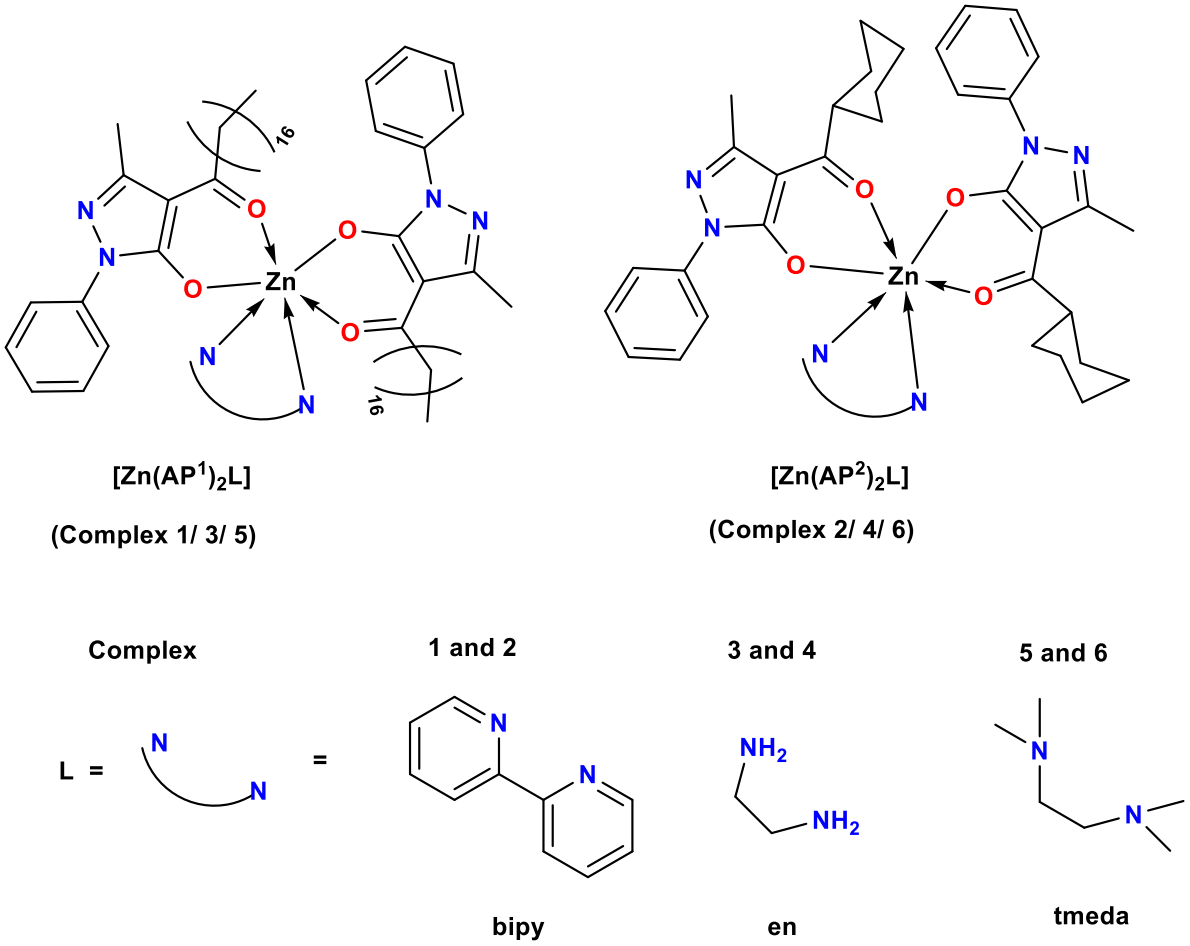

Fig. 2.2.4. Structures of mixed ligand zinc(II) complexes of 4-acylpyrazolone (AP^{1-2}) with secondary ligand (L).

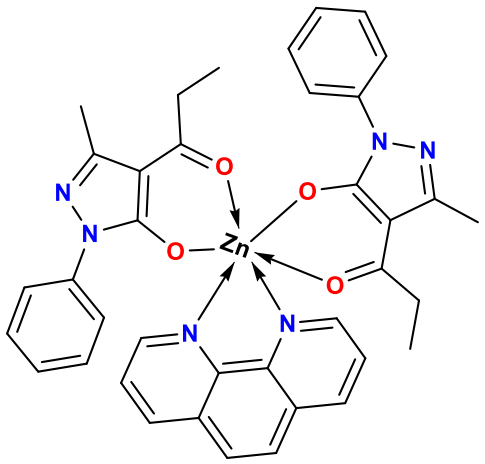

Fig. 2.2.5. Structure of mixed ligand zinc(II) complex of 4-acyl pyrazolone with 1,10-phenanthroline.

Objective and methodology of the present work

In the coordination chemistry, we object to synthesised ternary mixed ligand zinc(II) complexes of acylpyrazolones with bidentate secondary ligand as 2,2′-bipyridine /1,10-phenanthroline. In this chapter, mixed ligand zinc(II) complexes of acylpyrazolone and their structural analogues and characterized by various spectroscopic and analytical techniques. Single crystal X-ray diffraction study has been done and results revealed that synthesized mixed ligand zinc(II) complexes have an octahedral environment around zinc(II) ion.

2.2.2. Experimental

Materials and methods

Pyrazolones were obtained from Sidhdhanath industries, Sachin (Surat), India as gift samples. All necessary reagents and solvents were obtained from commercial sources. Zinc acetate, 2,2′-bipyridine and 1,10-phenanthroline were purchased from Spectrochem PVT. LTD., Mumbai. *P*-chloro benzoyl chloride was purchased from SRL Chemical, Mumbai.

Infrared (IR) spectra were recorded on Bruker Alpha Fourier transform IR (FT-IR) spectrometer as KBr pellets. ^{1}H NMR and ^{13}C NMR spectra of the ligand were recorded with an AV 400 MHz Bruker FT-NMR instrument. Single crystal data were collected on a Bruker CCD area-detector diffractometer. The electronic spectrum was recorded on a Perkin Elmer Lambda 35 UV-Vis spectrometer. A simultaneous TG/DTA was carried out on an SII EXSTAR6000 TG/DTA 6300 instrument. The experiments were performed in N_2 at a heating rate of 10 ºC min^{-1} in the temperature range 30–550ºC using an aluminium pan. The purity of the ligand and its complexes was evaluated by thin-layer chromatography. Gravimetric and volumetric analysis were performed for the determination of zinc after decomposition of the complex in nitric acid.

2.2.2.1. Syntheses of Compounds

2.2.2.1.1. Synthesis of ligands

Ligands (**L1**, **L2** and **L3**) have synthesized and used as the following method of chapter **2(a)** and previously reported the article.[7–9]

2.2.2.1.2. Synthesis of the ternary mixed ligand Zn(II) complexes

Synthesis of complex 4 $[Zn(L1)_2(bpy)]$

Preparation of complex **4** as follows, The metal salt zinc-acetate dehydrate ($Zn(CH_3COO)_2.2H_2O$) (0.219 g, 0.001 mol) was dissolved in methanol and the solution was added to a hot methanolic solution of the ligand (L1) (0.625 g, 0.002 mol) and 2,2′-bipyridine (0.154 g, 0.001 mol). After complete addition, a little amount of sodium acetate was added. The mixture was refluxed about for 5 h and cool it for overnight. After a night crystalline solid was obtained. The crystalline solid was filtered and washed with hot water and dried in air. M.P. >200ºC, Yield 82.42%, M.f.: $C_{42}H_{30}Cl_2N_6O_4Zn$ (F.w. 819.02); Metal estimation by gravimetrically and volumetrically Zn=7.12 %. **FTIR (KBr, cm^{-1}):** 1622 (m) (C=O, *p*-chloro benzoyl group), 1527 (s) (C=N, cyclic), 1469 (C-O, pyz ring), 480 (Zn-O), 422 (Zn-N); **^{1}H NMR (CDCl$_3$, 400MHz)** (δ *ppm):* 1.62 (s, 3H, CH_3-Pyz), 7.08-7.90 (m, 2H, phenyl of pyz), 8.01-9.06 (m, 4H, 2,2′-bipyridine).[7] **^{13}C NMR (CDCl$_3$, 100MHz):** δ 16.65, 105, 120, 121, 124, 126, 128, 128.5, 129, 136, 139, 140, 148, 149, 150, 167 and 190.

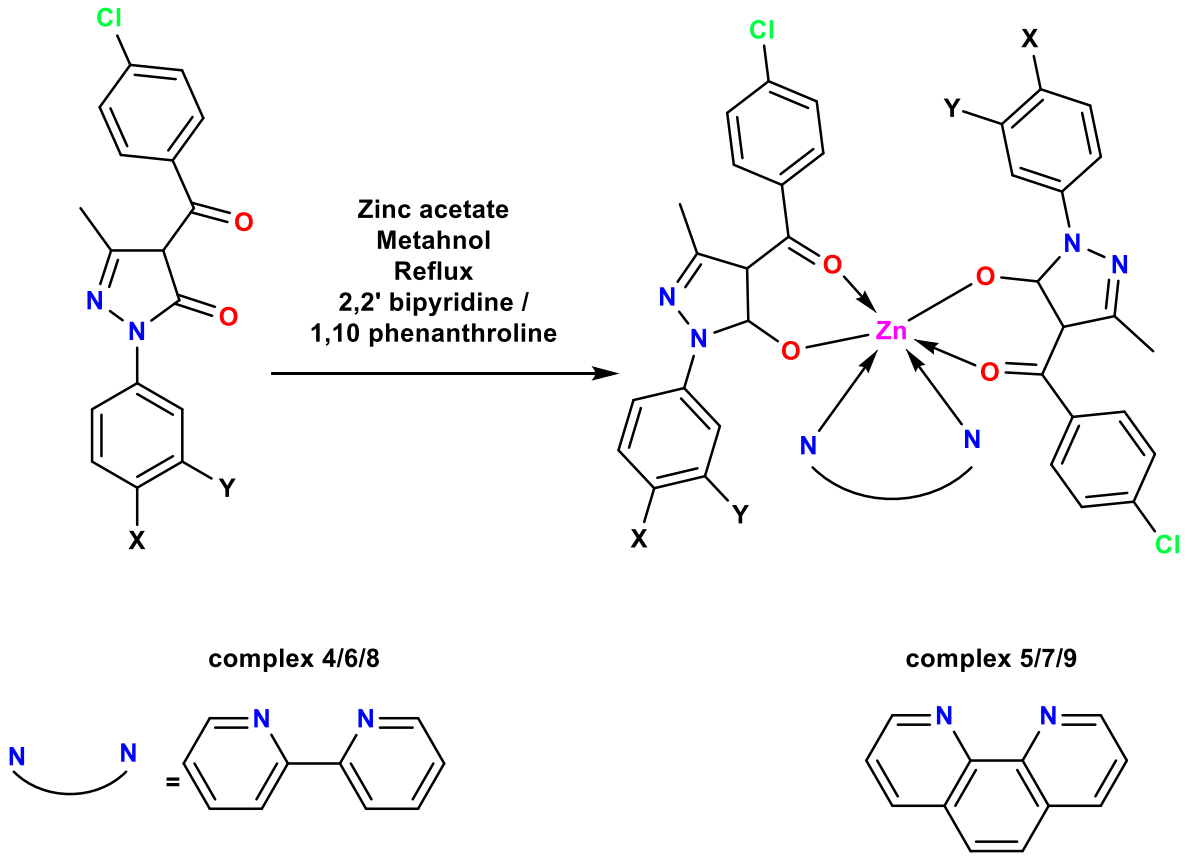

Scheme 2.2.1. Synthesis route for mixed ligand complexes **4-9.** For complex **4** & **5**: X=Y=-H, complex **6 & 7**: X=-H, Y=-Cl, and complex **8** & **9**: X=-CH_3, Y=-H.

Synthesis of complex 5 [Zn(L1)$_2$(phen)]

The procedure for the preparation of complex **5** is similar to that for complex **4** except for the replacement of 2,2′-bipyridine with 1, 10-phenanthroline.[7]

Yield: 86.7%. M.P.: >200°C.Anal. Calcd for $C_{48}H_{40}Cl_2N_6O_4Zn$: C, 63.98; H, 4.47; N, 9.33%, Found: C, 64.01, H, 4.55; N, 9.65%. M.w.: 901.17. Λ_m (S.cm^2.mol^{-1}): 9.7. Metal estimation by gravimetrically and volumetrically Zn=7.26%. **FTIR (KBr, cm^{-1}):** 1562(C=N, cyclic), 1622 (C=O, 4-chloro benzoyl group), 943(s) (N-N), 1436 (s) (Ar-C-C-). **^{1}H NMR (CDCl$_3$, 400MHz) δ *ppm*:**1.6 (s,3H, CH_3-tolyl), 2.2 (s, 3H, Pyz-C-CH_3) , 6.99-7.02 (d, 2H, aromatic-H, *J*=8Hz), 7.24-7.31(m, 2H, ar-H), 7.60-7.62 (d, 2H, aromatic-H, *J*=8Hz),7.72-7.74(d, 2H, 4-chloro benzoyl-, *J*=8Hz).9.30-9.31 (m, 1H, aromatic), 8.49-8.51(m, 1H, phen). Synthesis route for complexes **4-9** summarized in **Scheme 2.2.1.**

Complex 6, 7, 8 and 9 are prepared by following the method of complex 4 and 5.

Complex 6 [Zn(L2)$_2$(bpy)]

M.P. >200ºC, Yield 88.42%, Molecular formula: $C_{44}H_{34}Cl_4N_6O_4Zn$, F.W. 917.97 g/mol, metal estimation: 7.12%. **FTIR (KBr, cm^{-1}):** 1621 (m) (C=O p-chloro benzoyl group), 1597 (s) (C=N cyclic), 1470 (C-O, pyz ring), 481 (Zn-O), 439 (Zn-N); **^{1}H NMR (CDCl$_3$, 400MHz) δ *ppm:*** 1.62 (s, 3H, CH_3-Pyz), 7.08-7.90 (H- Ar protons of pyz), 8.01-9.06 (m, 4H, 2,2′-bipyridine). **^{13}C NMR (CDCl$_3$, 100 MHz) δ *ppm***: 16.5 (CH_3-pyz), 104, 117, 119, 121, 124, 126, 128, 129, 130, 134, 136, 139, 140, 141, 148, 149, 150, 166 and 190.

Complex 7 [Zn(L2)$_2$(phen)]

M.P. > 200ºC, Yield: 81.5%. Anal. Calcd for $C_{46}H_{34}Cl_4N_6O_4Zn$: C, 58.64; H, 3.47; N, 8.33%, Found: C, 58.65, H, 3.64; N, 8.92%. F.w.: 942.00 g/mol. Λ_m (S.cm^2.mol^{-1}): 9.5. Metal estimation by gravimetrically and volumetrically Zn=6.94%. **FTIR (KBr, cm^{-1}):** 1622 (C=O, 4-chloro benzoyl group), 1565(C=N, cyclic), 1433 (s) (Ar-C-C-), 956(s) (N-N), 583 (M-O), 491 (M-N). **^{1}H NMR (CDCl$_3$, 400MHz) δ *ppm*** 2.2 (s, 3H, Pyz-C-CH_3) , 7.01-7.02 (d, 2H, ar-H, *J*=8Hz), 7.26-7.33(m, 2H, ar-H), 7.70-7.82 (d, 2H, ar-H, *J*=8Hz),7.93-8.00 (d, 2H, 4-chloro benzoyl-, *J*=8Hz).9.33-9.35 (m, 1H, aromatic), 8.53-8.55 (m, 1H, phen). **^{13}C NMR (CDCl$_3$, 100 MHz) δ ppm** 16.58, 104, 117, 119, 124, 125, 126, 128, 129, 129.5, 130, 133, 136, 138, 139, 140, 141, 149, 149.5, 167 and 190.

Complex 8 [Zn(L3)$_2$(bpy)]

Yield 88.25%, Molecular formula: $C_{46}H_{40}Cl_2N_6O_4Zn$ (F.w. 877.14 g/mol), M.P. >200ºC; FTIR (KBr, cm^{-1}): 1626 (m) (C=O p-chloro benzoyl group), 1513 (s) (C=N cyclic), 1476 (C-O, pyz ring), 511 (Zn-O), 476 (Zn-N); **^{1}H NMR (CDCl$_3$, 400MHz) *δ ppm*** :1.62 (s, 3H, CH_3-pyz), 2.19(s, 3H, CH_3-toluyl), 6.99-7.68 (H-Ar, phenyl of pyz), 8.04-9.01 (m, 4H, 2,2′-bipyridine).[7] **^{13}C NMR (CDCl$_3$, 100MHz) *δ ppm:*** 16.67, 21, 120, 121, 126, 128, 129, 130, 140 and 150.

Complex 9 [Zn(L3)$_2$(phen)]

Yield: 82.60%. M.w.: 901.17. M.P.: >200°C. Molar conductance: Λ_m ($S.cm^2.mol^{-1}$): 9.5. Metal estimation by gravimetrically and volumetrically Zn=7.26%; Anal. Calcd for $C_{48}H_{40}Cl_2N_6O_4Zn$: C, 63.98; H, 4.47; N, 9.33%, Found: C, 64.01, H, 4.55; N, 9.65%. **FTIR (KBr, cm^{-1}):** 1622 (C=O, 4-chloro benzoyl group), 1562(C=N, cyclic), 943(s) (N-N), 1436 (s) (Ar-C-C-). **^{1}H NMR (CDCl$_3$, 400MHz) *δ ppm*:**1.6 (s,3H, CH_3-tolyl), 2.2 (s, 3H, Pyz-C-CH_3) , 6.99-7.02 (d, 2H, aromatic-H, *J*=8Hz), 7.24-7.31(m, 2H, ar-H), 7.60-7.62 (d, 2H, aromatic-H, *J*=8Hz),7.72-7.74(d, 2H, 4-chloro benzoyl-, *J*=8Hz), 9.30-9.31 (m, 1H, aromatic), 8.49-8.51(m, 1H, phen). **^{13}C NMR (CDCl$_3$, 100MHz) *δ ppm:*** 16.7, 21, 104.3, 120, 126.6, 128, 129, 129.1.

2.2.2.2. Single crystal X-ray crystallography

The single crystal X-ray crystallographic data of four complexes (**4, 6, 8 and 9**) are summarized in Table 2.2.1. Single crystal crystallographic data were collected on Bruker CCD area-detector diffractometer with graphite monochromated MoKα radiation (λ = 0.71073Å). Mercury was used for ORTEP views of complexes, crystal packing and H-bond diagrams of complexes are given in Fig. 2.2.9-Fig.2.2.20. Complexes **4. 6, 8 and 9** structures were solved by direct methods, using SHELXS97, SHELXL and SHELXS.[10] All non-hydrogen atoms of all molecules were located in the expected position in obtained structures. For the refinement, full-matrix least-squares refinement was carried out using SHELXS.[11] All hydrogen atoms were included as idealized atoms riding on the respective carbon atoms with C-H bond lengths appropriate to the carbon atom hybridization.[12,13]

Table 2.2.1. Structure refinement data of complex **4, 6, 8** and **9**.

	Complex 4	**complex 6**	**Complex 8**	**complex 9**
	$[Zn(L1)_2(bpy)]$	$[Zn(L2)_2(bpy)]$	$[Zn(L3)_2bpy]$	$[Zn(L3)_2phen]$
Empirical formula	$C_{44}H_{32}Cl_2N_6O_4Zn$	$C_{44}H_{30}Cl_4N_6O_4Zn$	$C_{49}Cl_2N_7O_5Zn$	$C_{51}H_{42}Cl_2N_7O_5Zn$
Formula weight	845.03	913.91	902.83	969.18
Crystal system	Monoclinic	Triclinic	monoclinic	triclinic
Space group	P21/c	P-1	$P2_1/n$	P-1
a/Å	9.4150(10)	9.0491(4)	12.5956(6)	13.4212(8)
b/Å	19.4466(16)	12.6789(6)	26.5655(10)	13.7150(8)
c/Å	22.572(2)	18.7081(6)	14.6544(7)	14.0396(7)
α/°	90.00	82.155(3)	90	88.005(4)
β/°	95.505(8)	79.592(3)	110.822(5)	80.209(4)
γ/°	90.00	81.754(4)	90	66.901(5)
Volume/$Å^3$	4113.6(7)	2075.78(15)	4583.2(4)	2341.0(2)
Z	4	2	4	2
ρcalcg/cm^3	1.364	1.462	1.308	1.375
μ/mm^{-1}	0.777	0.900	0.705	0.694
Crystal size/mm^3	0.7 × 0.3 × 0.1	0.3 × 0.2 × 0.2	0.3 × 0.2 × 0.2	0.3 × 0.2 × 0.2
Radiation	MoKα (λ = 0.71073)	MoKα (λ = 0.71073)	MoKα (λ = 0.71073)	MoKα (λ = 0.71073)
Reflections collected	20658	45888	51601	51456
Independent reflections	8070 [R_{int} = 0.0450, R_{sigma} = 0.0441]	10074 [R_{int} = 0.0450, R_{sigma} = 0.0441]	11254 [R_{int} = 0.0873, R_{sigma} = 0.0834]	11368 [R_{int} = 0.1462, R_{sigma} = 0.1772]
Data/restraints/parameters	8070/0/553	10074/0/534	11254/0/577	11368/0/601
Goodness-of-fit on F2	1.042	1.030	1.039	1.007
Final R indexes [I>=2σ (I)]	*R1 = 0.0510, wR2 = 0.1270*	R_1 = 0.0469, wR_2 = 0.0932	R_1 = 0.0814, wR_2 = 0.2186	R_1 = 0.0718, wR_2 = 0.1206
Final R indexes [all data]	*R1 = 0.0961, wR2 = 0.1547*	R_1 = 0.0867, wR_2 = 0.1098	R_1 = 0.1519, wR_2 = 0.2646	R_1 = 0.2135, wR_2 = 0.1701
CCDC No.	1870327	1985004	1985005	1985006

2.2.3. Results and discussion

In this chapter, six heteroleptic zinc(II) complexes have been prepared by following the scheme 2.2.2. described below;

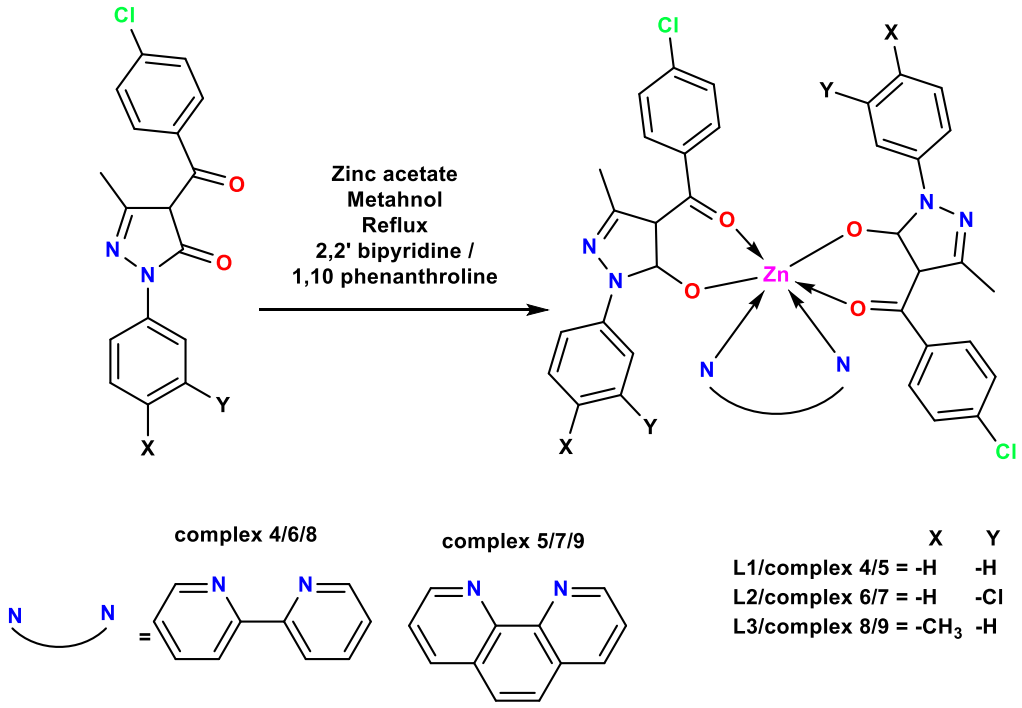

Scheme 2.2.2. Synthesis route of complexes **4-9**.

All these complexes are yellowish solid, stable at room temperature and soluble in DMF and DMSO.

The detailed characterization of these complexes is described in succeeding sections.

2.2.3.1. Crystal structures complexes

The crystallographic data of complexes **4, 6, 8** and **9** are given in Table 2.2.1. The structures with atom numbering schemes are represented in respective figures. Selected bond length and bond angles of complexes **4-9** are given in respective Tables.

2.2.3.1.1. Crystal structure of $[Zn(L1)_2(bpy)]$ complex 4

Crystallographic data of complex **4** presented in Table 2.2.1 and complex structure illustrated in Fig. 2.2.6. Selected bond length and bond angles are given in Table 2.2.3. Here, complex 4 has six-coordinate Zn(II) with four O-atoms of two bidentate acyl pyrazolones and two N-atoms coordinated of 2,2′-bipyridine . Two-two oxygen atoms from L1 and two nitrogen atoms from 2,2′-bipyridine compose equatorial planes with the least plane deviation of 0.011Å and

the Zn(II) metal ion strays from the equatorial plane 0.001Å. The coordination plane around Zn(1) ion is composed of O(2), O(3), N(1) and N(2) atoms and regular bond distances of Zn(1)–O(2), Zn(1)–O(3), Zn(1)–N(1) and Zn(1)- N(2) are 2.030(2) Å, 2.053(2) Å, 2.108(3) Å and 2.131(3) Å respectively. Two oxygens [O(1) and O(4)] of L1 are in axial positions with distance from the equatorial plane are 2.092 Å and 2.113 Å respectively.[6,7,14,15] The angles of O(2)–Zn(1)–N(1), O(3)–Zn(1)–N(2)and O(1)–Zn(1)–O(4) are 168.06(12)°, 170.50(12)° and 167.81(9)°, respectively, which are deviated from the theoretical value of 180° of proper geometric structure. Therefore, the local coordination geometry around the Zn(II) centre can be described as a distorted octahedron. The angles of complex **4** for O(2)–Zn(1)–O(1) (86.16(10)º), O(3)–Zn(1)–O(1)(85.82(9)º), O(1)–Zn(1)–N1) (95.29(11)º), O(1)–Zn(1)–N(2) (94.34(10)º), O(2)–Zn(1)–O(4) (87.54(10)º), O(3)–Zn(1)–O(4) (84.68(9)º), O(4)–Zn(1)–N1) (93.03(11)º) and O(4)–Zn(1)–N(2) (96.28(10)º) have deviated from 90º angle between the axial line and equatorial plane. Therefore geometry around the zinc ion in the complex is distorted octahedral (*see* Fig. 2.2.7).[14,16]

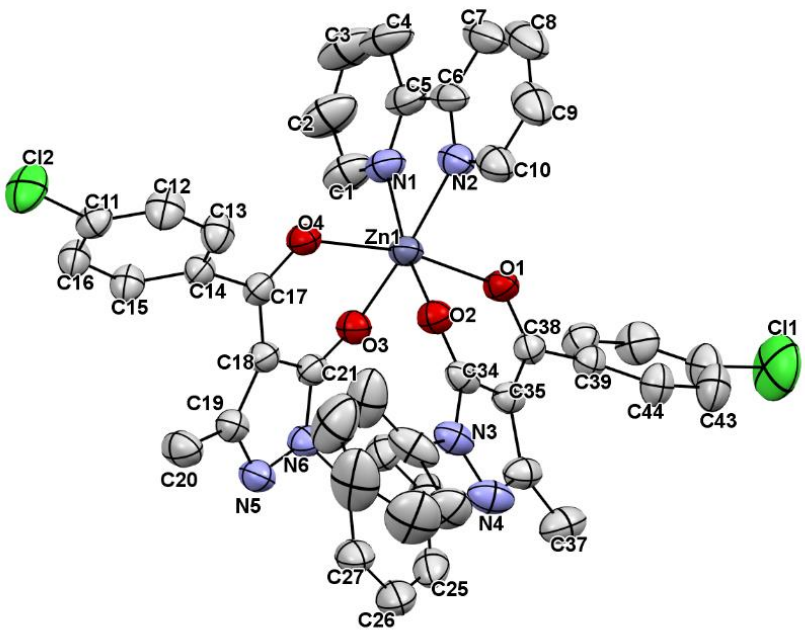

Fig. 2.2.6. ORTEP ellipsoid diagram with 35% probability of complex **4**, H-atoms are omitted for clarity.

Intermolecular H-bond has shown in the complex **4** packing system between Oxygen atom (O(4)) of *p*-chloro benzoyl of L1 and a hydrogen atom (H(3)) of 2,2′-bipyridine (Fig. 2.2.8)

where H-bond parameters are given in Table 2.2.2 and crystal packing system presented in the Fig. 2.2.9.[7]

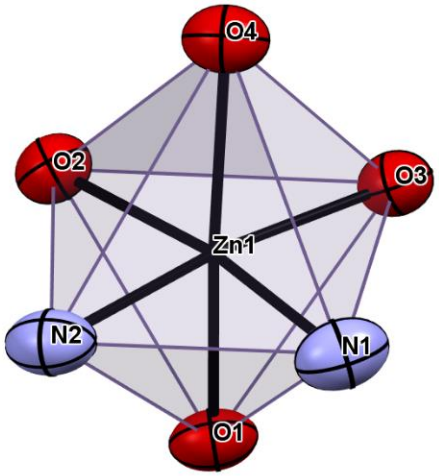

Fig. 2.2.7. Distorted octahedral geometry around Zn(II) ion in the complex **4**.

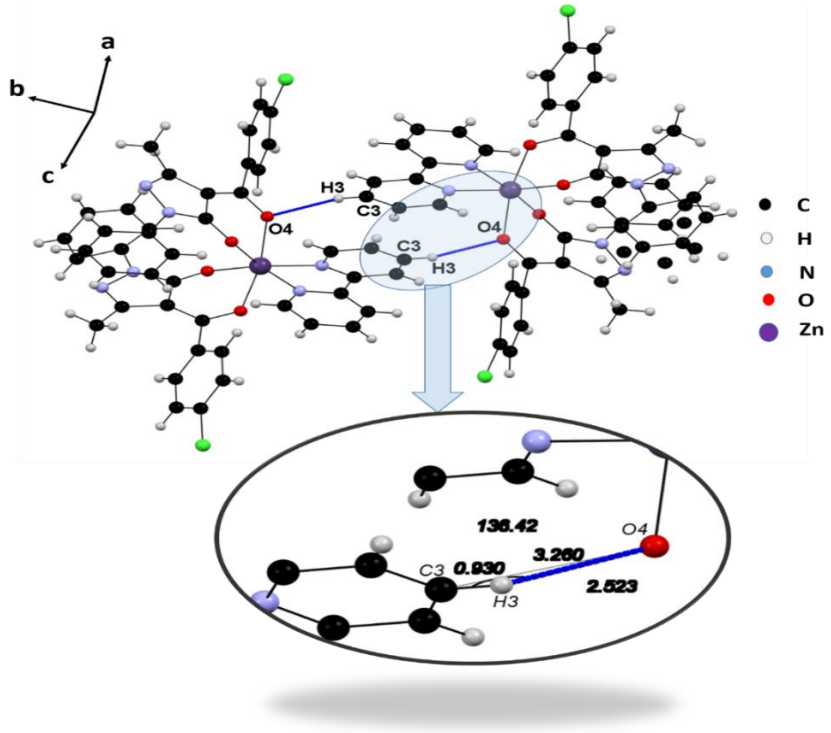

Fig. 2.2.8. Plot of intermolecular H-bond in the complex 4 $[Zn(L1)_2(bpy)]$.

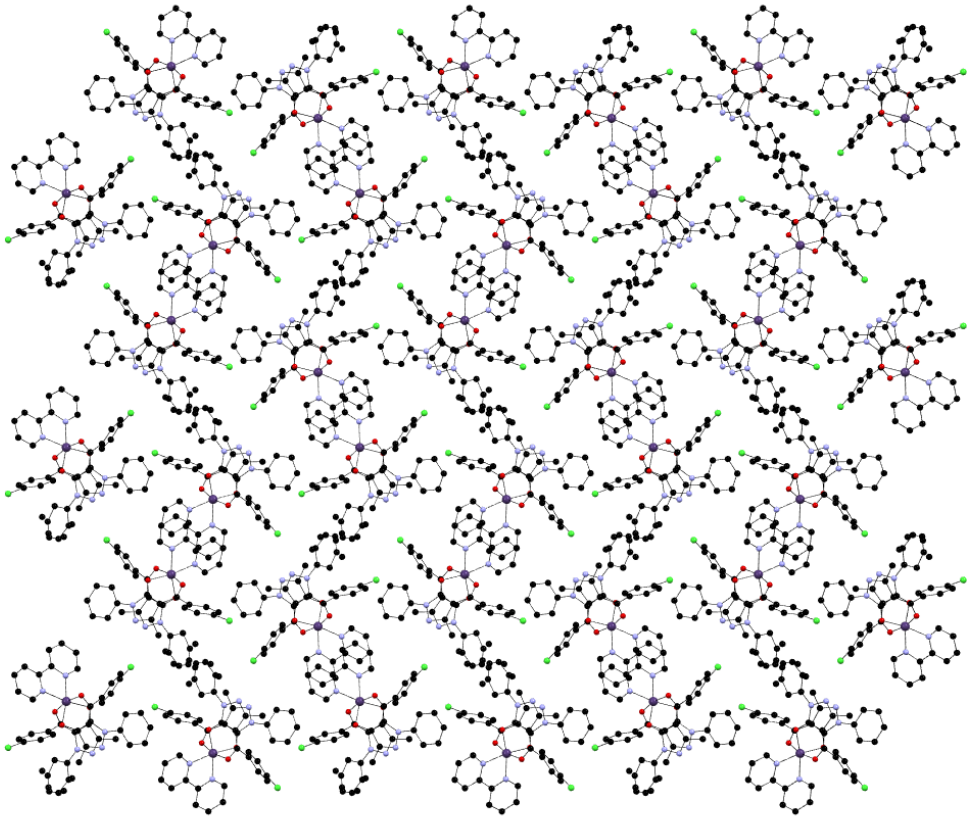

Fig. 2.2.9. The packing arrangement of Complex **4** viewed down the a-axis.

2.2.3.1.2. Crystal structure of [Zn(L2)$_2$(bpy)] (complex 6).

The single crystal X-ray analysis for complex **6**, the structure had common formula ML$_2$L' (where L= L2 and L¢ is 2,2′-bipyridine). In the complex, zinc(II) ion Hexa coordinated by four oxygen atoms (O1, O2, O3 and O4) of two acyl pyrazolone ligand (L2) and two nitrogen atoms (N5 and N6) of the 2,2′-bipyridine . The structure of complex **6** is shown in Fig. 2.2.10 and selected bond lengths and bond angles are displayed in Table 2.2.3 The coordination geometry styled as octahedral in which two oxygens [O(2) and O(3)] from two L2 and two nitrogens [N(5) and N(6)] from 2,2′-bipyridine compose equatorial planes. Deviation of coordination atoms O(2), O(3), N(5) and N(6) from the mean plane are 0.0073, 0.069, 0.077 and 0.081 Å, respectively.

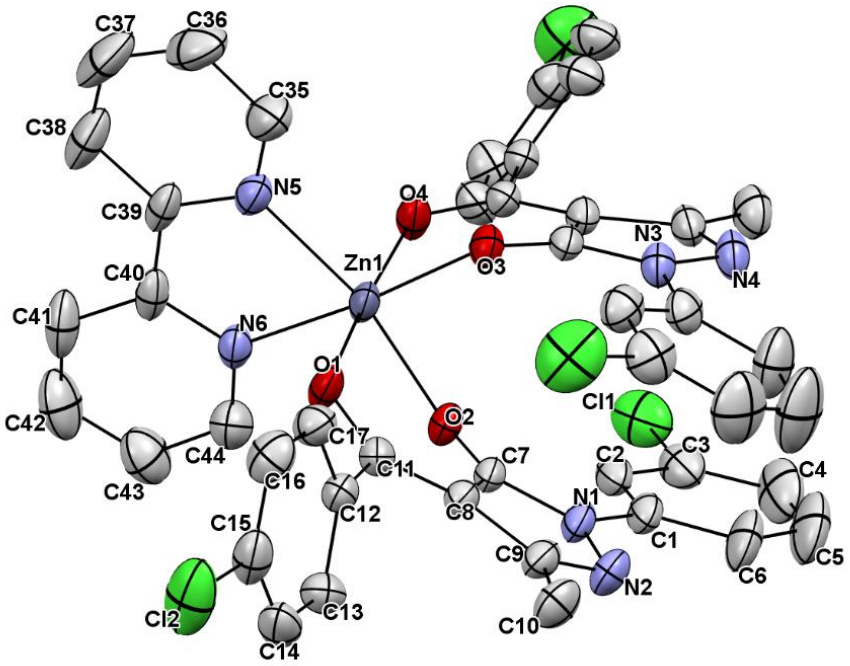

Fig. 2.2.10. ORTEP ellipsoid with 35% probability diagram of Complex **6**. H-atoms and needless atomic numbers are omitted for clarity.

The Zn(II) metal ion, which strays from the equatorial plane 0.008 Å. The coordination plane around Zn(II) ion composed of O(2), O(3), N(5) and N(6) atoms and regular bond distances of Zn(1)–O(2), Zn(1)–O(3), Zn(1)–N(5) and Zn(1)- N(6) are 2.069(15) Å, 2.061(17) Å, 2.150(2) Å and 2.140(2) Å respectively. Two oxygens [O(1) and O(4)] of L2 are in axial positions with distance from the equatorial plane are 2.109 Å and 2.129 Å respectively.[7,9]

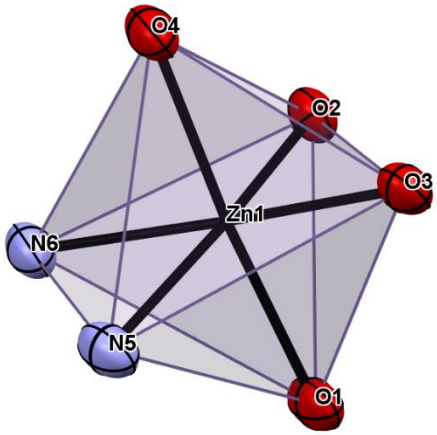

Fig. 2.2.11. Distorted Octahedral geometry around zinc(II) ion in the complex **4**.

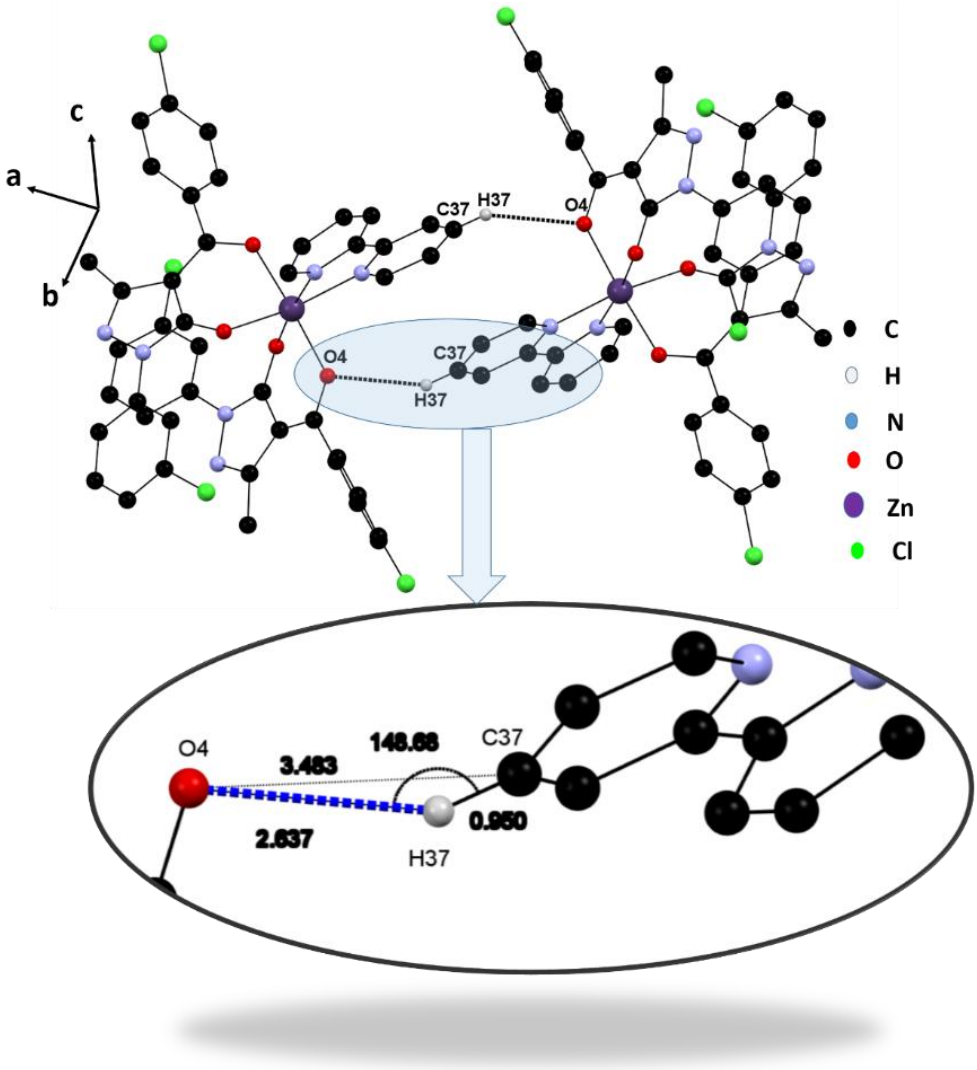

Fig. 2.2.12. Intermolecular H-bond in complex **6** $[Zn(L2)_2(bpy)]$.

The angels of O(2)–Zn(1)–N(5), O(3)–Zn(1)–N(6) and O(1)–Zn (1)–O(4) are 167.91(7)°, 174.87(7)° and 175.91(6)°, respectively, which are deviated from the theoretical value of 180° of proper geometric structure. Therefore, the local coordination geometry around the Zn(II) center can be described as a distorted octahedron.

The angles of the O(2)–Zn(1)–O(1), O(3)–Zn(1)–O(1), O(1)–Zn(1)–N5), O(1)–Zn(1)–N(6), O(2)–Zn(1)–O(4), O(3)–Zn (1)–O(4), O(4)–Zn(1)–N(5) and O(4)–Zn(1)–N(6) are 86.65(6) °, 90.15(7) °, 89.10(7) °, 93.57(7) °, 91.67(6) °, 86.13(7)°, 100.59(8)° and 90.25(7)° respectively, which are deviated from 90° angle between the axial line and equatorial plane. Therefore geometry around the zinc ion in the complex is distorted octahedral (*see* Fig.2.2.11).[6,7,14] Complex **6** having intermolecular H-bond between a Hydrogen atom (H37-C37) of 2,2′-bipyridine and O-atom (O4) of acylpyrazolone moiety (Fig. 2.2.12). Crystal packing system depicted in Fig. 2.2.13.

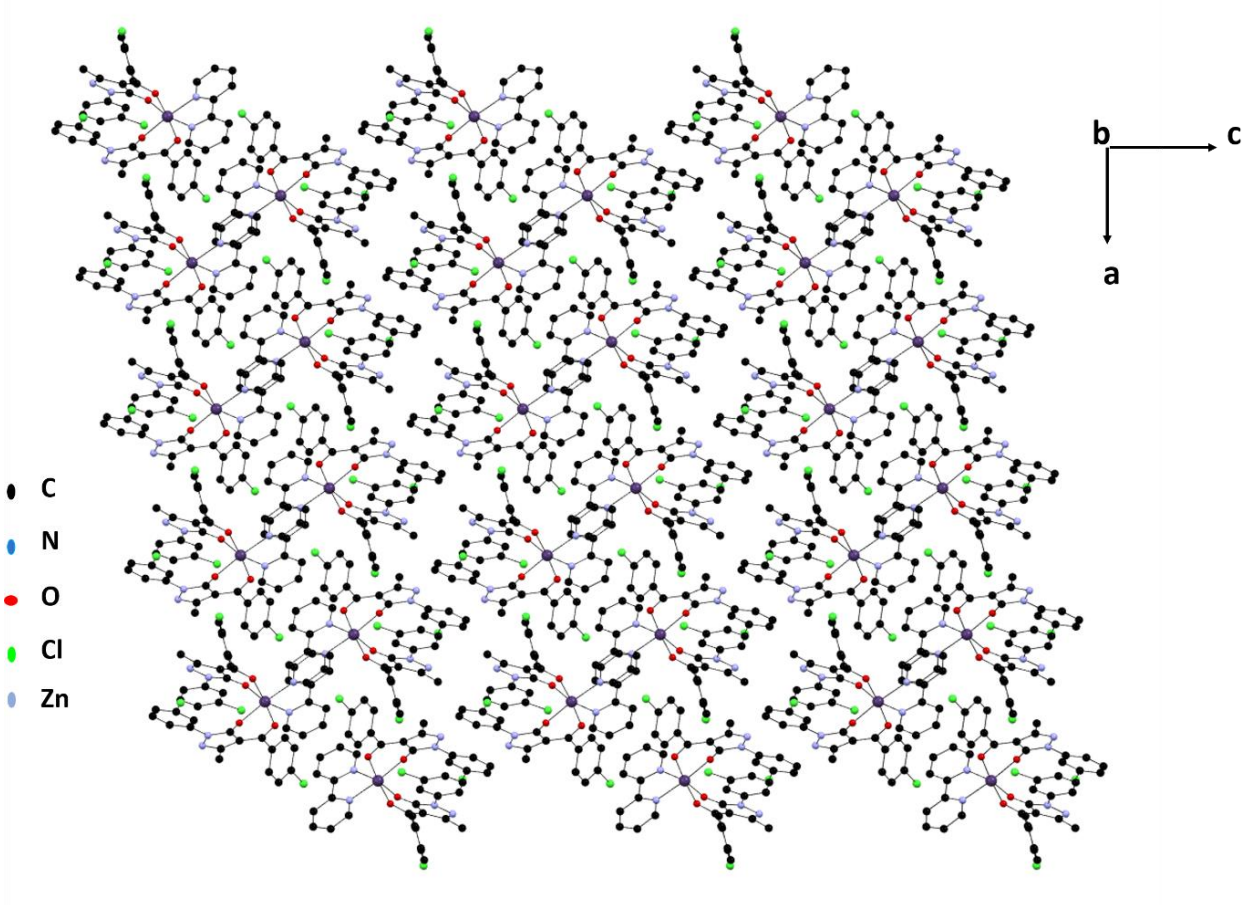

Fig. 2.2.13. Crystal packing viewed down from 'b' axis of complex **6**. The 2,2′-bipyridine rings were arranged parallel to each other.

Table 2.2.2. Hydrogen–bonding geometry (esd's in parentheses).

Complex	**D-H...A**	**d(D-H)/** Å	**d(H-A)/** Å	**d(D-A)/** Å	**D-H-A/°**
4	C3-H3...O4	0.930	2.523	3.260	136.42
6	C37-H37...O4	0.950	2.637	3.483	148.68
8	(i) C44-H44...O5	0.930	2.584	3.180	122.38
	(ii)C43-H43...O2	0.930	2.610	3.457	151.69
9	C45-H45...O1	0.930	2.615	3.446	149.19

Symmetry code: **4:** -x,1/2+y,1/2-z**, 6:** -x,-y,-z**, 8:** 1/2-x,1/2+y,1/2-z

3.1.4. Crystal structure of $[Zn(L3)_2(bpy)]$ (complex 8)

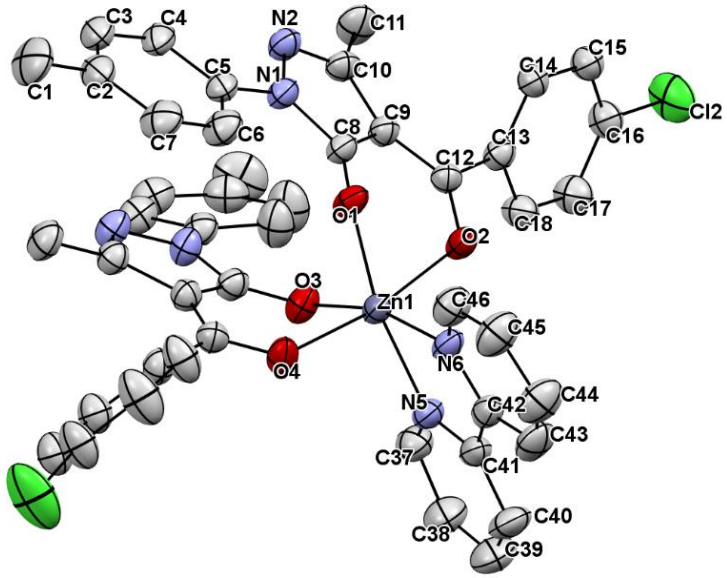

Fig. 2.2.14. ORTEP ellipsoid diagram with 35% probability of complex **8**, H-atoms are omitted for clarity.

Complex **8** has also 2,2′-bipyridine with two acyl pyrazolones (L3). Selected bond length and bond angles of complex **8** presented in Table 2.2.3. The single crystal X-ray analysis for complex **8**, the structure had general formula ML_2L' (where, L=L3 and L' is 2,2′-bipyridine).

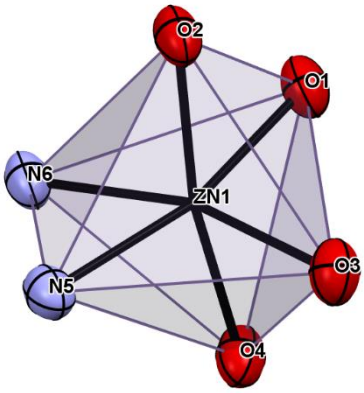

Fig. 2.2.15. Distorted octahedral geometry shown down b-axis around Zn(II) ion the complex **8** $[Zn(L3)_2bpy]$.

The zinc (II) ion is Hexa coordinated by four oxygen atoms (O1, O2, O3 and O4) of two acyl pyrazolone ligand (L3) and two nitrogen atoms (N5 and N6) of the 2,2′-bipyridine . The

structure of complex **8** is illustrated in Fig. 2.2.14. Two oxygens [O(1)and O(3)] from two L3 and two nitrogens [N(5) and N(6)] from 2,2′-bipyridine creates the equatorial plane. Deviation of coordination atoms O(1), O(3), N(5) and N(6) from the mean plane are 0.128, 0.131, 0.157 and 0.154 Å, respectively. The Zn(II) metal ion, which strays from the equatorial plane 0.015Å.

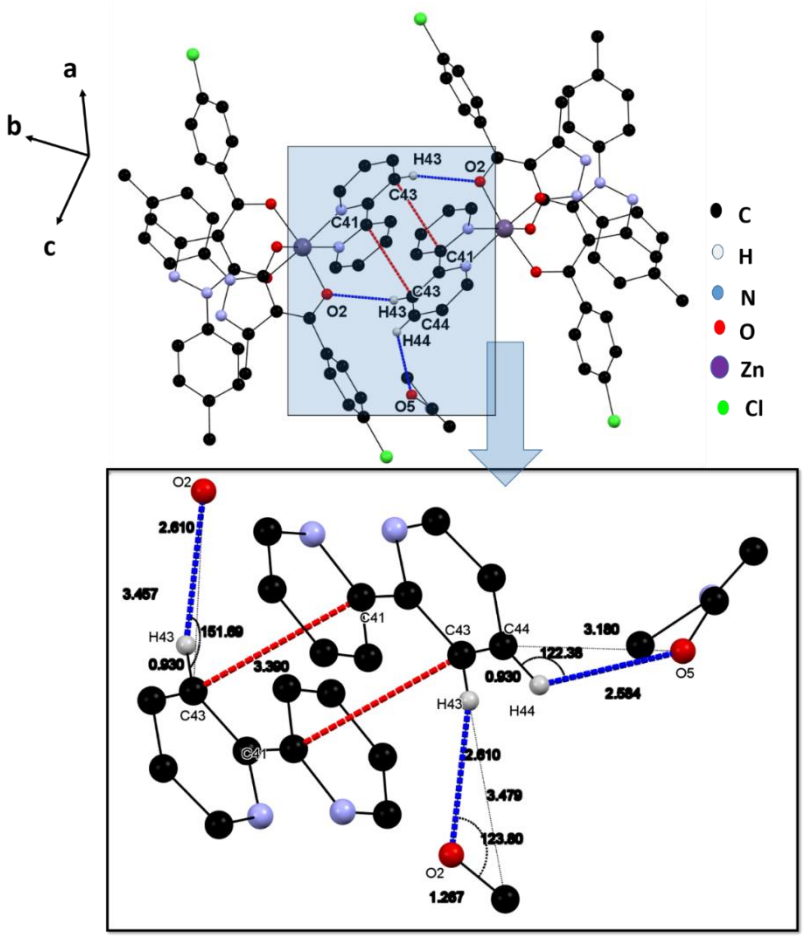

Fig. 2.2.16. Inter molecular H-bond and pi-pi stacking in the complex **8** [$Zn(L3)_2(bpy)$].

The coordination plane around Zn(II) ion is composed of O(1), O(3), N(5) and N(6) atoms. Regular bond distances of Zn(1)–O(1), Zn(1)–O(3), Zn(1)–N(5) and Zn(1)- N(6) are 2.071(3) Å, 2.064(3) Å, 2.126(4) Å and 2.111(4) Å respectively. Two oxygens [O(2) and O(4)] of L3 are in axial positions with distance from the equatorial plane are 2.144 Å and 2.080 Å respectively.[7,9]

The angles of O(1)–Zn(1)–N(5), O(3)–Zn(1)–N(6) and O(2)–Zn (1)–O(4) are 168.02(14)°, 164.78(15)° and 170.44(13)°, respectively, which are deviated from the theoretical value of 180° of proper geometric structure. Therefore, the local coordination geometry around the Zn(II) centre can be described as a distorted octahedron (Fig. 2.2.15).

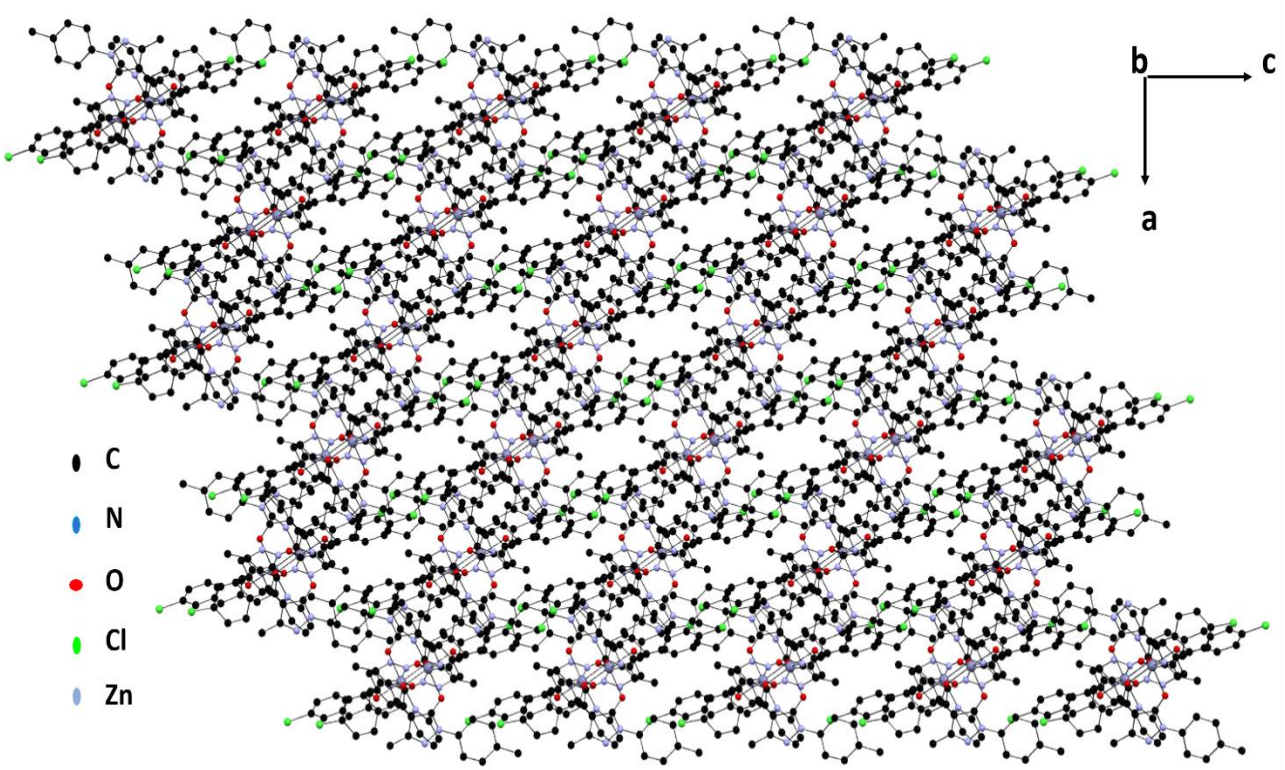

Fig. 2.2.17. Crystal packing viewed down from '*b*' axis of complex **8**. The bipyridyl rings were arranged parallel to each other of complex **8**.

The angles of the O(2)–Zn(1)–O(1)(83.89(13)°), O(3)–Zn(1)–O (1)(83.89(13)°), O(2)–Zn(1)–N(5)(98.68(13)°), O(2)–Zn(1)–N(6) (89.83(14)°), O(1)–Zn(1)–O(4) (99.07(14) °), O(3)–Zn (1)–O(4) (88.20(14)°), O(4)–Zn(1)–N(5) (85.69(14)°) and O(4)–Zn(1)–N(6) (86.83(14)°) deviate from 90° angle between the axial line and equatorial plane. Therefore geometry around the zinc(II) ion in the complex is distorted octahedral (Fig. 2.2.15).[6,7,14] Complex displayed π-π stacking and intermolecular H-bond (Fig. 2.2.16). Face to face pi-pi stacking shows between bipyridyl rings and two intermolecular H-bond showed, first H-bond showed between H-atoms (C44-H44) of 2,2′-bipyridine and O-atom(O5) of DMF and second H-bond showed between H-atom(C43-H43) of 2,2′-bipyridine and O-atom(O2) of acyl pyrazolone (Fig. 2.2.17).

3.1.5. Crystal structure of $[Zn(L3)_2(phen)]$ (complex 9).

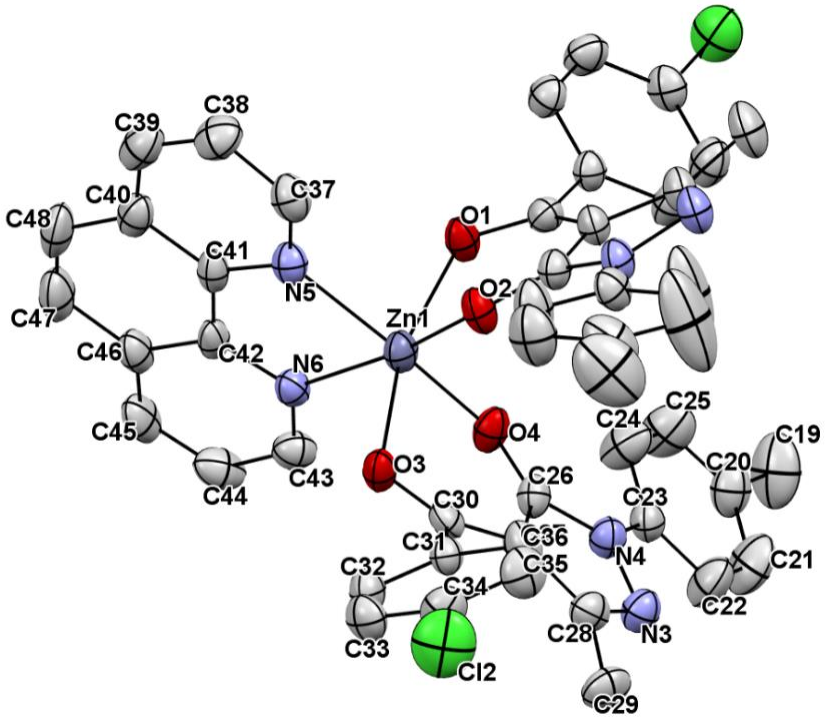

Fig. 2.2.18. ORTEP ellipsoid with 35% probability of complex **9**, H-atoms and solvent molecule are omitted for clarity.

The mixed ligand complex **9**, 1,10-phenanthroline as a secondary ligand in structure. Selected bond lengths and bond angles are illustrated in Table 2.2.3.As shown in Fig. 2.2.18, Two oxygen atoms O(2) and O(3) of each 4-acyl pyrazolone (L3) are generated equatorial plane with two nitrogen atoms of 1,10-phenanthroline. Deviation of coordination atoms O(2), O(3), N(5) and N(6) from the mean plane are 0.108 Å, 0.111 Å, 0.130 Å and 0.131 Å, respectively. The Zn(II) metal ion, which strays from the equatorial plane 0.018 Å. The coordination plane around Zn(II) ion is composed of O(2), O(4), N(5) and N(6) atoms. Regular bond distances of Zn(1)–O(2), Zn(1)–O(4), Zn(1)–N(5) and Zn(1)- N(6) are 2.042(3) Å, 2.034(3) Å, 2.144(4) Å and 2.154(3) Å, respectively.[7,17,18] Two oxygen atoms O(1) and O(3) of acyl pyrazolone (L3) are at axial position. Angles between O(2)-Zn(1)-N(6), O(4)-Zn(1)-N(5) and O(1)-Zn(1)-O(3) are 166.95(13)°, 164.65(12)°, and 163.50(10)° respectively. These angles have deviated from the theoretical value of 180° of proper geometric structure. Therefore, the local coordination geometry around the Zn(II) center can be described as a distorted octahedron (Fig. 2.2.19).

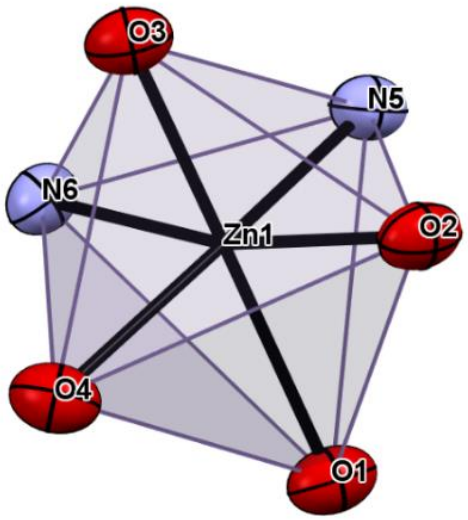

Fig. 2.2.19. Distorted octahedral geometry showed down the b-axis of zinc(II) complex [Zn(L3)$_2$phen].

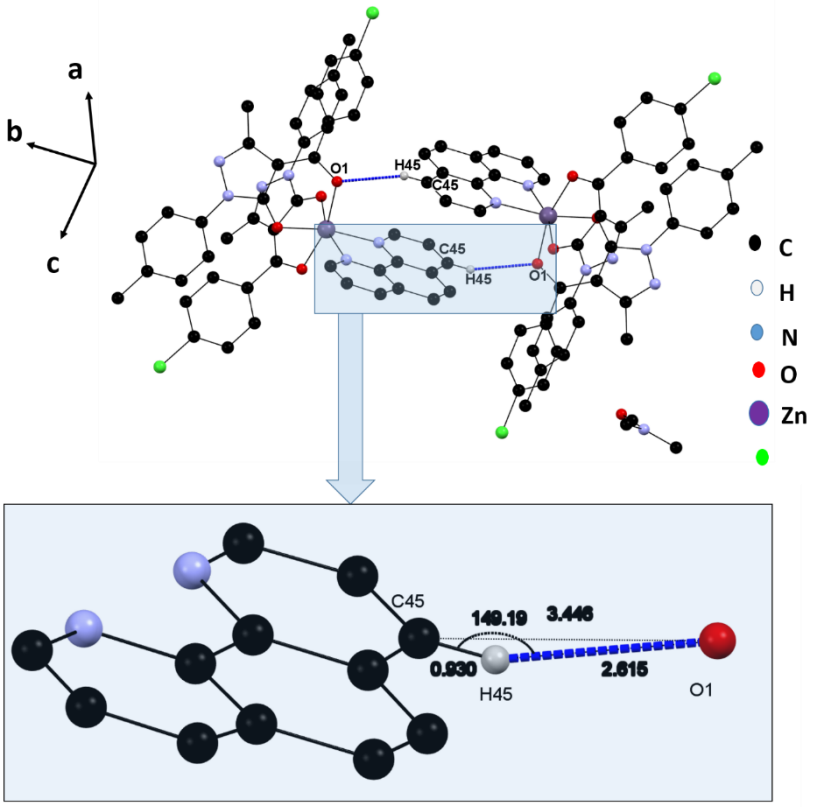

Fig. 2.2.20. Inter molecular H-bond in complex **9** [Zn(L3)$_2$(phen)].

The angles of the O(4)–Zn(1)–O(2), O(4)–Zn(1)–N(6), N(5)–Zn(1)–N(6), O(2)–Zn(1)–N(5), O(1)–Zn(1)–O(4), O(3)–Zn(1)–O(4), O(1)–Zn(1)–N(5) and O(3)–Zn(1)–N(6) are 101.76(12)°, 90.37(13)°, 76.73(14)°, 91.90(13)°, 83.87(11)°, 87.02(11)°, 90.08(12)° and 94.03(11)° respectively, which are deviated from 90° angle between the axial line and equatorial plane. Therefore geometry around the zinc ion in the complex is distorted octahedral (Fig. 2.2.19).[6,7,9] In the complex **9**, there is intermolecular H-bond between electropositive hydrogen (C45-H45) atom of 1, 10-phenanthroline and electronegative O-atom (O(1)) of acyl pyrazolone. H-bond parameters and symmetry presented in Table 2.2.2 and H-bond diagram presented in Fig. 2.2.20. Complex 9 packing system is shown in Fig. 2.2.21.

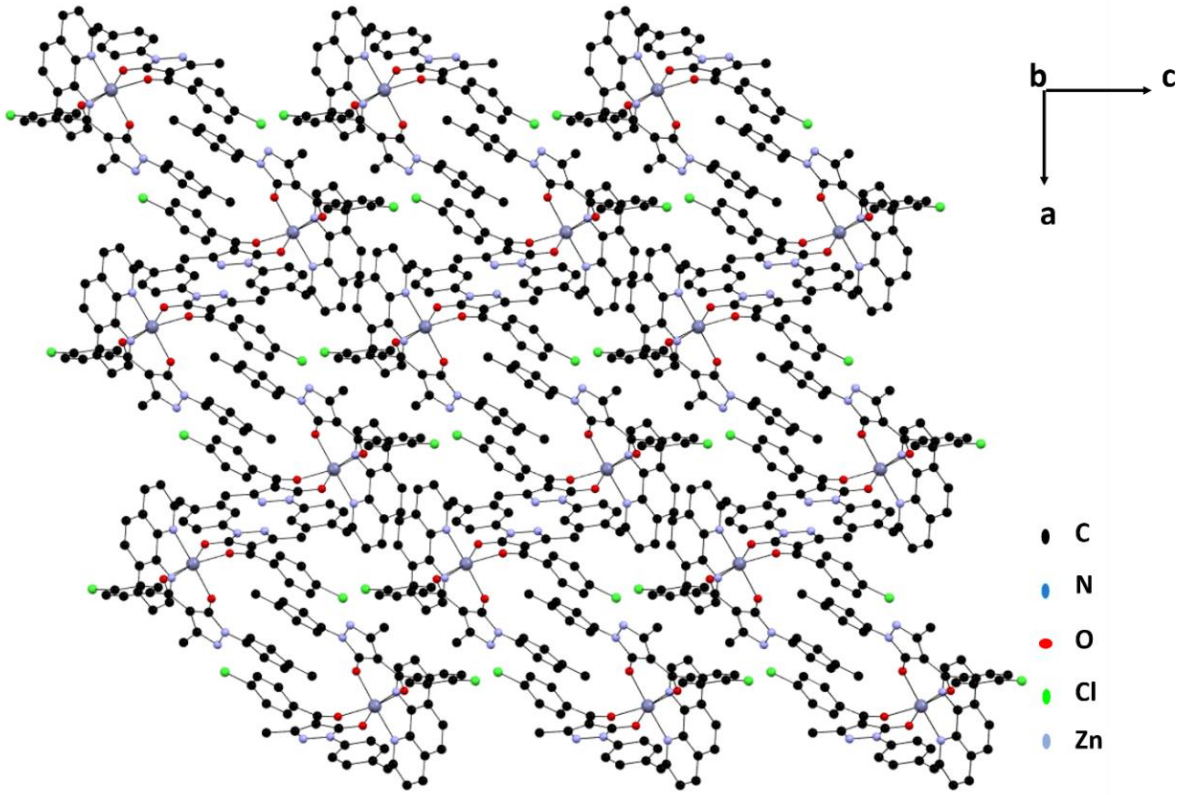

Fig. 2.2.21. Crystal packing system viewed down from 'b' axis of complex **9**.

Table 2.2.3. Selected bond angle and bond length for complexes **4, 6, 8** and **9.**

Complex **4**

Atom	**Length/Å**	**Atom**	**Angle/°**
Zn1-O2	2.030(2)	O2-Zn1-O3	97.67(10)
Zn1-O3	2.053(2)	O2-Zn1-O1	86.16(10)
Zn1-O1	2.104(2)	O3-Zn1-O1	85.82(9)
Zn1-N1	2.108(3)	O2-Zn1-N1	168.06(12)
Zn1-O4	2.126(2)	O3-Zn1-N1	94.25(13)
Zn1-N2	2.131(3)	O1-Zn1-N1	95.29(11)
C21-O3	1.258(4)	O2-Zn1-O4	87.54(10)
C21-N6	1.357(4)	O3-Zn1-O4	84.68(9)
C21-C18	1.421(5)	O1-Zn1-O4	167.81(9)
N2-C10	1.313(5)	N1-Zn1-O4	93.03(11)
N2-C6	1.341(5)	O2-Zn1-N2	91.81(12)
C18-C17	1.407(4)	O3-Zn1-N2	170.50(12)
C18-C19	1.429(5)	O1-Zn1-N2	94.34(10)
C19-N5	1.308(4)	N1-Zn1-N2	76.26(15)
C19-C20	1.495(5)	O4-Zn1-N2	96.28(10)
C16-C11	1.363(5)	O3-C21-N6	123.6(3)

complex 6

Atom	**Length/Å**	**Atom**	**Angle/°**
Zn1-O4	2.1225(16)	O4-Zn1-N6	90.25(7)
Zn1-O3	2.0610(17)	O4-Zn1-N5	93.26(7)
Zn1-O1	2.1187(16)	O3-Zn1-O4	86.13(7)
Zn1-O2	2.0693(15)	O3-Zn1-O1	90.15(7)
Zn1-N6	2.140(2)	O3-Zn1-O2	90.74(6)
Zn1-N5	2.150(2)	O3-Zn1-N6	174.87(7)
Cl2-C15	1.740(3)	O3-Zn1-N5	100.59(8)
Cl1-C3	1.740(3)	O1-Zn1-O4	175.91(6)

Cl4-C32	1.743(3)	O1-Zn1-N6	93.57(7)
O4-C28	1.263(3)	O1-Zn1-N5	89.10(7)
O3-C24	1.273(3)	O2-Zn1-O4	91.67(6)
complex **8**			
Atom	**Length/Å**	**Atom**	**Angle/°**
Zn1-O2	2.138(3)	O3-Zn1-O2	90.21(14)
Zn1-O3	2.064(3)	O3-Zn1-O1	98.68(13)
Zn1-O1	2.071(3)	O3-Zn1-O4	85.69(14)
Zn1-O4	2.103(3)	O3-Zn1-N5	91.52(15)
Zn1-N5	2.126(4)	O3-Zn1-N6	164.78(15)
Zn1-N6	2.111(4)	O1-Zn1-O2	83.89(13)
Cl2-C16	1.734(5)	O1-Zn1-O4	88.20(14)
Cl1-C34	1.732(6)	O1-Zn1-N5	168.02(14)
O2-C12	1.265(5)	O1-Zn1-N6	94.31(14)
O3-C26	1.267(6)	O4-Zn1-O2	170.44(13)
		O4-Zn1-N5	98.89(15)
complex 9			
Atom	**Length/Å**	**Atom**	**Angle/°**
Zn1-O3	2.160(3)	O3-Zn1-O1	163.50(10)
Zn1-O2	2.042(3)	O2-Zn1-O3	81.95(11)
Zn1-O1	2.160(3)	O2-Zn1-O1	86.47(11)
Zn1-O4	2.034(3)	O2-Zn1-N6	166.95(13)
Zn1-N6	2.154(3)	O2-Zn1-N5	91.90(13)
Zn1-N5	2.144(4)	O4-Zn1-O3	87.02(11)
Cl1-C16	1.744(4)	O4-Zn1-O2	101.76(12)
Cl2-C34	1.734(4)	O4-Zn1-O1	83.87(11)
O3-C30	1.260(4)	O4-Zn1-N6	90.37(13)
O2-C8	1.262(5)	O4-Zn1-N5	164.65(12)
O1-C12	1.268(5)	N6-Zn1-O3	94.03(11)

2.2.3.2. ^{1}H and ^{13}C NMR spectral study

Complex 4

In the ^{1}H NMR spectrum of complex **4**, Spectrum shows a singlet at 1.61 δ ppm, which confirm the presence of a methyl group. A triplet in the aromatic region at 7.07 δ ppm indicates proton at 4th position of the phenyl ring. Multiplet at 7.19-7.32 δ ppm indicates aromatic protons of L1 ligand. The spectrum shows two triplets at 7.58-7.6 δ and 8.01-8.02 δ ppm confirm aromatic protons of the phenyl ring and a proton of 2,2′-bipyridine , respectively. A doublet at 9.05-9.06 δ ppm indicates proton of 2,2′-bipyridine which is near to N-atom in the ring.

^{13}C NMR spectrum of the complex **4**, the spectrum shows 18 peaks in the spectrum, which correspond to the presence of 18 carbons of different chemical environment. The spectrum shows a signal at 16.6 δ ppm, which confirm a methyl group of pyrazolone. Two carbon signals at 166.6 and 189.7 δ ppm specify C-O and C=O in the complex creation. Other signals are due to the L1 and bpy in the complex.

Complex 5 [Zn(L1)$_2$phen]

In the ^{1}H NMR spectrum of complex **5**, Spectrum shows a singlet at 1.62 δ ppm due to three proton of the methyl group of L1. The spectrum shows many multiplets in the aromatic region specified aromatic protons in the complex formation. A singlet at 9.35 δ ppm due to the proton of phen which near to N-atom in the moiety.

Complex 6 [Zn(L2)$_2$bpy]

In complex **6**, ^{1}H NMR spectrum shows a singlet at 2.2 δ ppm confirm methyl group of L2. The spectrum shows doublet at 7.00-7.02 δ ppm specified a proton and a triplet at 7.12-7.26 δ ppm confirm two protons of phenyl group of L2. The spectrum shows a triplet and two doublets of aromatic protons of 2,2′-bipyridine observed in the range 8-9.1 δ ppm.[6,7] Many multiplets signals show in the aromatic region for aromatic protons of the L2 ligand and 2,2′-bipyridine in the complex.

In the ^{13}C NMR spectrum, there were twenty signals displays in the spectrum which is a good proof of the formation of ternary zinc(II) complex of 4-acylpyrazolone and 2,2′-bipyridine . The spectrum shows a signal at 16.6 δ ppm confirms a methyl group of acylpyrazolone. The spectrum shows signals at 104, 150 and 169 δ ppm due to the stretching frequency of C=C, C=N and C-O, respectively. Two signals show at 139 and 139.9 δ ppm due to two C-Cl of the

ligand in the complex. The spectrum shows two signals at 148 and 149 δ ppm due to two C-N of 2,2′-bipyridine as a secondary ligand.

Complex 7 [Zn(L2)$_2$phen]

In the ^{1}H NMR spectrum of complex **7**, the spectrum shows singlet at aliphatic region confirm one methyl group of L2 and others protons in the aromatic region indicated aromatic protons of primary and secondary ligands. Protons of *m*-chlorophenyl observed with a singlet, two doublets and a triplet in region 7.01-7.80 δ ppm. The spectrum shows a doublet at 9.33-9.35 δ confirm a proton of bpy.^{1}H NMR spectrum is good agreement of formation of ternary Zn(II) complex.

In the ^{13}C NMR spectrum of complex **7**, the spectrum shows the signal at 16.5 δ due to the methyl group at the C3 position of acyl pyrazolone. Lower range signals show at 190 δ and 167 δ ppm due to carbonyl carbon and *p*-chloro benzoyl of L2. Two peaks show at 149 and 149.5 δ ppm confirm two C=N of pyrazolone ring. All other ^{13}C signals observe their expected region.

Complex 8 [Zn(L3)$_2$bpy]

In the ^{1}H NMR of complex **8,** two singlets show at 1.6 and 2.2 δ ppm confirm methyl and toluyl group of L3 respectively. The spectrum shows multiplets signals in an aromatic region due to aromatic protons of L3 and 2,2′-bipyridine .[6,7] Spectrum shows a doublet at 9.00-9.02 δ ppm for 2,2′-bipyridine proton (H-C-N). ^{1}H NMR spectrum is good agreement of structure formation of ternary Zn(II) complex of acyl pyrazolone and 2,2′-bipyridine .

Complex 9 [Zn(L3)$_2$phen]

In the ^{1}H NMR spectrum of complex **9**, Spectrum shows two singlets at 1.66 and 2.28 δ ppm for methyl of pyrazolone and toluyl respectively.[6,7] Spectrum shows a doublet at 9.30-9.32 δ ppm confirm 1,10-phenanthroline proton (H-C-N). Results are the good agreement of structure formation of ternary zinc(II) complex of acyl pyrazolone and 1,10-phenanthroline.[6,7] ^{1}H & ^{13}C NMR spectra of complexes are presented in Fig.2.2.22 – Fig. 2.2.29.

Such a type of heteroleptic Zn(II) complexes of acylpyrazolones give the possible geometrical isomerism. In this chapter, this kind of study couldn't performed due to lack of facilities. Marchetti *et al.*, reported zinc(II) complexes perform low temperature NMR studies in deuteorochloroform to eventually confirm or exclude more isomers in solution.[5]

^{1}H and ^{13}CNMR spectra

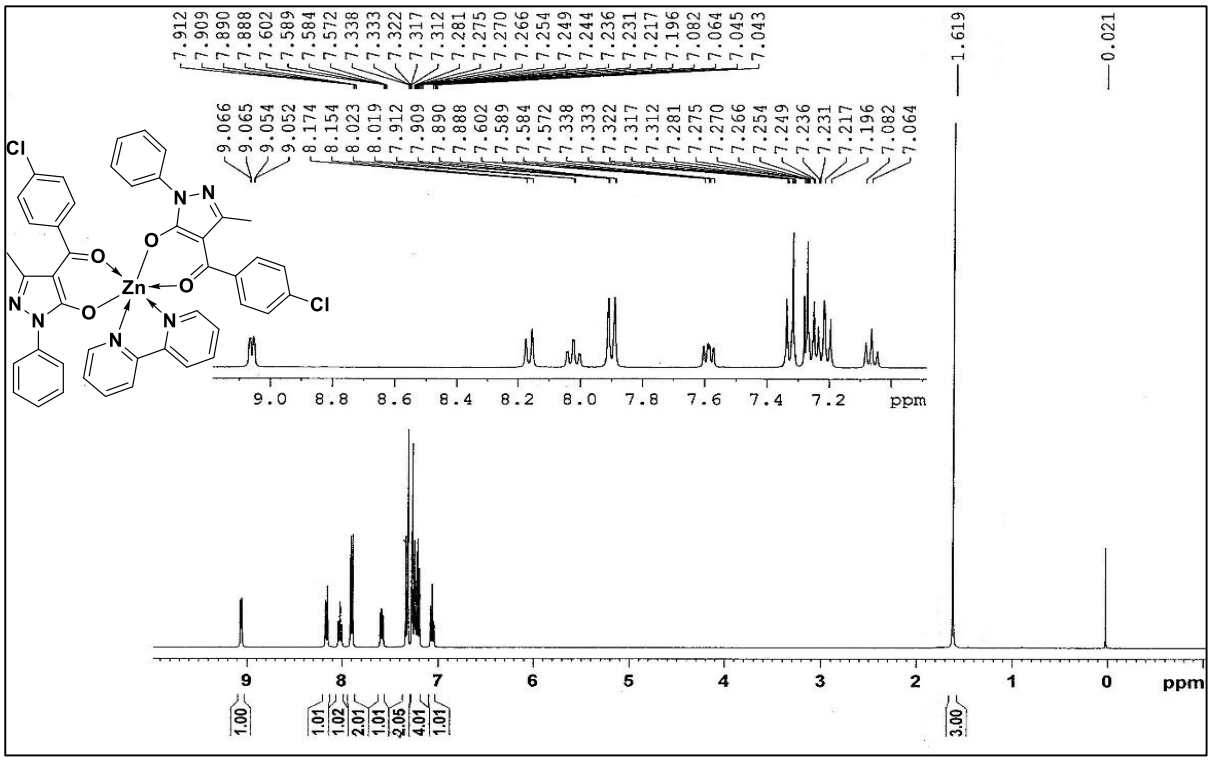

Fig. 2.2.22. ^{1}H NMR spectrum of complex 4 [Zn(L1)$_2$bpy].

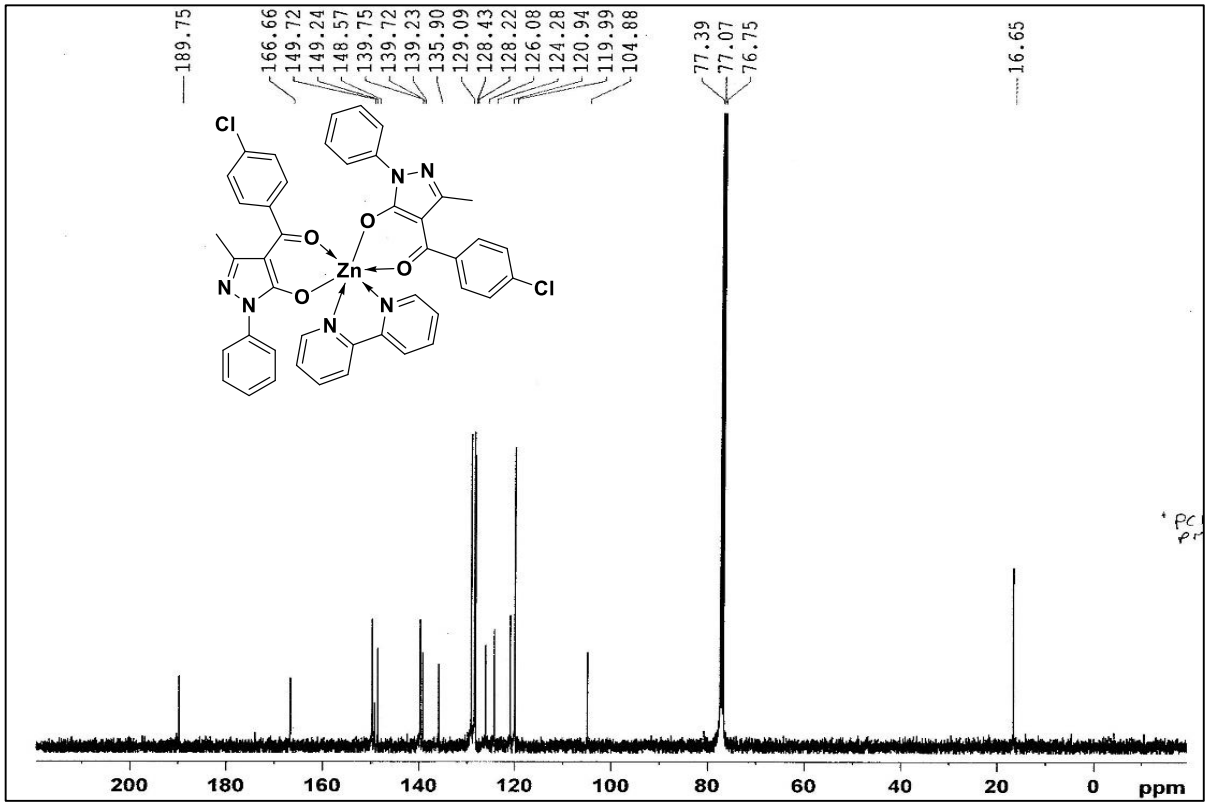

Fig. 2.2.23. ^{13}C NMR spectrum of complex **4** [Zn(L1)$_2$(bpy)].

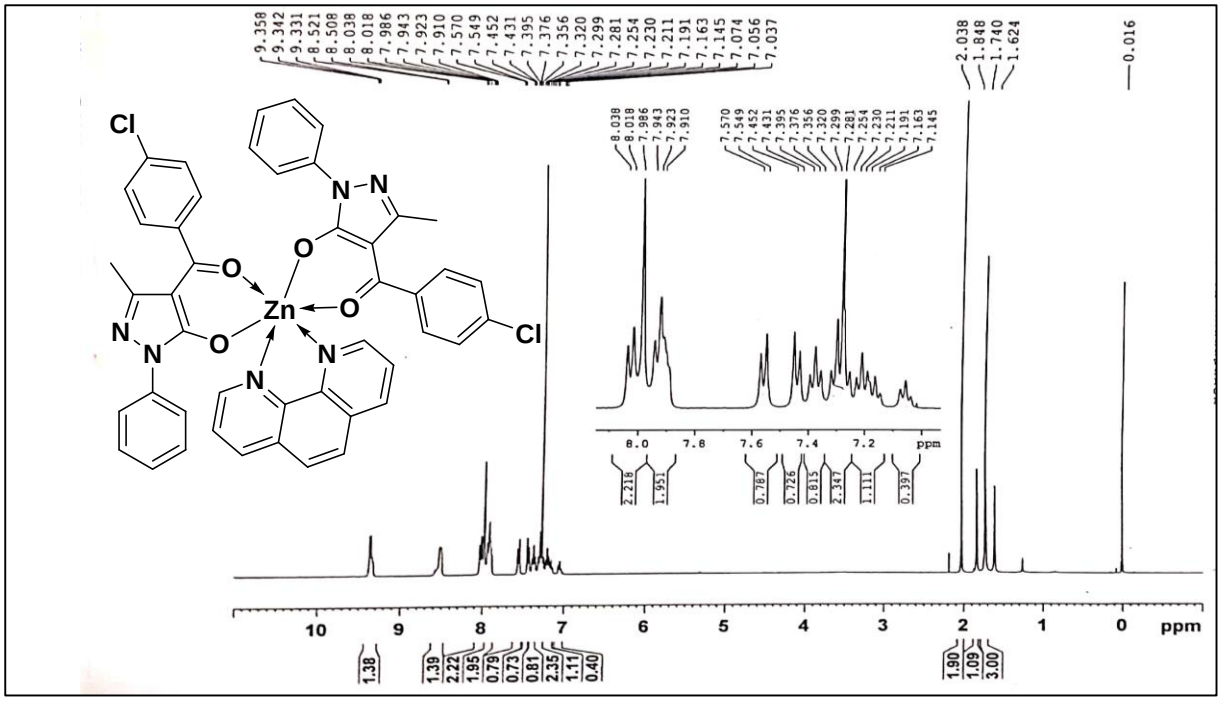

Fig. 2.2.24. ^{1}H NMR spectrum of complex **5** [Zn(L1)$_2$phen].

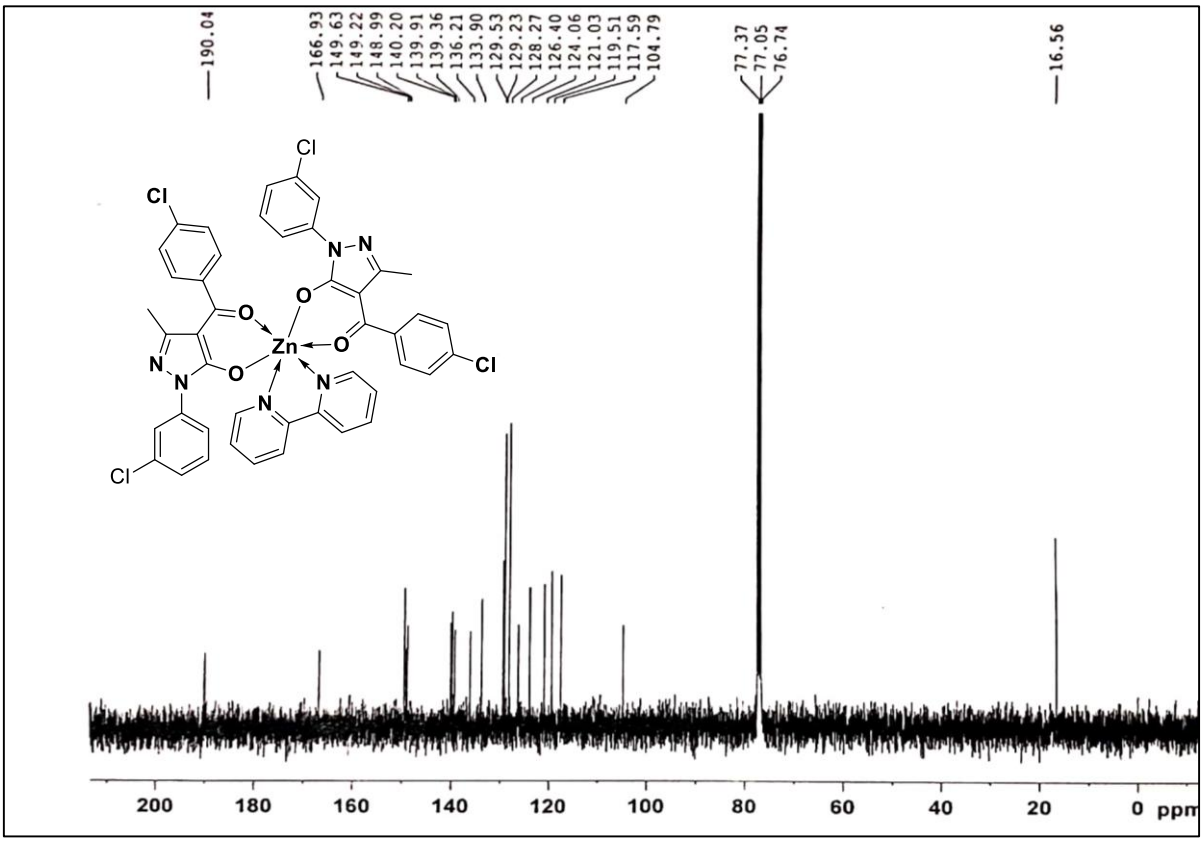

Fig. 2.2.25. ^{13}C NMR spectrum of complex **6** [Zn(L2)$_2$bpy].

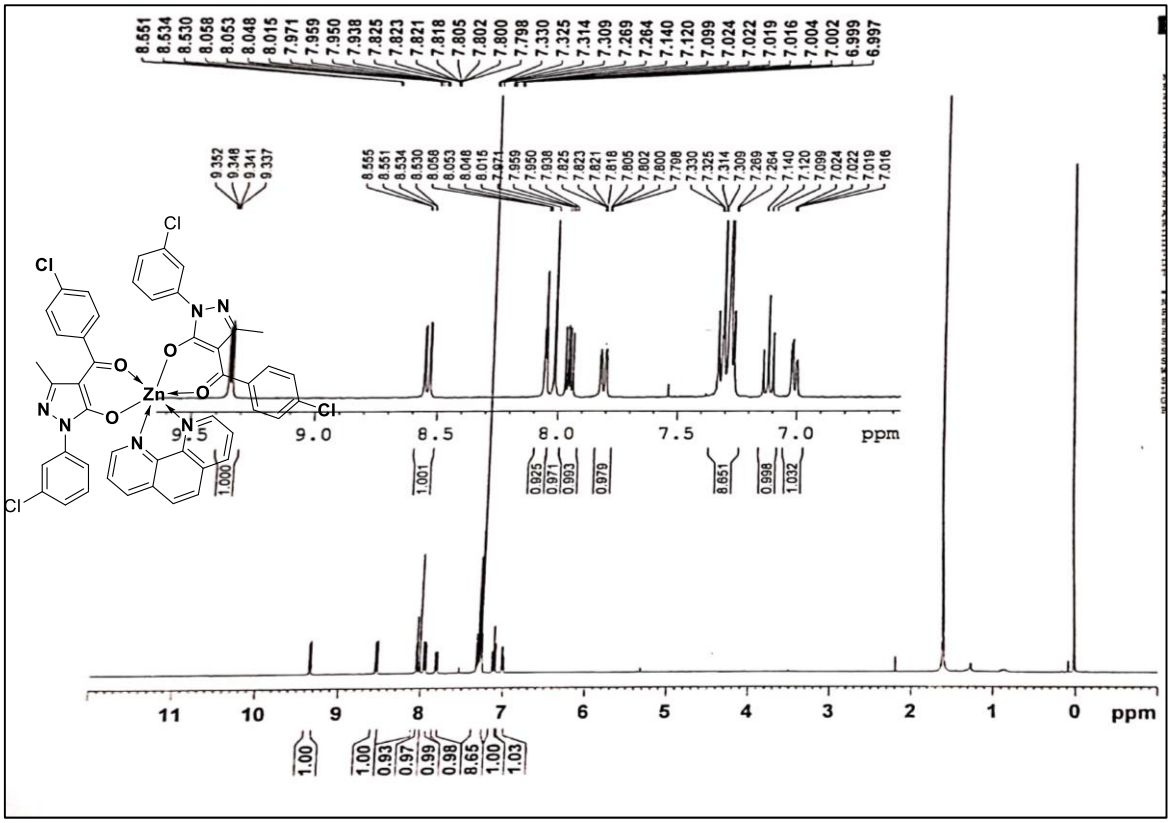

Fig. 2.2.26. ^{1}H NMR spectrum of complex **7** [Zn(L2)$_2$phen].

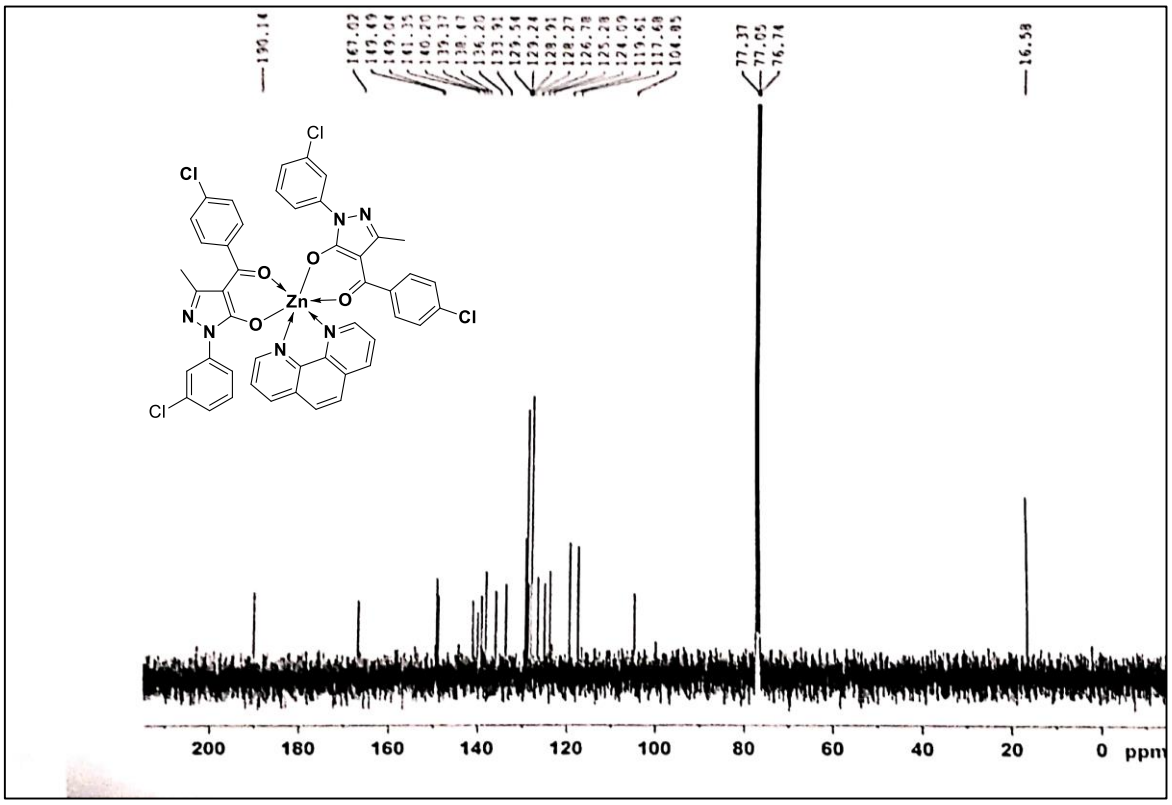

Fig. 2.2.27. ^{13}C NMR of complex **7** [Zn(L2)$_2$phen].

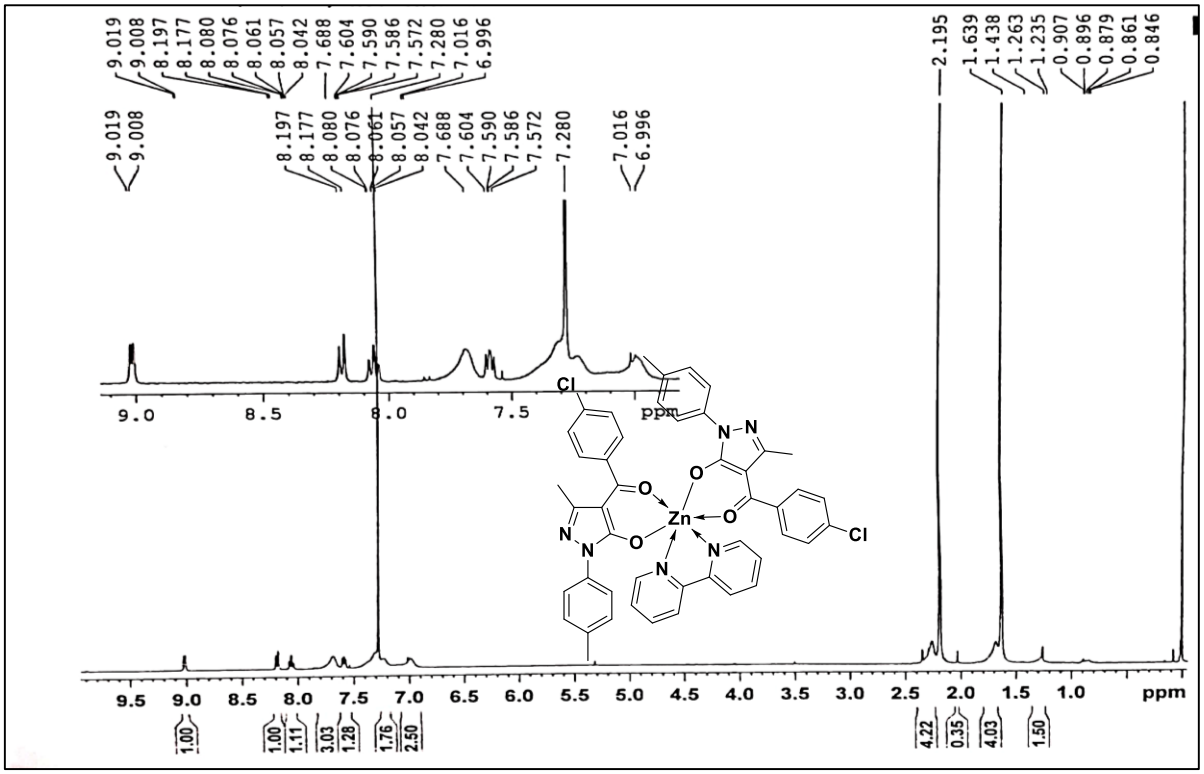

Fig. 2.2.28. ^{1}H NMR spectrum of complex **8** [Zn(L3)$_2$bpy].

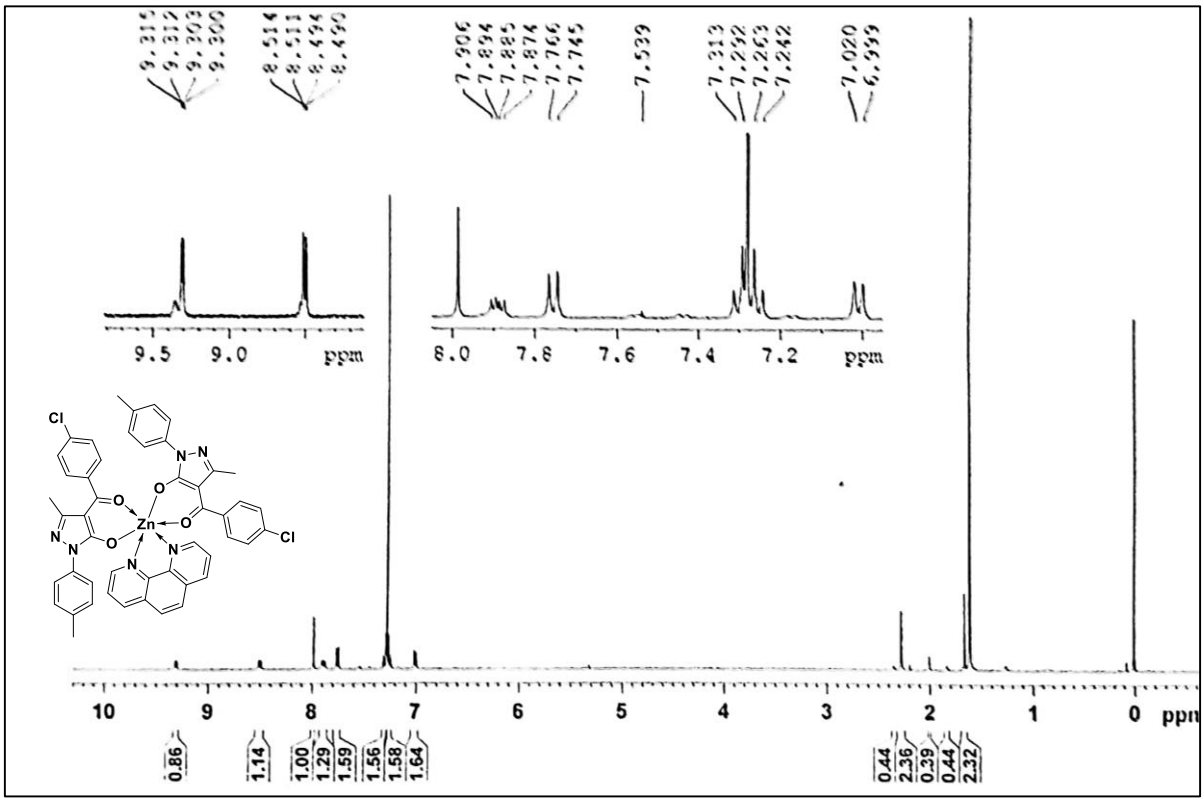

Fig. 2.2.29. ^{1}H NMR spectrum of complex **9** [Zn(L3)$_2$phen].

2.2.3.3. FTIR spectroscopy

The FTIR spectra of the complexes **4-9**, in the complex **4** FTIR spectrum, the spectrum shows a band at 1622 cm^{-1} assigned to υ(C=O) of *p*-chloro benzoyl of ligand L1 and a sharp peak at 1527 cm^{-1} due to the υ(C=N) of pyrazolone. Two small peaks at 420 and 480 cm^{-1} due to υM-O and υM-N, respectively[6,7,9,19]. In the FTIR spectrum of complex **5**, strong band observes at 1619 cm^{-1} due to the υ(C-O) stretching frequency. Pyrazolone υ(C=N) stretching exhibits at 1588cm^{-1} in the spectrum. The spectrum shows bands at 421 and 475 cm^{-1} for the stretching frequency of the metal-ligand bond of M-N and M-O, respectively. In the spectrum of complex **6,** the spectrum shows a sharp peak at 1621 cm^{-1}, which assign to υC=O of acylpyrazolone. The spectrum shows two peak at 471 and 439 cm^{-1} due to M-N and M-O stretching frequency, respectively. In the spectrum of complex **7,** the spectrum shows the carbonyl stretching of *p*-chloro benzoyl of L2 at 1622 cm^{-1}. The stretching frequency of υ(C=N) of pyrazolone exhibits at 1565 cm^{-1}. Compare to ligand spectrum, the new band detects in the complex spectrum at 1467 cm^{-1} is attributed to υ(C-O) stretching of pyrazolone ligands, which one was converted from C=O to C-O in the complexation reaction. Metal ligand M-O and M-N stretching frequencies exhibit at 439 and 481 cm^{-1}, respectively in FTIR spectrum. In the FTIR spectrum of complex **8,** absorptions show at 1626 and 1564 cm^{-1} due to $\upsilon CO_{(ketone)}$ and υC=N respectively. New bands show at 476 cm^{-1} and 415 cm^{-1} due to the *ν*(Zn-O) and *ν*(Zn-N), respectively.[7,20,21] In the spectrum of Complex **9,** the stretching frequencies show at 1622 and 1562 cm^{-1} due to $\upsilon CO_{(ketone)}$ and υC=N of L3 respectively. The spectrum shows new bands at 476 and 424 cm^{-1} due to the metal-ligand bond of υM-O and υM-N, respectively. Comparison between FT-IR spectra of ligands and complexes revealed that complex **4, 6** and **8** contain 2,2′-bipyridine and complex **5, 7** and **9** contain 1,10-phenanthroline with corresponding acyl pyrazolone ligand.[7,20,21] FTIR spectra are presented in Fig. 2.2.30-Fig. 2.2.35.

FTIR spectra

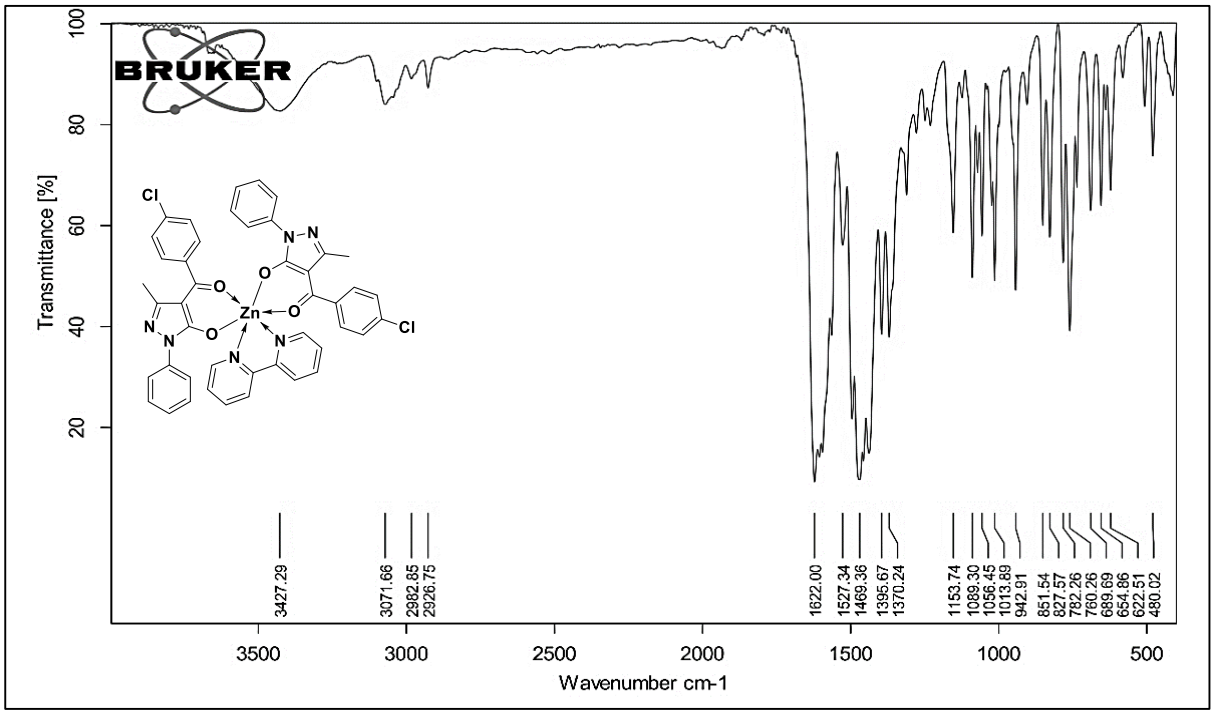

Fig. 2.2.30. FTIR spectrum of complex **4** $[Zn(L1)_2bpy]$.

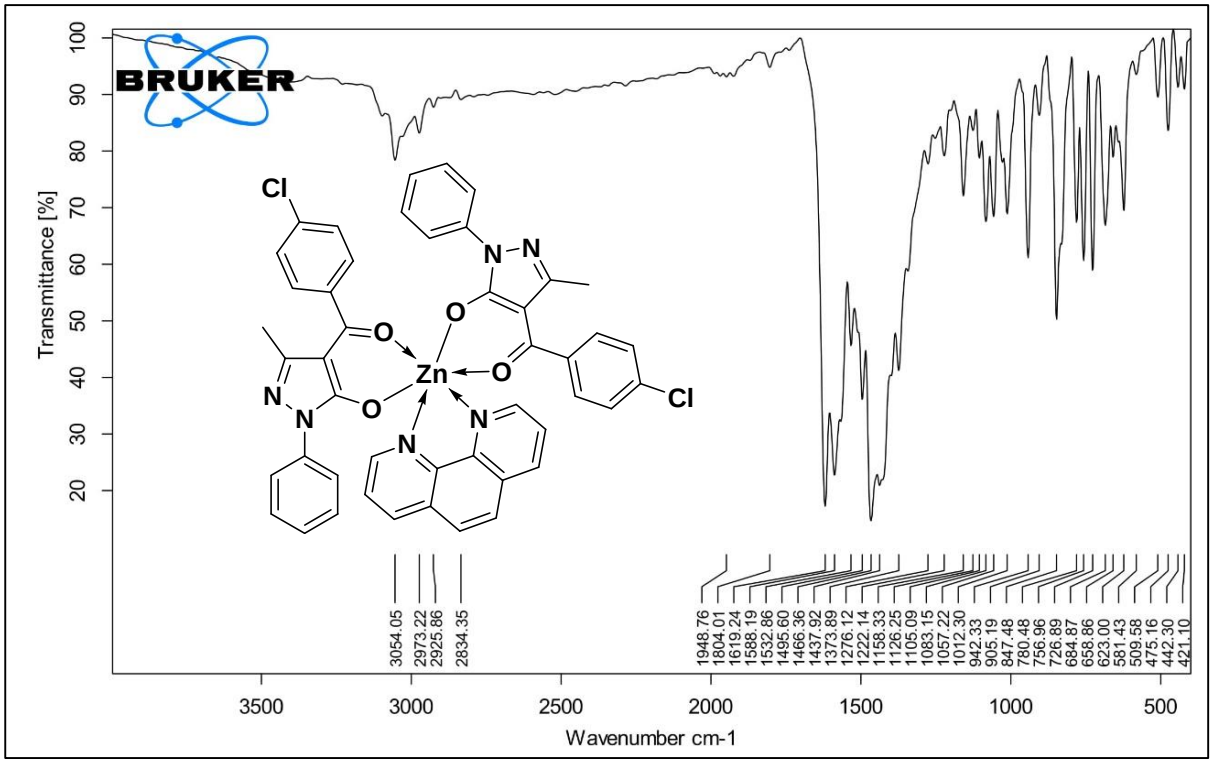

Fig. 2.2.31. FTIR spectrum of complex **5** $[Zn(L1)_2phen]$.

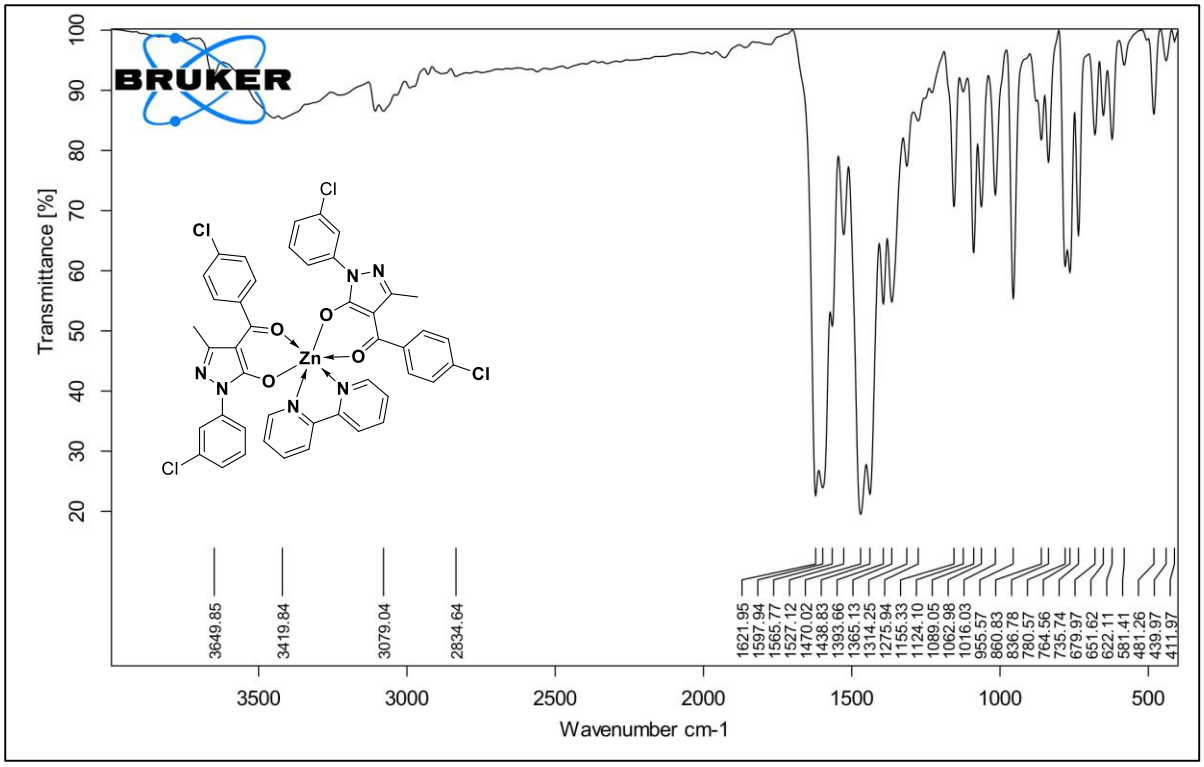

Fig. 2.2.32. FTIR spectrum of complex **6** $[Zn(L2)_2bpy]$.

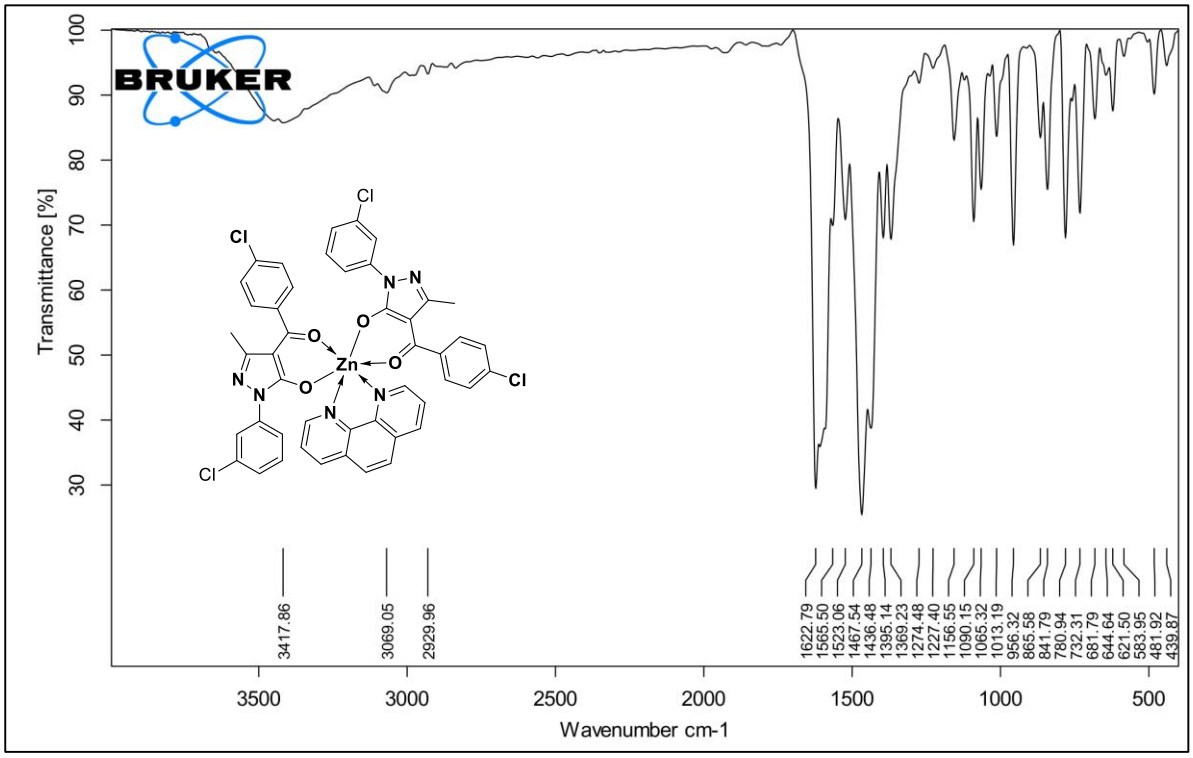

Fig. 2.2.33. FTIR spectrum of complex **7** $[Zn(L2)_2phen]$.

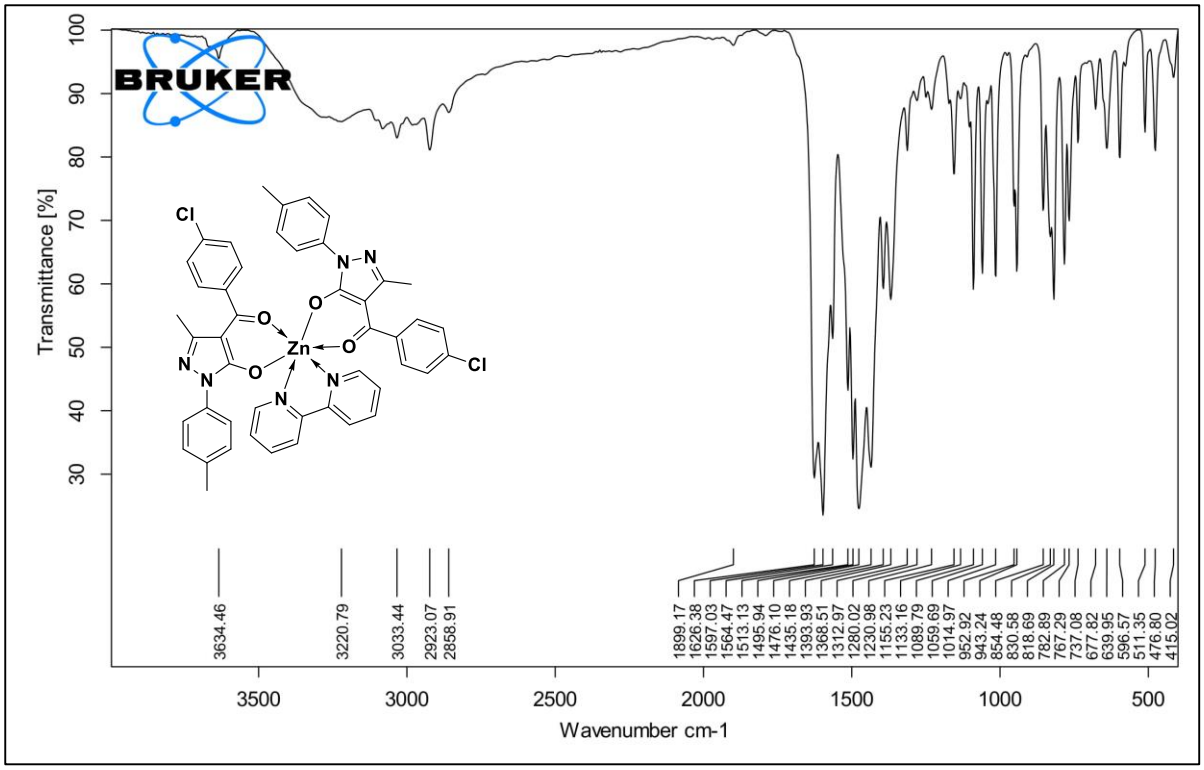

Fig. 2.2.34. FTIR spectrum of complex **8** [Zn(L3)$_2$bpy]

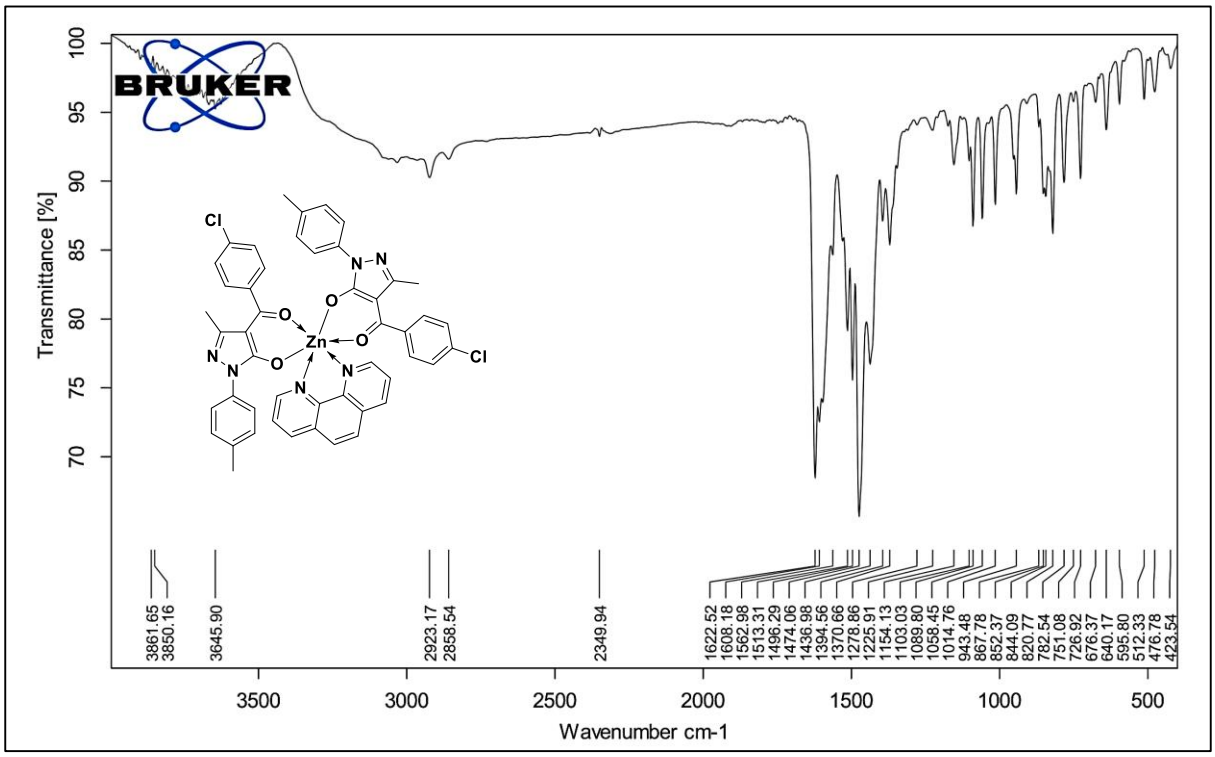

Fig. 2.2.35. FTIR spectrum of complex **9** [Zn(L3)$_2$phen].

2.2.3.4. Electronic spectral studies

Electronic spectra of ligands (L1, L2 and L3) and their zinc complexes **4-9** were recorded in DMSO (Fig. 2.2.36). Ligands and complexes were completely soluble in DMSO. In the Uv/Vis spectra of complexes, the first intense band is attributed to a ligand-centred (LC) π–π* transition localized on the aromatic rings of the ligand, while the shoulder due to its metal coordination and no d-d band was observed as expected for d^{10} configuration. Compounds bearing the coordinated *N*, *N*-aromatic ligands, also an intense band at 280 nm, and LMCT band at around 350-360 nm, all due to the 2,2′-bipyridine and 1,10-phenanthroline ligand.

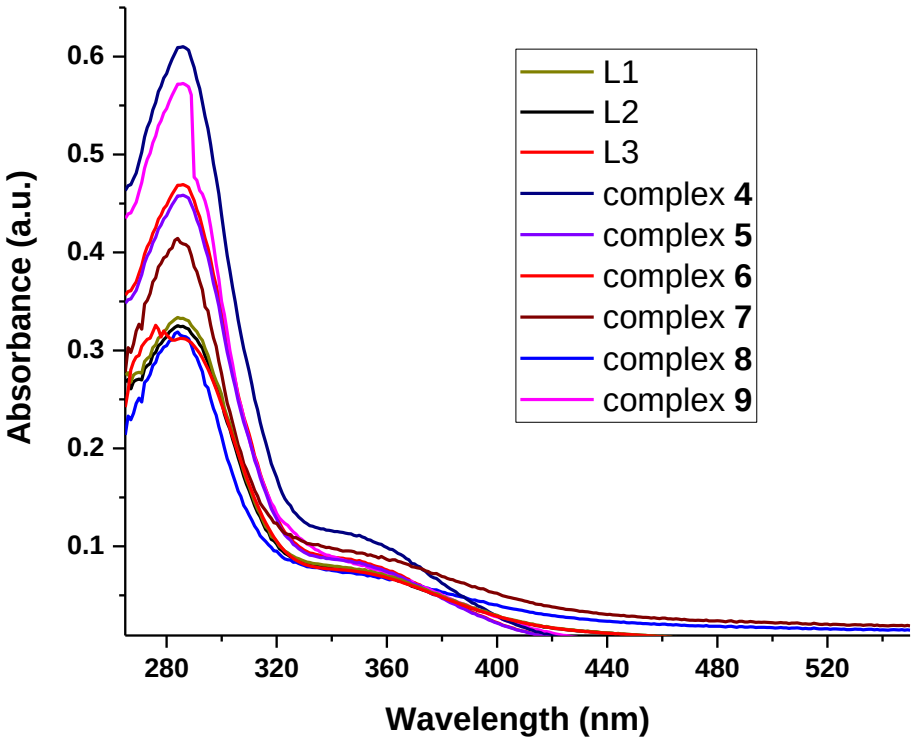

Fig. 2.2.36. UV-Vis spectra of ligands and complexes **4-9**.

2.2.3.5. Thermogravimetric analysis.

In the TGA graph of complexes **4-9**, the complexes were observed air stable (Fig.2.2.37). The thermal study was carried out using the thermogravimetric technique with a heating rate of 10 $^{o}C\ min^{-1}$.

TGA of complex 4 [Zn(L1)$_2$bpy]

In the TGA plot of complex **4,** there was no degradation up to 200 ºC, therefore, the good agreement of lattice water or methanol molecule absent in the complex structure. The compound shows stable in high temperature. Degradation starts after 200 ºC due to pyrolysis of a ligand in the complex.[7]

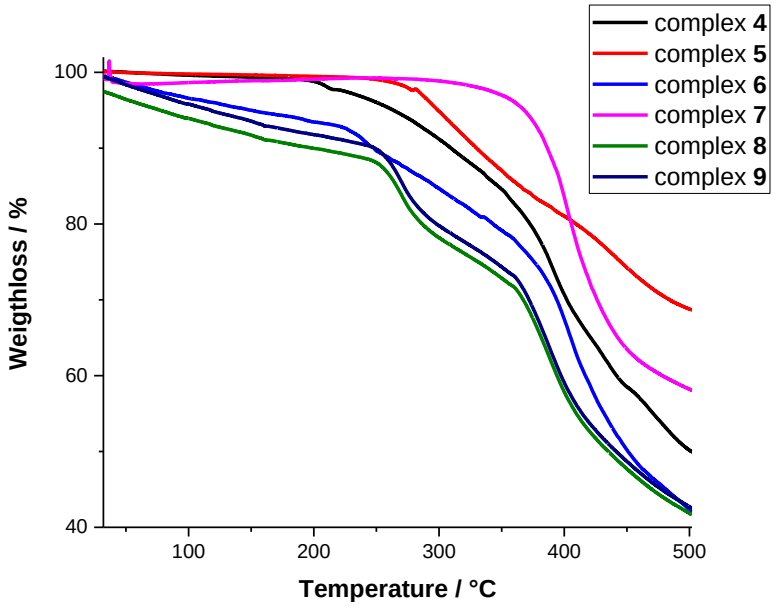

Fig. 2.2.37. Thermogravimetric analysis of complex **4-9.**

TGA of complex 5 [Zn(L1)$_2$phen]

In the TGA graph of complex 5, there was degradation start after 200 ºC due to the pyrolysis of ligand molecules. Ternary zinc(II) complex shows thermally and air stable in the TGA plot.

TGA of complex 6 [Zn(L2)$_2$(bpy)]

The complex **6** was observed air stable. TGA plot revealed Complex **6** has high thermal stability. Slowly Degradation was started up to 250 ºC is due to the lattice solvent molecule. The second degradation starts after 250 ºC due to pyrolysis of primary ligand L2 and secondary ligand 2,2′-bipyridine coordinated molecules present in the complex.[7,8]

TGA of complex 7 [Zn(L2)$_2$phen]

The plot of complex **7** revealed thermally stable and air stable ternary Zn(II) complex of acyl pyrazolone and phen. This complex showed highly thermally stable up 250ºC temperature.

Degradation starts after 250ºC due to degradation of coordinated acyl pyrazolone and phen in the complex.

TGA of complex 8 [Zn(L3)$_2$(bpy)]

The TGA revealed that the zinc complex **8** was found to be air stable and to have high thermal stability. Degradation observed after 240ºC due to pyrolysis of coordinated acyl pyrazolone ligand (L3)and secondary ligand (bpy) molecule in the complex[7].

TGA of complex 9 [Zn(L3)$_2$(phen)]

From the TGA plot, complex **9** found air stable and to have high thermal stability revealed from the TGA plot (Fig. 2.2.37). Degradation observed after 250 ºC due to pyrolysis of coordinated primary ligand (L3) and secondary ligand (phen) molecule in the zinc(II) complex[7].

2.2.3.6. Molar conductance study

The molar conductivity measured for all the complexes in 10^{-3} M DMSO solution is found to be below 14 ohm^{-1} cm^2 mol^{-1}. So the conductance measurements suggest that they are non-electrolytes.[22] The conductivity values are given in Table 2.2.4.[8]

Table 2.2.4. Molar conductance of ligands and complexes **4-9**.

Compound code	**Λ_m (s cm^2 mol^{-1})**
L1	9.7
L2	9.8
L3	8.8
[Zn(L1)$_2$(byp)] **4**	11.7
[Zn(L1)$_2$(phen)] **5**	13.2
[Zn(L2)$_2$(byp)] **6**	12.4
[Zn(L2)$_2$(phen)] **7**	12.4
[Zn(L3)$_2$(byp)] **8**	10.2
[Zn(L3)$_2$(phen)] **9**	9.8

Conclusion

The 4-acyl pyrazolone ligands (L1-L3) have been prepared by the acylation of pyrazolone derivatives with 4-chloro benzoyl chloride. All three ligands have been characterized by IR, X-ray crystal study, ^{1}H NMR, and ^{13}C NMR spectroscopy. Ternary Zn(II) complexes **4-9** of these ligands have been synthesized and fully characterized by metal estimation, molar conductance, UV/Vis, FTIR, Thermogravimetric analysis, ^{1}H and ^{13}C NMR, and single crystal X-ray study. The X-ray analyses of the complexes 4-9 revealed that all complexes were ternary mixed ligands complexes of acylpyrazolones with 2,2′-bipyridine and 1,10-phenanthroline. From the NMR spectroscopy and single crystal X-ray study confirm that all complexes having distorted octahedral geometry. The lower molar conductance values of the complexes reveal that all complexes are non-electrolytes.

References:

1 F. Marchetti, R. Pettinari and C. Pettinari, *Coord. Chem. Rev.*, 2015, **303**, 1–31.

2 K. M. Vyas, R. N. Jadeja, D. Patel, R. V. Devkar and V. K. Gupta, *Polyhedron*, 2014, **80**, 20–33.

3 F. Marchetti, C. Pettinari, A. Cingolani, D. Leonesi, A. Drozdov and S. I. Troyanov, *J. Chem. Soc. - Dalt. Trans.*, 1998, **0**, 3325–3333.

4 B. T. Thaker, K. R. Surati and C. K. Modi, *Russ. J. Coord. Chem. Khimiya*, 2008, **34**, 25–33.

5 F. Marchetti, C. Di Nicola, R. Pettinari, C. Pettinari, I. Aiello, M. La Deda, A. Candreva, S. Morelli, L. De Bartolo and A. Crispini, *Eur. J. Inorg. Chem.*, 2020, **2020**, 1027–1039.

6 R. N. Jadeja, M. Chhatrola and V. K. Gupta, *Polyhedron*, 2013, **63**, 117–126.

7 I. U. Shaikh, R. K. Patel, V. A. Mevada, V. K. Gupta and R. N. Jadeja, *ChemistrySelect*, 2019, **4**, 8286–8294.

8 I. Shaikh, R. N. Jadeja and R. Patel, *Polyhedron*, 2020, **183**, 114528.

9 I. Shaikh, A. Vohra, R. Devkar and R. Jadeja, *Eur. J. Chem.*, 2019, **10**, 131–138.

10 University of Gottingen, *G.M. Sheldrick, SHELXS97 and SHELXL97*, Germany, 1997.

11 C. K. Johnson, *ORTEP II; Report ORNL-5138,* Oak Ridge, TN, 1976.

12 A. L. Spek, *PLATON for Windows,* University of Utrecht, Netherlands, September., 1999.

13 M. Nardelli, *J. Appl. Crystallogr.*, 1995, **28**, 659–665.

14 H. Li, G. C. Xu, L. Zhang, J.-X. Guo and D.-Z. Jia, *Polyhedron*, 2013, **55**, 209–215.

15 R. N. Jadeja, K. M. Vyas, V. K. Gupta, R. G. Joshi and C. Ratna Prabha, *Polyhedron*, 2012, **31**, 767–778.

16 M. H. Sadhu, J. K. Saini, S. S. Ingle and S. B. Kumar, *ChemistrySelect*, 2018, **3**, 6203–6208.

17 Z.-Y. Yang, R.-D. Yang, F.-S. Li and K.-B. Yu, *Polyhedron*, 2000, **19**, 2599–2604.

18 H. Y. Luo, J. Y. Li, Y. Li, L. Zhang, J. Y. Li, D. Z. Jia and G. C. Xu, *RSC Adv.*, 2016, **6**, 114997–115009.

19 S. J. Archibald, in *Comprehensive Coordination Chemistry I I*, eds. J. A. McCleverty and T. J. B. T. Meyer, Pergamon, Oxford, 2003, pp. 1147–1251.

20 K. Nakum and R. N. Jadeja, *Zeitschrift für Naturforsch. B*, 2018, **73**, 713–718.

21 R. J. Yadav, K. M. Vyas and R. N. Jadeja, *J. Coord. Chem.*, 2010, **63**, 1820–1831.

22 W. J. Geary, *Coord. Chem. Rev.*, 1971, **7**, 81–122.

Published paper

Polyhedron 183 (2020) 114528

Contents lists available at ScienceDirect

Polyhedron

journal homepage: www.elsevier.com/locate/poly

Three mixed ligand mononuclear Zn(II) complexes of 4-acyl pyrazolones: Synthesis, characterization, crystal study and anti-malarial activity

Irfan Shaikh [a], R.N. Jadeja [a,*], Rajesh Patel [b]

[a] Department of Chemistry, Faculty of Science, The Maharaja Sayajirao University of Baroda, Vadodara 390 002, India
[b] Department of Bioscience, Veer Narmad South Gujarat University, Surat 395007, India

ARTICLE INFO

Article history:
Received 20 February 2020
Accepted 18 March 2020
Available online 23 March 2020

Keywords:
Acyl pyrazolone
Antimalarial
Mixed ligand complex
Single crystal
Zinc(II) complexes

ABSTRACT

Three novel mixed ligand Zn(II) complexes {complex **1** = $[Zn(L1)_2(bpy)]$, complex **2** = $[Zn(L2)_2(bpy)]$, complex **3** = $[Zn(L2)_2(phen)]$, where bpy = 2,2′-bipyridine and phen = 1,10-phenanthroline} of 4-(4-chlorobenzoyl)-2-(3-chlorophenyl)-5-methyl-2,4-dihydro-3H-pyrazol-3-one (HL1) and 4-(4-chlorobenzoyl)-5-methyl-2-(p-tolyl)-2,4-dihydro-3H-pyrazol-3-one (HL2) were synthesized and characterized by ^{1}H and ^{13}C NMR, FTIR, TG-DTA, UV–Vis, elemental analysis, molar conductance and single crystal X-ray structure determination. Based on analytical and spectroscopic techniques, all the three Zn(II) complexes were found to have a distorted octahedral geometry. The ligands and the complexes were screened for antimalarial activity against *plasmodium falciparum*. The zinc(II) complexes showed greater antimalarial activity than their parent ligands.

1. Introduction

The two nitrogen atoms of an amidic ketone containing pyrazolone react with acid chlorides to give substitution on the 4th position of the pyrazolone, giving the commonly named 4-acyl pyrazolone. 4-Acyl pyrazolones have proven to be very useful in coordination chemistry as an –OO bidentate ligand [1–8]. There are reports in the literature on metal complexes of 4-acyl pyrazolones for d-block metals which display good antimalarial, anticancer, antibacterial, antifungal and catalytic activities.[2,6,8–11]

The lack of zinc can be a problem in biological systems and is responsible for various disease states [6,12]. Zinc has been used to reduce gastro toxicity, in which any extra drug binds to zinc and is released from the human body [13,14]. Malaria is an infectious disease caused by a parasite called *Plasmodium* and it is a serious problem for human health, especially in the so-called "Third World" [15]. The diseases are mainly caused by the main five parasite species: *Plasmodium falciparum*, *Plasmodium vivax*, *Plasmodium malariae*, *Plasmodium ovale* and *Plasmodium knowlesi* [16]. Amongst them, *Plasmodium falciparum* is the most deadly. Malaria is an entirely preventable and treatable mosquito-borne illness. However, drug resistance to currently available drugs increases multiple fold in the real world [17]. This prompted us to explore better treatment for *Plasmodium falciparum*. Pyrazolone derivatives complexed with the zinc(II) metal have been investigated [18]. The current study explores 4-acyl pyrazolones and their zinc(II) complexes, which show promising antimalarial activity [4]. The studies performed using *in vitro* assays on *P. falciparum* strains with various concentrations of the metal complexes and ligands showed that the complexes were able to inhibit the parasite growth in a more effective manner than the parent compounds. With the same dose, the metal complexes showed greater activity than the ligands against malaria [4,19–22].

* Corresponding author.
E-mail address: rjadeja-chem@msubaroda.ac.in (R.N. Jadeja).

https://doi.org/10.1016/j.poly.2020.114528
0277-5387/

2. Experimental

2.1. Materials and methods

The pyrazolones were obtained from Sidhdhanath Industries, Sachin (Surat), India as free gift samples. All necessary reagents and solvents were obtained from commercial sources. Zinc acetate, 2,2′-bipyridine and 1,10-phenanthroline were purchased from Spectrochem PVT. LTD., Mumbai. *P*-chloro benzoyl chloride was purchased from SRL Chemical, Mumbai.

Infrared (IR) spectra were recorded on a Bruker Alpha Fourier transform IR (FT-IR) spectrometer as KBr pellets. ^{1}H NMR spectra of the ligands were recorded with an AV 400 MHz Bruker FT-NMR instrument. Single crystal data were collected on a Bruker